Leibniz-Institut für Katalyse e.V. an der Universität Rostock

The Chemistry of Cyanophosphide and Phosphafluorene: Insights into Structure and Reactivity

Dissertation

In Kumulativer Form

Zur Erlangung des akademischen Grades

doctor rerum naturalium (Dr. rer. Nat.)

der Mathematisch-Naturwissenschaftlichen Fakultät

der Universität Rostock

vorgelegt von

Ayu Afiqah Nasrullah,

Geboren am 13.02.1987 in Kuala Lumpur, Malaysia

Rostock, 2025

https://doi.org/10.18453/rosdok_id00005658

Selbstständigkeitserklärung

Ich versichere hiermit an Eides statt, dass ich die vorliegende Arbeit selbständig angefertigt und ohne fremde Hilfe verfasst habe, keine außer die von mir angegebenen Hilfsmittel und Quellen dazu verwendet habe und die den benutzten Werken inhaltlich und wörtlich entnommenen Stellen als solche kenntlich gemacht habe.

Place, date, signature

Rostock, den 01.12.2025, Ayu Afiqah Nasrullah

Die vorgelegte Arbeit wurde in der Zeit von Apr 2023 bis Juli 2025 am Leibniz-Institut für Katalyse e.V., einem An-Institut der Universität Rostock, in der Arbeitsgruppe von Dr. Christian Hering-Junghans und Prof. Dr. Eszter Baráth angefertigt.

The presented work was carried out between April 2023 and July 2025 at the Leibniz Institute for Catalysis e.V., an affiliated institute of the University of Rostock, in the working group of Dr. Christian Hering-Junghans and Prof. Dr. Eszter Baráth.

Gutachter:
Dr. habil. Christian Hering-Junghans, Leibniz-Institut für Katalyse
Prof. Dr. Eszter Baráth, Leibniz-Institut für Katalyse
Prof. Dr. Rudolf Pietschnig, Universität Kassel, Institut für Chemie

Datum der Einreichung: 18.07.2025

Datum der Verteidigung: 28.10.2025

Acknowledgements

First and foremost, all praise be to Allah S.W.T, Most Gracious and Most Merciful. I am thankful to the Almighty Allah for giving me the blessing, strength, knowledge, ability and opportunity to undertake this study and complete it satisfactory. This thesis would not have been possible without the guidance and the help of several individuals who in one way or another contributed and extended their valuable assistance in my PhD journey.

I am grateful to my supervisor, Prof. Dr. Eszter Barath for her guidance, support, and always keep track on my progress and ensure that I complete my PhD within the time frame available to me as an international student. I would also like to express my deepest gratitude to my supervisor, Dr. Christian Hering-Junghans for his invaluable guidance, support, and mentorship throughout my research journey. Working under his supervision has been an incredibly enriching experience. I am grateful for the opportunity to learn and develop hands-on skills in air-sensitive chemistry − an area I had no prior knowledge and experience, but through his guidance and trust, I have grown into an independent researcher. His dedication and passion for research inspires me, his openness, patience and readiness to help, makes him more than just a supervisor, but a remarkable role model, demonstrating not only technical excellence but also humility and unwavering commitment to science.

I would like to extend my thanks to University of Malaysia Sabah (my employer) for the study leave and allowing me to pursue my PhD in Germany, Majlis Amanah Rakyat (MARA) for providing me with a scholarship and LIKAT, Rostock for allowing me to conduct the research for this thesis in this highly reputed institute. Also, my appreciation goes out to Dr. Anke Spannenberg, Dr. Wolfgang Baumann, Mr. Andreas Koch, Mrs. Astrid Lehmann, Mrs. Susann Buchholz, Mrs. Sandra Leiminger, and the other colleagues of the analytic department for their precise analysis and generous support.

I am indebted to wonderful members of my group, Kushik, Dr. Jan-Erik Siewert, Dr. Andrey Petrov, Max Neubauer, Dr. Edgar Zander, Katharina Konieczny, Claas Schünemann, Dr. Shasha Zheng, Dr. Soumyadeep Chakrabortty, Dr. Ana Franco, Dr. Fabian Kallmeier, Dr. Wietse Smit, Dr. Andrea Dell'Aqua, Dr. Sergey Tin and others for being so accommodating and providing a pleasant working atmosphere. It was so easy working with all of you and I will always cherish the time that we spent together.

Finally, I would also like to extend my deepest thanks to my beloved husband, Mohd Nazrie Salasian, for his unwavering support, understanding, and patience throughout my PhD journey. His encouragement, sacrifices and belief in my abilities have been my anchor through the most challenging time. Thank you for being the biggest cheerleader of my life, my best friend and my partner for life and for always being there for me through thick and thin. I am equally grateful to my beloved parents, Mr. Nasrullah and Mrs. Rosnida, my siblings, my parents in law for their constant love, moral support, and prayers – even from afar. Their faith in me has given me strength, and their presence in my life has been a source of comfort and motivation throughout this long and demanding journey.

My heartfelt gratitude goes to everyone – both mentioned and unmentioned – who has contributed in any way to this journey. Your kindness and companionship have made my stay in Germany truly memorable and my PhD journey more bearable. Thank you for being part of this chapter in my life.

Abstract

Phosphorus chemistry has undergone a significant revival, particularly within catalysis and synthetic methodology, reflecting its expanding utility in modern chemical research. This thesis explores low-valent phosphorus chemistry, focusing on cyanophosphides ([RPCN]$^-$) and phosphorus heterocycles, using sterically demanding terphenyl substituents to enable novel reactivity. The [^{Dipp}TerPCN]$^-$ (^{Dipp}Ter = 2,6-Dipp-C_6H_3; Dipp = 2,6-*i*Pr_2-C_6H_3) anion was established as a robust platform, exhibiting unprecedented P–CN/P–NC coordination isomerism upon O_2 oxidation, with the cyanide form thermodynamically favored — highlighting dynamic electronic behavior in P(V) adducts. Building on this foundation, the second section of the thesis demonstrates that [^{Dipp}TerPCN]$^-$ served as a cyanophosphide transfer reagent. The reactions with $GeCl_2$ yielded a unique chlorogermylene dimer with Ge···NC interactions or a diphosphanylgermylene,, while PCl_3/$AsCl_3$ afforded diphosphane/arsaphosphane species via dehydrohalogenation. These results expand cyanophosphide chemistry into new P−E (E = Ge, P, As) frameworks. In addition, frustrated Lewis pair (FLP) reactivity was demonstrated using a ^{Dipp}Ter-derived phosphafluorene. Coordination to AuCl, BH_3, or S gave quaternized derivatives, while the combination with $B(C_6F_5)_3$ and terminal arylacetylenes enabled regio- and stereoselective formation of zwitterionic alkenyl phosphonium borates—a rare transformation for phosphorus heterocycles. Minimal substituent effects on arylacetylenes suggest a generalizable activation mode governed by the phosphafluorene–borane system. Collectively, sterically tailored phosphorus centers unlock novel reactivity: cyanophosphides exhibit structural dynamism (isomerism) and transfer capabilities, while dibenzophosphole analogs facilitate FLP-mediated alkyne activation. This work advances main-group chemistry in reactive intermediates (phosphinidenes, germylenes) and functional materials, establishing new synthetic paradigms for phosphorus-based systems.

Zusammenfassung

Die Phosphorchemie hat eine bedeutende Wiederbelebung erfahren, besonders in der Katalyse und Synthesemethodik, was ihre wachsenden Nutzungsmöglichkeiten in der modernen chemischen Forschung unterstreicht. In dieser Dissertation wurde die Chemie niedervalenter Phosphorverbindungen erforscht mit einem Fokus auf Cyanophosphiden ([RPCN]$^-$) und Phosphorheterocyclen,, wobei sterisch anspruchsvolle Terphenyl-Substituenten neuartige Reaktivität ermöglichen. Das [^{Dipp}TerPCN]$^-$ (^{Dipp}Ter = 2,6-Dipp-C_6H_3; Dipp = 2,6-*i*Pr_2-C_6H_3) - Anion wurde als robuste Syntheseplattform etabliert und zeigt nach Oxidation mit O_2 eine beispiellose P–CN/P–NC-Koordinationsisomerie, wobei die Cyanid-Form thermodynamisch bevorzugt wird – ein Beleg für das dynamische elektronische Verhalten von P(V)-Addukten. Basierend darauf dient [^{Dipp}TerPCN]$^-$ als Cyanophosphid-Transferreagenz: Reaktionen mit $GeCl_2$ ergaben ein einzigartiges Chlorgermylen-Dimer mit Ge···NC-Wechselwirkungen oder ein Diphosphanylgermylen, während PCl_3/$AsCl_3$ über eine Dehydrohalogenierung Diphosphan-/Arsaphosphan-Spezies lieferten. Diese Resultate erweitern die Cyanophosphid-Chemie auf neue P–E-Gerüste (E = Ge, P, As). Zusätzlich wurde FLP-Reaktivität (Frustrated Lewis Pair) an einem ^{Dipp}Ter-abgeleiteten Phosphafluoren demonstriert. Koordination dieses Phosphafluorens an AuCl, BH_3 oder S führte zu quaternären Derivaten, während die Kombination mit $B(C_6F_5)_3$ und terminalen Arylacetylenen regio- und stereoselektiv zwitterionische Alkenylphosphonium-Borate ergab – eine seltene Transformation für Phosphorheterocyclen. Minimale Substituenteneffekte an den Arylacetylenen deuten auf einen verallgemeinerbaren Aktivierungsmechanismus hin, der durch das Phosphafluoren-Boran-System bestimmt wird. Zusammenfassend erschließen sterisch modulierte Phosphorzentren neuartige Reaktivitäten: Cyanophosphide zeigen strukturelle Dynamik (Isomerie) und Transferfähigkeiten, während Dibenzophosphol-Analoga FLP-vermittelte Alkinaktivierung ermöglichen. Diese Arbeit erweitert die Hauptgruppenchemie reaktiver Intermediate (Phosphinidene, Germylene) und funktioneller Materialien und etabliert neue synthetische Paradigmen für phosphorbasierte Systeme.

Table of Contents

List of Abbreviations

15-c-5	15-crown-5
18-c-6	18-crown-6
2.2.2-crypt	4,7,13,16,21,24-Hexaoxa-1,10-diazabicyclo[8.8.8]hexacosane
AgOTf	silver triflate
Bu	n-butyl
C_6D_6	benzene-d_6
^{Cl}Ter	2,6-(2,6-$Cl_2C_6H_2$)$_2$-C_6H_3
Cy	Cyclohexyl
DBP	dibenzophosphole
DFT	densiti functional theory
Dipp	2,6-*i*$Pr_2C_6H_2$
^{Dipp}Ter	2,6-(2,6-*i*$Pr_2C_6H_2$)$_2$-C_6H_3
Dmap	4-NMe_2-C_6H_4N
DPM	dipyrromethene
e.g.	Example
EDG	electron donating group
EIND	1,1,3,3,5,5,7,7-octaethyl-1,2,3,5,6,7-hexahydro-s-indacen-4-yl
equiv.	Equivalent
Et	Ethyl
EWG	electron withdrawing group
FLP	frustrated lewis pair
G	Gramm
H	Hours
Hz	Hertz
IDipp	1,3-Bis((2,6-isopropyl-phenyl)imidazol-2-ylidene)
I*i*Pr_2	1,3-diisopropylimidazol-2-ylidene
IMe_4	1,3,4,5-Tetra((Methyl)imidazol-2-ylidene)
IMes	1,3-Bis((2,4,6-trimethyl-phenyl)imidazol-2-ylidene)
*i*Pr	Isopropyl
IR	infrared spectroscopy
KHMDS	K[N($SiMe_3$)$_2$]
LP	lone pairs

LUMO	lowest unoccupied molecular orbital
[M]	metal
M	meta
Me	methyl
^{Me}IMes	1,3-Bis((2,4,6-trimetyl-phenyl)-4,5-bis(methyl)imidazol-2-ylidene)
MeO	methoxy
Mes	2,4,6-$CH_3C_6H_2$
Mes*	2,4,6-*t*BuC_6H_2
^{Mes}Ter	2,6-(2,4,6- $CH_3C_6H_2)_2$-C_6H_3
NaHMDS	Na[$N(SiMe_3)_2$]
NBO	natural bond orbital
NHC	N-heterocyclic carbene
NHO	N-heterocyclic olefin
NMR	nuclear magnetic resonance
O	ortho
Ph	phenyl
PNP	N[2-$P(CHMe_2)_2$-4-methylphenyl]$_2$
r.t.	room temperature
*t*Bu	tert-butyl
Tht	Tetrahydrothiophen
Tipp	2,4,6-*i*$Pr_3C_6H_2$
^{Tipp}Ter	2,6-(2,4,6-*i*$Pr_3C_6H_2)_2$-C_6H_3
Tol	toluene
Xyl	xylene

1 Introduction

1.1 Phosphanylidenephosphoranes

Species of the general type R−P(R'$_3$) are generally referred to as phosphanylidinephosphoranes. These species feature a divalent phosphorus atom bearing two lone pairs of electrons (LP) and a strongly electron-donating PR'$_3$ substituent. Multiple nomenclature systems have been used to describe these species, reflecting divergent bonding interpretations. The term phosphanylidene-σ^4-phosphorane specifies a tetrahedral phosphorus center bearing four σ-bonds (Scheme 1, **II**). When applying the λ-convention, these species are designated as 1λ^5-diphosphenes (R'$_3$P=PR), highlighting a formal P=P double bond and a pentavalent, tetracoordinate P(V) center at one phosphorus (Scheme 1, **I**). The phosphane moiety (PR'$_3$) exhibits lability and can undergo thermal/photochemical extrusion or be displaced by stronger Lewis bases, prompting the alternative designation as phosphane-stabilized phosphinidenes (Scheme 1, **III**). The latter term is interchangeable with phosphanediyls.[1] Phosphanylidenephosphoranes of the type R–P(PR'$_3$) are often termed as phospha-Wittig reagents by isolobal replacement of the CR$_2$ in classic Wittig reagents R$_2$C=PR'$_3$ with a phosphinidene fragment P−R. These systems have proven indispensable in synthesizing complex organophosphorus architectures and for elucidating novel phosphorus-centered reactivity.[2] Burg and Mahler were the first to report on the action of an excess of PMe$_3$ on the phosphorus homocycles, tetramers (PCF$_3$)$_4$ and pentamers (PCF$_3$)$_5$, noting the reversible formation of F$_3$C−P(PMe$_3$), a phosphanylidenephosphorane.[3-4] Further analysis revealed that the NMR spectra are influenced by the concentration of free PMe$_3$, indicating an exchange of coordinated PMe$_3$.

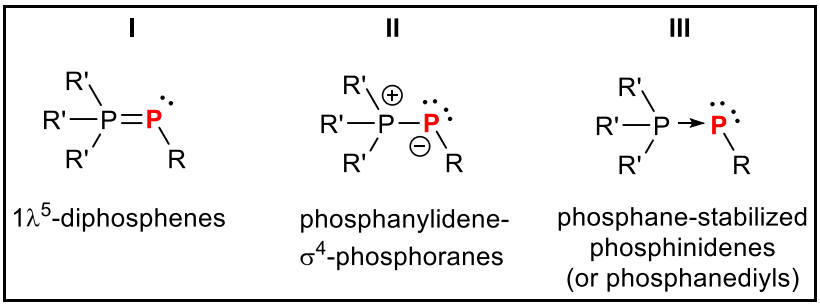

Scheme 1. Different nomenclatures for phosphanylidenephosphoranes of the general formula R−P(PR'$_3$).[1]

Aryl-substituted phosphanylidenephosphoranes Ar–P(PR'$_3$), pioneered by Protasiewicz and co-workers, represent the most widely utilized class of these compounds. The discovery emerged unexpectedly during attempts to synthesize ^{Mes}Ter-substituted diphosphenes from Cp$_2$Zr(PMe$_3$)P^{Mes}Ter[5] and ^{Mes}TerPCl$_2$ (similar to Stephan's Cp$_2$Zr(PMe$_3$)PMes* work).[6] Instead of the anticipated formation of product mixtures, ^{Mes}Ter–P(PMe$_3$) was identified (Scheme 2, top). Subsequently, a rational synthesis was developed using sterically hindered aryldichlorophosphanes (ArPCl$_2$), excess PMe$_3$, and Zn as a reductant. Although the role of zinc dust may seem redundant, it proves crucial for achieving high yields as the system performs poorly with PMe$_3$ as the sole reagent (PMe$_3$ is also oxidized during the reaction, giving Cl$_2$PMe$_3$).[7] This method enabled access to diverse derivatives with varying aryl-substituents (Ar = Mes*,[7] EIND,[8] ^{Cl}Ter,[9] ^{Mes}Ter,[7, 10] ^{Dipp}Ter,[11] ^{Tipp}Ter[12]; Scheme 2 bottom). These compounds function as phospha-Wittig reagents, reacting with aldehydes to yield phosphaalkenes (R$_1$R$_2$C=P−Ar) while liberating O=PMe$_3$, analogous to the Wittig reaction in classic organic chemistry.

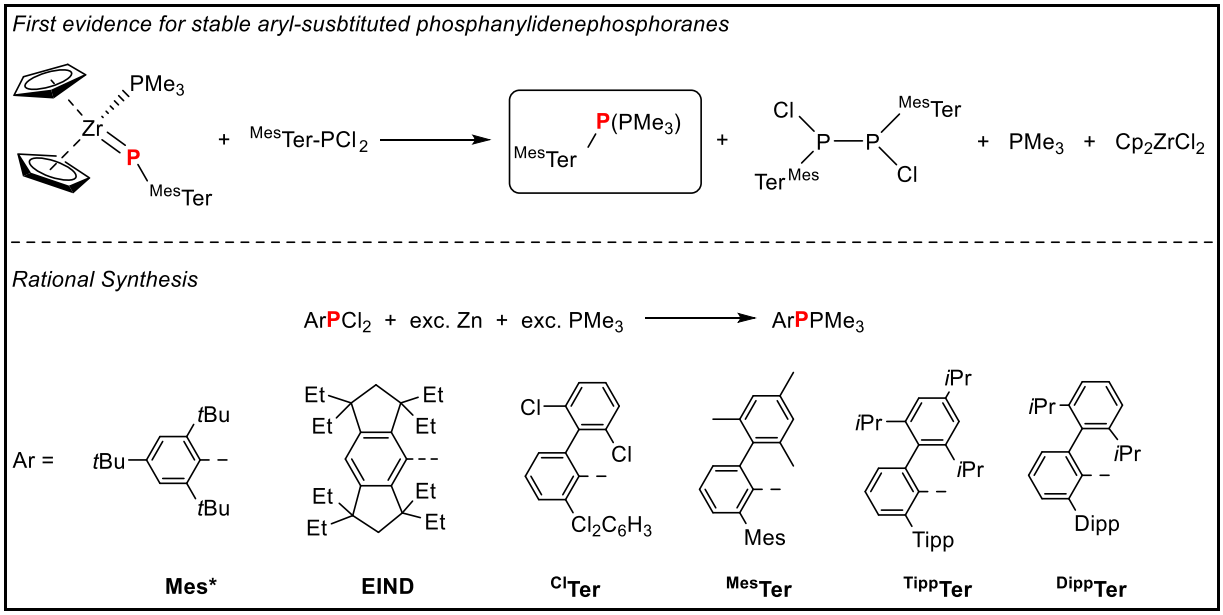

Scheme 2. First, serendipitous synthesis of ^{Mes}Ter−P(PMe$_3$) (top) and rational synthesis of Ar−P(PMe$_3$) along with different aryl-substituents commonly used to obtain robust phospha-Wittig reagents (bottom).

Phosphanylidenephosphoranes feature electron-rich (Scheme 1), dicoordinate phosphorus centers, as evidenced by their shielded ^{31}P NMR signals between ca. −10 and.80 ppm in the region typical of phosphonium P atoms. The ^{31}P NMR chemical shifts for dicoordinate phosphorus atoms (where phosphorus has two bonds and one lone pair, typically in

phosphinidenes (R−P) or phosphaalkenes(P=C)) generally fall in a highly deshielded range between ca. 200 and 500 ppm due to reduced electron density and low coordination number. Additionally, large $^{1}J_{PP}$ coupling constants (430-700 Hz) indicate potential multiple bonding between the P atoms of phosphanylidene-σ^4-phosphoranes, comparable to that observed in diphosphenes (e.g., Mes*P=PMes, $^{1}J_{PP}$ = 574 Hz).[13-14] Structural characterization of some derivatives revealed remarkably short P−P bond distances (ca. 2.06-2.15 Å) between the dicoordinate and tetracoordinate phosphorus centers. These values are significantly shorter than the theoretically predicted P−P single bond length (Σr_{cov}(P−P) = 2.22 Å) and approach the expected double bond distance (Σr_{cov}(P=P) = 2.04 Å), further supporting the presence of multiple bonding interactions.[15] Bearing two lone pairs of electrons on the dicoordinate P atom, phosphanylidene-σ^4-phosphoranes are expected to be potent ligands toward transition metals and able to react with Lewis acids as well as other electrophiles. Burg and Mahler reported the first synthesis of highly unstable acyclic trifluoromethyl derivative of P,P-ylide, F_3C–P(PMe_3) at low temperature (Scheme 3, **IV**).[4, 16] Subsequent work by Weber and Fluck,[17] Fritz,[18-19] and Regitz[20] expanded this class with further examples such as stable P,P-ylide **IV**.

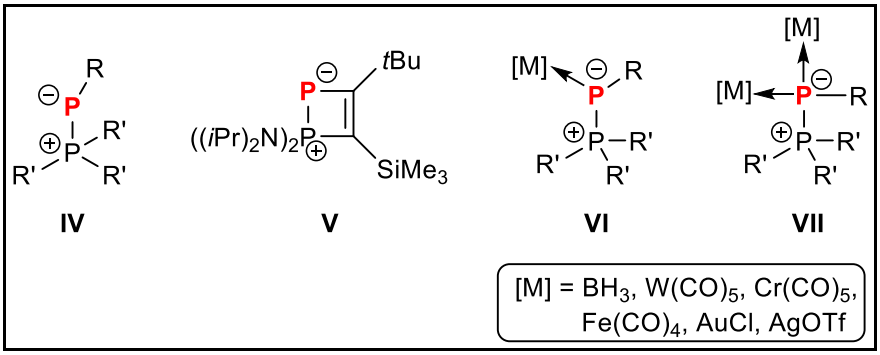

Scheme 3. Selected examples of phosphanylidenephosphorane complexes.

A cyclic P,P-ylide 1λ^5,2λ^3-1,2-diphosphete (Scheme 3, **V**) was synthesized by Regitz and Bertrand via photolysis of phosphanyl(silyl)diazomethane and *tert*-butylphosphaalkyne.[21-22] Reactivity towards transition metal fragments were shown in Mathey's mononuclear [$W(CO)_5$(RP−PR'$_3$)] complexes (Scheme 3, **VI**), accessed via phosphate reduction[23] and Scheer's dinuclear complexes (Scheme 3, **VII**) from reactions of a Cp*-phosphinidene with tungsten precursors.[24] Protasiewicz and co-workers have shown the successful syntheses of Lewis acid diadducts using the sterically unhindered Lewis acids AuCl and AgOTf in combination with stable acyclic aryl phospha-Wittig derivatives (e.g., Mes*–P(PMe_3)).[25]

Similar observations were made by Kilian and co-workers in a peri-substituted acenaphthene system (a cyclic P,P-ylide (**V**)) giving related gold diadducts (e.g., $[MesP(AuCl)_2(PMe_3)]_2$).[26-27] Additional complexes with diverse metals (Cr, W, Mo, Fe) highlight the structural variability. [16, 22-23, 25-28] Scheme 3 underscores the evolution from early unstable species to well-characterized complexes, emphasizing the synthetic potential of phospha-Wittig reagents.

1.2 Phosphanylidenephosphorane as R−P Transfer Agent

One of the key features of phosphanylidenephosphoranes is their ability to act as phosphinidene transfer agents. In this context, phosphanylidenephosphoranes serve as precursors to phosphinidene moieties (R–P), which can be delivered under mild, controlled conditions. The transfer process often proceeds via an associative substitution pathway, replacing the PR'_3 fragment with a stronger nucleophile or electrophile. This behavior has been utilized to synthesize P–E bonds where E represents transition metals or main-group elements. The reactivity can be rationalized by considering the electronic structure of $R{-}P(PMe_3)$. The LUMO of the model compound $H{-}P(PH_3)$ exhibits significant σ* character associated with the P−P bond. This suggests that photolysis or reaction with a nucleophile should promote P−P bond cleavage and release of the phosphinidene fragment (H−P).

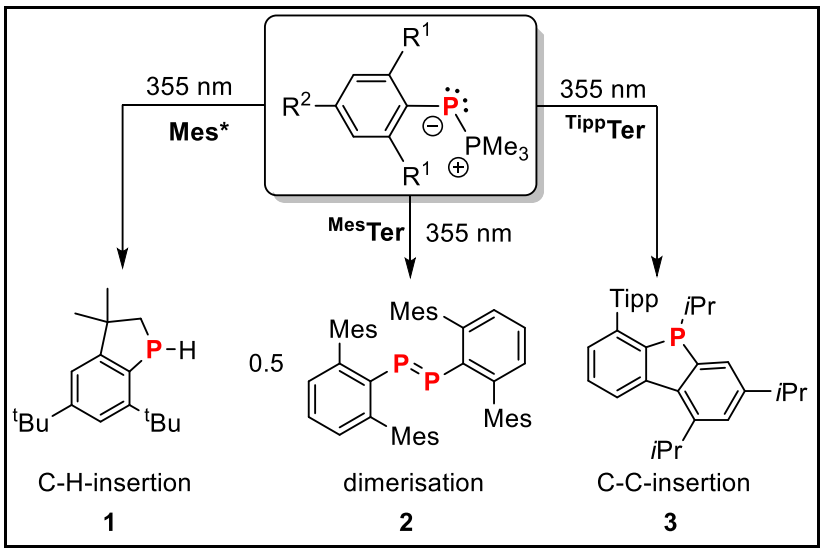

Scheme 4. Three different fates of phosphinidenes generated from $Ar{-}P(PMe_3)$ upon photolytic cleavage.

Upon laser irradiation (355 nm) of aryl-substituted phosphanylidenephosphoranes Ar–P(PMe$_3$) (Ar = Mes*, ^{Mes}Ter, ^{Tipp}Ter) bearing bulky aryl groups on the phosphanylidene P atom in C_6D_6 solution, generates the corresponding phosphinidenes Ar–P (Scheme 4).[12] Analysis by ^{31}P NMR spectroscopy confirmed the release of free PMe$_3$ and revealed distinct reaction pathways depending on the aryl substituent. For Mes*–P(PMe$_3$), the known 3,3-dimethyl-5,7-di-tert-butylphosphaindane (**1**) was formed, which is a decomposition product of the transient Mes*–P, forming through insertion of the phosphinidene P atom into a vicinal C–H bond of the *o*-*t*Bu-group. Photolysis of ^{Mes}Ter–P(PMe$_3$) yielded the diphosphene (^{Mes}TerP)$_2$ (**2**) alongside PMe$_3$, and the inherent photolytic stability of this diphosphene prevented further degradation (Scheme 4, middle). Photolytic P–P bond cleavage in the phospha-Wittig reagent ^{Tipp}TerP(PMe$_3$) produced Tipp-phosphafluorene (**3**) as the primary product forming through Ar–P insertion into one of the flanking *i*Pr-group in the Tipp-substituent. Pointing in the same direction, Protasiewicz and co-worker showed the cyclo-addition of Mes*–P(PMe$_3$) and ^{Mes}Ter–P(PMe$_3$) with *o*-quinones affording 1,3,2-dioxophospholanes rather than producing the expected 1,2-diphosphaalkenes (from phospha-Wittig type reactivity) (Scheme 5, left).[29] The reaction using 3,5-di-*tert*-butyl-*o*-benzoquinone (**5**) gives excellent yields while reaction with tetrachloro-*o*-benzoquinone (**4**) resulted in low yields. Moreover, phosphinidene transfer to transition metals was shown for ^{Mes}Ter–P(PMe$_3$) when combined with Cp$_2$Zr(PMe$_3$)$_2$ yielding Cp$_2$Zr(P^{Mes}Ter)(PMe$_3$) (**6**) with a characteristic deshielded ^{31}P NMR signal at 762 ppm corresponding to the phosphinidene P atom (Scheme 5, right). In addition, the first vanadium(V) phosphinidine complex (PNP)V=PMes*(CH*t*Bu) was furnished upon treatment of (PNP)V(CH$_2$*t*Bu)$_2$ (PNP = N[2-P(CHMe$_2$)$_2$-4-methylphenyl]$_2$) with Mes*–P(PMe$_3$) at 50 °C for 12 h.[30]

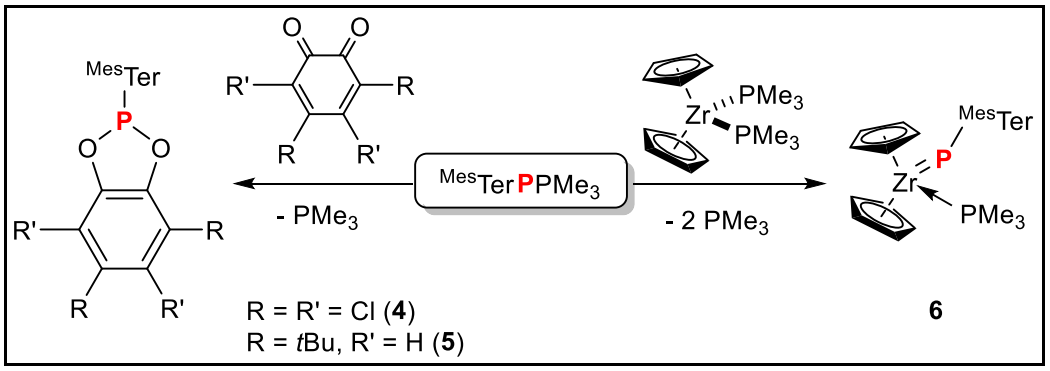

Scheme 5 Oxidative addition of Ar–P(PMe$_3$) to *o*-quinones (left) and R-P transfer to access terminal transition metal phosphinidene complexes (right).

Aldehydes react with phosphanylidenephosphoranes analogously to Wittig reagents to yield phosphaalkenes.[7] This P(I) transfer represents a simple, direct synthetic route to low-valent P(III) molecules. Thus, the addition of stronger Lewis bases to ArP(PMe_3) should result in a facile exchange of PMe_3 alongside the respective Lewis base. The reaction of ArP(PMe_3) (Ar = Mes*, ^{Mes}Ter, ^{Dipp}Ter) and NHCs (NHC = IMe_4, I*i*Pr_2, IMes, ^{Me}IMes) gives clean conversion into NHC-phosphinidene adducts NHC=PAr (**7**, Ar = Mes*; NHC = IMe_4, IMes, ^{Me}IMes) upon prolonged heating to 80 °C to 105 °C in C_6D_6, while at room temperature the desired formation was not observed (Scheme 6 (a)).[11]

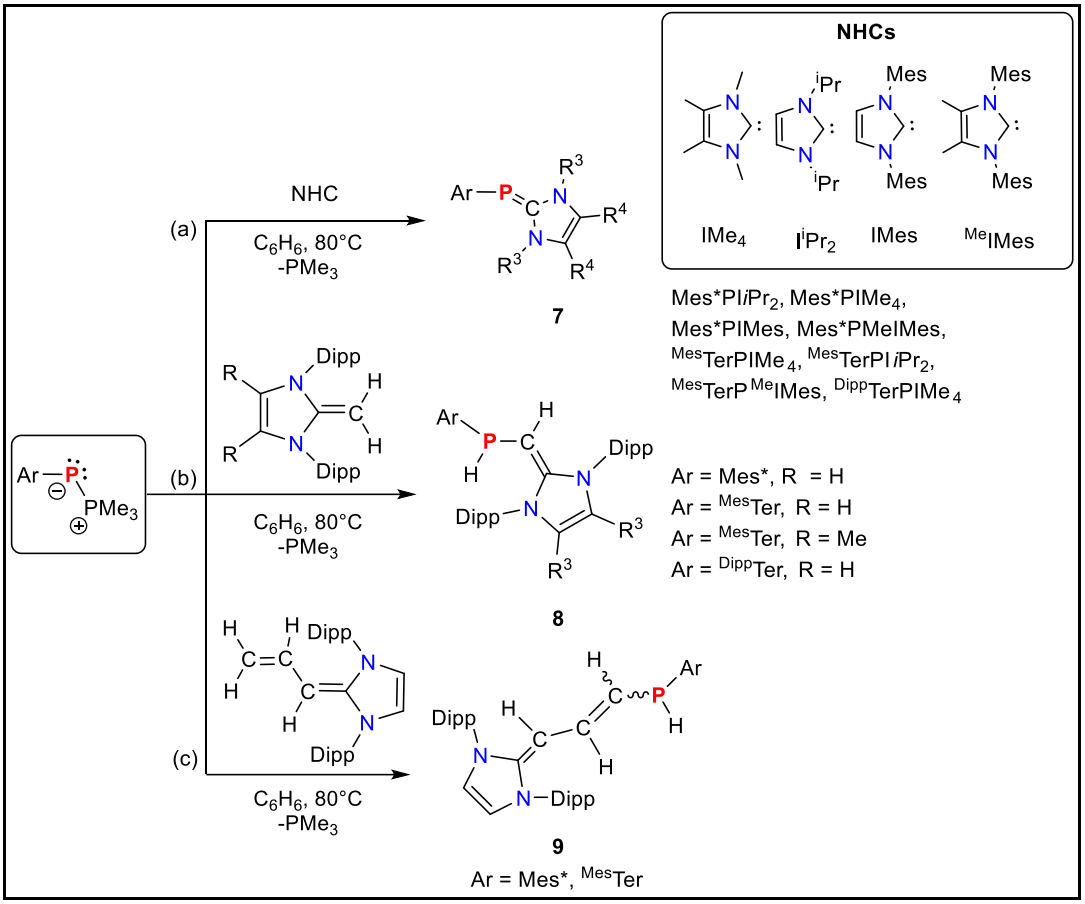

Scheme 6. Ar–P(PMe_3) as precursor for NHC-phosphinidene adducts (a) and C(sp^2)-H activation in the reaction with NHOs and enediamines to access P-substituted NHOs or butadienes, respectively (b, c).

DFT-studies and the inspection of the intrinsic bond orbitals (IBOs) are in line with an initial nucleophilic attack of the NHC at the σ* P–P orbitals and thus, an S_N2-type substitution is proposed. As outlined in Scheme 6, this protocol offers an alternative pathway to NHC phosphinidene adducts,[31] versatile ligands used in transition metal chemistry.[32] Unlike NHCs, N-Heterocyclic olefins (NHOs) act as strong σ-donors with negligible π-accepting ability.[33-34]

The reaction of IDippCH$_2$ with Mes*−P(PMe$_3$) in C$_6$D$_6$ at 80 °C afforded the P-substituted NHO IDippC(H)P(H)Mes* (**8**, Scheme 6 (b)), confirmed by a doublet in the ^{1}H NMR spectrum between 4.11-5.29 ppm ($^1J_{PH} \approx 210$ Hz), indicative of a PH proton. Extending this methodology, treating the enediamine IDippC$_3$H$_4$[35] with Ar−P(PMe$_3$) (Ar = Mes*, ^{Mes}Ter) affords γ-P-substituted enediamines IDippC$_3$H$_3$P(H)Ar (**9**, Scheme 6 (c)). These adopt predominantly *E*-1,3-diene configurations in solution, while the *Z*-configured diene (IDippC$_3$H$_3$P(H)Mes*) was observed in the solid state.[11]

The phosphinidene transfer capability extends to reactions with other simple organic nucleophiles, where Ar−P(PMe$_3$) reacts with isonitriles (R–NC) to form new 1,3-phosphaazaallenes (ArPCNR). In the case of *t*Bu−NC these phosphaazaallenes can thermally eliminate *iso*-butene to yield cyanophosphines (ArP(H)CN).[36] Heating 1:1 mixtures of the phospha-Wittig reagents Ar−P(PMe$_3$) (Ar = Mes*, ^{Mes}Ter, ^{Dipp}Ter) and isonitriles (*t*BuNC, XylNC; Xyl = 2,6-Me$_2$C$_6$H$_3$) to 80 °C for 16 h in benzene or *n*-hexane solution afforded six examples of the phosphaazaallenes ArPCNR (**10**, Scheme 7). Subsequent prolonged heating of the *t*Bu-substituted phosphaazaallenes (ArPCN*t*Bu) to 105 °C induced conversion to the cyanophosphines ArP(H)CN (**11**), along with *iso*-butene elimination. Furthermore, treatment of ^{Dipp}TerP(H)CN with K[N(SiMe$_3$)$_2$] (KHMDS) was shown to give an isolable cyanophosphide (**12**, Scheme 7). Furthermore, Mes*PCN*t*Bu underwent hydroborylation across the C=N bond using Piers' borane (HB(C$_6$F$_5$)$_2$), yielding the heterobutadiene derivative Mes*P=C(H)−N(B(C$_6$F$_5$)$_2$)*t*Bu

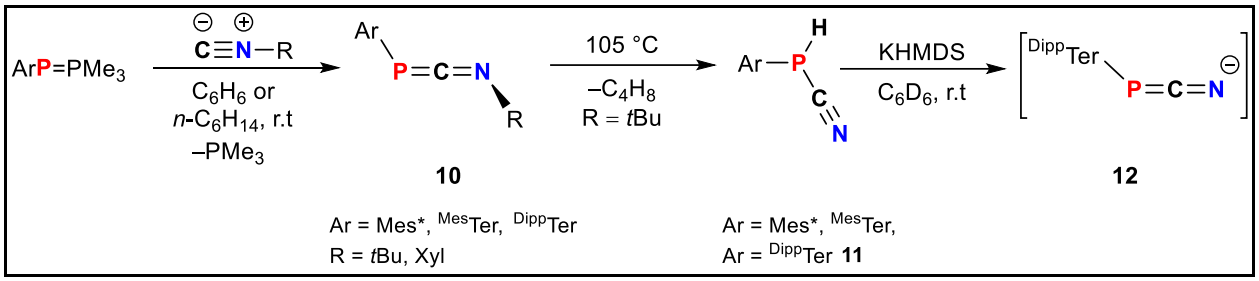

Scheme 7. Facile PMe$_3$ for CN—R exchange reactions to afford 1,3-phosphaazaallenes **10**, which upon heating yielded cyanophosphine **11** and further deprotonation to form cyanophosphide **12**.

Hering-Junghans and co-workers have synthesized phospha- and arsaalumenes, ^{Dipp}TerPnAlCp* (**13**, Pn = P, As) by heating 4:1 mixtures of ^{Dipp}Ter—Pn(PMe$_3$) and (Cp*Al)$_4$ (Scheme 8).[37] After recrystallization from *n*-hexane, these compounds formed thermally stable violet (Pn = P) or blue (Pn = As) crystalline solids under inert conditions. This strategy

leveraged PMe_3 as an innocent and volatile leaving group, analogous to prior work with alanediyls and organic azides. In contrast, using ^{Mes}Ter—P(PMe_3) under identical conditions did not yield the expected phosphaalumene.[38] Instead, a second Al(I) fragment (from $(Cp^*Al)_4$ or $Cp^{3t}Al$[39]) (Cp^{3t} = 1,2,4-*t*$Bu_3C_5H_2$) added across the putative P=Al bond, forming ^{Mes}TerP($AlCp^x$)$_2$ (x = *, 3t). This reactivity showcases the potential of phospha-Wittig reagents in phosphinidene transfer and arsa-Wittig reagents for arsinidene transfer in accessing novel heterodiatomic multiple bonds between main-group elements.[40]

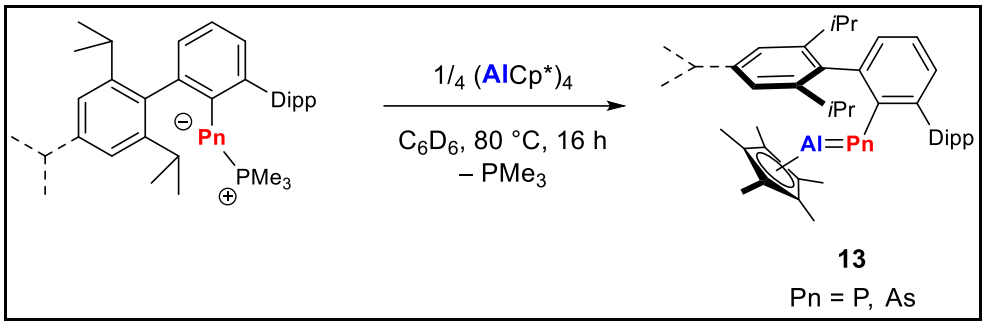

Scheme 8. PMe_3 for Cp*Al-exchange to afford phospha- and arsaalumenes.

Later, the group demonstrated the facile activation of N–H bonds in NH_3 using Ar–P(PMe_3) (Ar = Mes*, ^{Mes}Ter, ^{Dipp}Ter) without the need for metal, yielding isolable secondary aminophosphines, $ArP(H)NH_2$ (**14**, Scheme 9). This reactivity was extended to primary and secondary amines, including chiral variants. Phospha-Wittig reagents thus provide a direct route to P–N bonds from diverse amine substrates.[41]

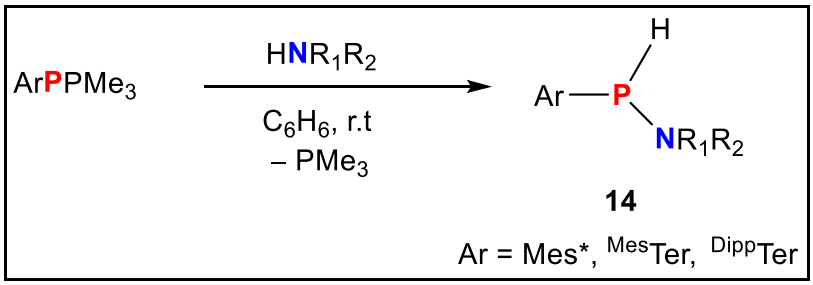

Scheme 9. N-H bond activation in HNR_1R_2 using phospha-Wittig reagents (Ar–$PPMe_3$).

1.3 Formal Phosphinidene Cyanide Adducts

Cyanophosphines (R_2P–CN/RP(H)CN) represent a pivotal class of organophosphorus compounds, historically valued as precursors to phosphinidenes (R–P) and ligands in coordination chemistry. The ambidentate nature of the cyanide group introduces unique electronic properties, characterized by strong σ-donation and moderate π-acceptance, which modulates the phosphorus electrophilicity and facilitates complex formation with transition metals.[42] Cyanophosphines of the general type RP(H)CN (R = alkyl, aryl) have long remained elusive and were either found to be unstable,[43] or to be stabilized only by coordination to a transition metal.[44] Streubel and co-workers showed that the 1,3-phosphaazaallene complex $(Me_3Si)_2HC$–P($W(CO)_5$)CN*t*Bu undergoes thermal loss of *iso*-butene to give the corresponding cyanophosphine tungsten complex (**15**, Scheme 10 (a)).[45] In 2001 the reaction of dicyanophosphines ($RP(CN)_2$) with equimolar amounts of Schwartz's reagent ($[Cp_2Zr(H)Cl]_n$) was shown to afford the methyl, *tert*-butyl, and Mes* derivatives of cyanophosphines, respectively (**16**, Scheme 10 (b)).[46] Our group has demonstrated the synthesis of cyanophosphines through the reaction of Ar−P(PMe_3) and *t*Bu-NC to afford 1,3-phasphaazallene which later upon heating at 105 °C, converted to cyanophosphine (**11**) (Scheme 7), *vide supra*. The limited research on cyanophosphines motivated our investigation into this underexplored class of compounds.

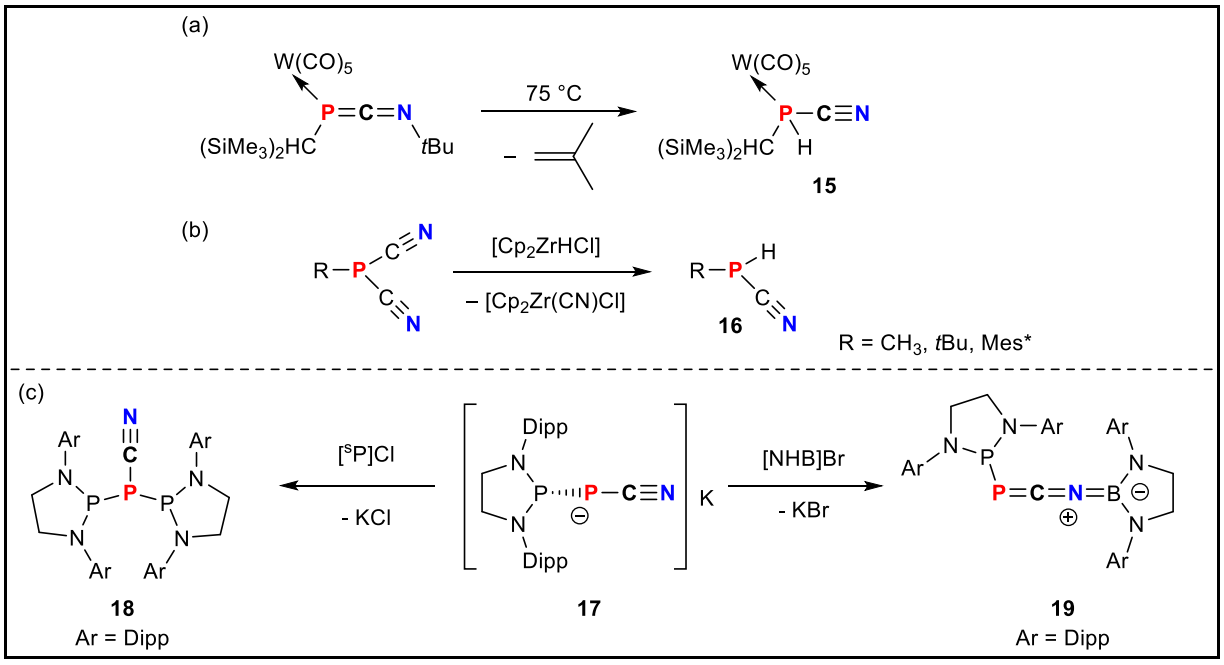

Scheme 10. Previous work on cyanophosphine synthesis (a,b) and examples of salt metathesis of cyanophosphide **17** (c).

A transformative advancement emerged with the recognition that anionic cyanophosphides $[RPCN]^-$ serve as isolable phosphinidene equivalents (through MCN elimination). This concept garnered recognition through work by Schmidtpeter et al. through reductive decyanation of $P(CN)_3$ where the first dicyanophosphides $[P(CN)_2]M$ were isolated,[47] and alternative synthetic strategies have surfaced since this initial report.[48-49] Cyanophosphides can be considered as the formal cyanide adducts of phosphinidenes and are thus another class of P-compounds in the (+1)-oxidation state.[50] Later, Schmidtpeter and co-workers synthesized $[PhPCN]^-M^+$ (M^+ = Na, K, $[N(PPh_3)_2]$) via reaction of $(PhP)_5$ with cyanide salts, observing equilibrium mixtures that shift toward $[PhPCN]^-$ with weakly coordinating cations.[51-52] Recently, Grützmacher *et al.* developed alkali metal phosphanyl cyanophosphides ($[^sP]PCN)M$ (**17**, Scheme 10 (c)) (M = Na, K; $[^sP]$ = $[(H_2CNDipp)_2P]$) through oxygen for nitrogen exchange between phosphanyl phosphaketenes ($[^sP]PCO$) and $M[N(SiMe_3)_2]$, releasing $O(SiMe_3)_2$. These species serve as versatile PCN^- transfer agents, exhibiting ambident nucleophilicity ($[^sP]PCN)^-$ yields either P- or N-functionalized product (**18**/**19**, Scheme 10 (c)).[53] On the other hand, Wolf and co-workers observed the formation of the phosphanyl-substituted cyanophosphides $[R_2PPCN]^-$ (R = Ph, Cy, *t*Bu, $N(iPr)_2$) as counter anions for anionic cobalt *cyclo*-triphosphido complexes.[54] Building on this, our group has shown that terphenyl cyanophosphines can be deprotonated with KHMDS to afford [^{Dipp}TerPCN]K and addition of 2.2.2-cryptand quantitatively yielded the ion-separated salt [^{Dipp}TerPCN][K(2.2.2-crypt)].[36]

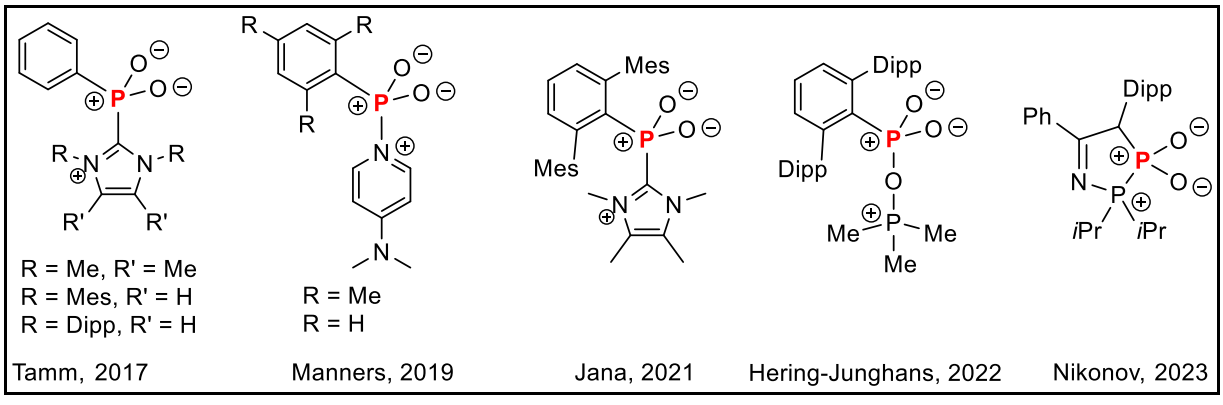

Scheme 11. Examples of reported dioxophosphorane $ArPO_2$ species.

Cyanophosphides represent rare phosphorus(I) species, prompting investigation into the air oxidation of sterically shielded [(^{Dipp}TerPCN)K], which might result in the formation of the corresponding dioxophosphorane cyanide adducts. Previous studies report several

stabilized forms of $^{Dipp}TerPO_2$, including its dimer $[^{Dipp}TerPO_2]_2$,[55] and $OPMe_3$ adduct $[^{Dipp}TerPO_2(OPMe_3)]$ (Scheme 11).[56] Beside the adducts of $^{Dipp}TerPO_2$, literature documents NHC adducts of $PhPO_2$,[57] $^{Mes}TerPO_2$,[58] dmap-adducts (dmap = 4-NMe_2-C_6H_4N),[59] and a cyclic phosphine-stabilized amino-dioxophosphorane (Scheme 11).[60] Notably, free dioxophosphoranes have only been isolated in argon matrixes and were characterized by vibrational spectroscopy.[61-63]

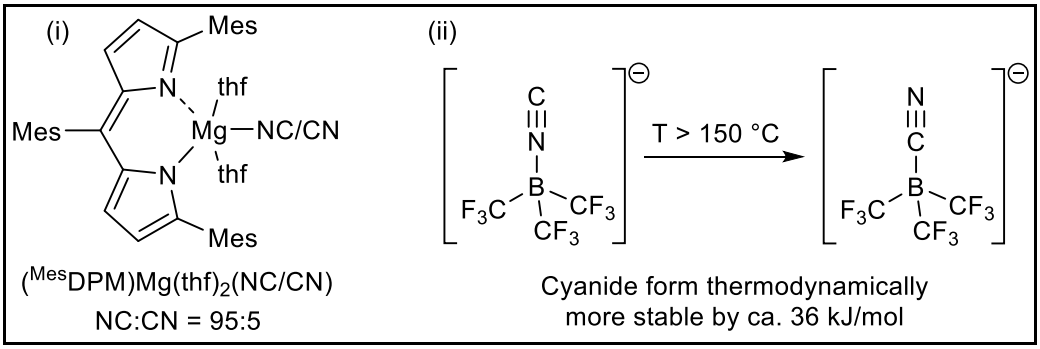

Scheme 12. CN/NC coordination isomerism in magnesium and boron species.

Recently, we have reported a series of crown ether complexes [(^{Dipp}TerPCN)M(crown)] (M = Na, K; crown = 15-crown-5, 18-crown-6), with structural diversity in the solid-state dependent on the metal ion or crown ether. Investigation of their reactivity towards dry air, nitrous oxide and sulfurization, lead to the discovery of coordination isomerism in dioxophosphorane cyanides.[64] Similar CN/NC isomerization phenomena in main-group compounds have been observed for magnesium and boron systems (Scheme 12). For a dipyrromethene-supported magnesium complex (^{Mes}DPM-Mg, Scheme 12(i)), X-ray crystallography revealed predominant solid-state existence as the Mg–NC isomer (95%), with only minor Mg–CN contribution (5%).[65] Conversely, the borate anion $[(F_3C)_3B–CN]^-$ was shown experimentally (via DSC) to be thermodynamically favored over its $[(F_3C)_3B–NC]^-$ isomer by 35.2 kJ mol^{-1} (Scheme 12(ii)).[66] Coordination isomerism remains exceptionally rare in main group compounds.[65-68] Seminal contribution include Inoue's report of thermally induced SiP/PSi-isomerism in the heavier nitrile derivative ($(SiTol_3)(SiMe_3)_2Si$)SiP(IPr) (IPr = $(HCNDipp)_2C$).[68] while the Goicoechea group discovered a [B]–OCP to [B]–PCO ([B] = $(HCNDipp)_2B$) isomerism catalysed by *t*Bu−NC.[67] In contrast, our findings on the oxidation of cyanophosphides with S_8 and N_2O afforded isomer-free $[^{Dipp}TerPS_2(CN)]^-$ and anionic phosphinidene monoxide adducts, respectively, where no coordination isomerism was observed.[64] We have also demonstrated reactions of cyanophoshine (^{Dipp}TerP(H)CN) with

ECl_n (E = Ge, n = 2; E = P, As, n = 3) using either salt metathesis or base-assisted dehydrohalogenation[69] These findings will be further elaborated in Chapter 3.

1.4 Dibenzophospholes

Dibenzophospholes (DBP's) are tricyclic heteroaromatic compounds featuring a central five-membered P-containing ring fused to two benzene rings, also termed phosphafluorenes. The first dibenzophospholes were described in the 1950's, and the interest towards these compounds surged in the early 21st century due to their potential in organic electronics and the possibility of designing new π-conjugated, electroluminescent materials for optoelectronic devices.[70] Important reviews regarding brief introduction to phospholes (**I**) (Scheme 13) and other organophosphorus derivatives in the context of molecular electronics were published by Réau,[71] Baumgartner,[72-73] and Hissler.[74] Dibenzophospholes (**II**) together with dibenzofurans (**III**), dibenzothiophenes (**IV**) and carbazoles (**V**) formally belong to a family of heteroatom-substituted analogs of fluorenes (**VI**), or fluorene anions (Scheme 13).

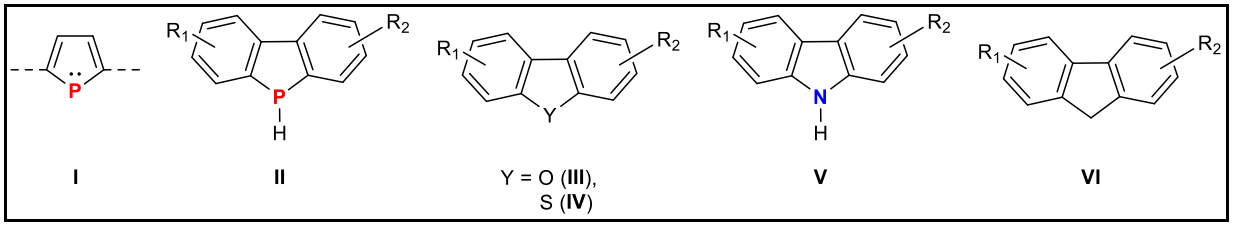

Scheme 13. Fluorene and heterofluorene derivatives.

Réau and Baumgartner primarily developed phosphole-containing oligo-and polythiophene materials, whereas Hissler's review comprehensively covered non-fused phospholes and diheteroaromatic derivatives of phospholes fused to thiophene, pyrrole, furan, pyridine and other P-derivatives which were incorporated into electronic devices. In 2015, Gouygou have discussed the application-potential of phosphole-based ligands, including dibenzophospholes in both metal- and organo-catalyzed reactions.[75] A recent review by Bałczewski and co-workers summarizes the literature on the newest synthetic approaches towards DBP's and

outlines functionalization strategies as well as their applications as optoelectronic materials from 2001-2016.[70]

P-phenyl dibenzophosphole was first reported by Wittig and co-workers in 1953,[76] and considerable efforts have been devoted to establishing structural diversity.[76-78] An updated overview on synthetic strategies for the construction of dibenzophosphole scaffolds classified by their reaction modes was provided in a review by Sakai, Hattori and co-workers. The synthetic strategies in the formation of the ring units in dibenzophosphole can be categorized into three types (Scheme 14): (a) formation of a phosphole ring using compound with pre-existing benzene units, (b) formation of a fused-benzene ring into a multi-substituted phosphole core and (c) sequential formation of the phosphole skeleton followed by the fused-benzene ring.[79]

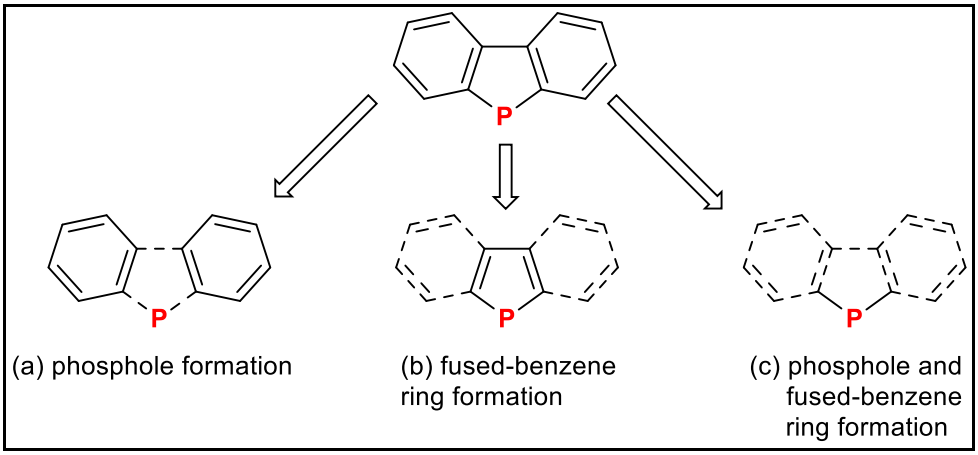

Scheme 14. Overview of the synthetic strategies of a dibenzophosphole scaffold.

In 1999, Power and co-workers reported that the reduction of an *m*-terphenyldichlorophosphine (^{Tipp}TerPCl$_2$, (**24**)) with magnesium in THF gave the Tipp-phosphafluorene (**3**) as the cyclized product (Scheme 15, b).[80] Around the same time, the Protasiewicz group reported on the photolysis (365 nm) of phospha-Wittig reagent, ^{Tipp}TerP(PMe$_3$) (**21**) to generate the same Tipp-phosphafluorene (**3**) (Scheme 15, a).[12] Later, they have shown that using activated magnesium (Mg*) has a profound impact on the reduction of **24** to give Tipp-phosphafluorene (**3**) as the sole product (Scheme 15, b).[81] Complementing this, our group observed ^{Dipp}Ter–P generation and subsequent cyclization to phosphafluorene (**22**) through two pathways: (i) thermal decomposition (50°C, 2h) of isolated phosphagallene ^{Dipp}TerPGaCp* (**25**) (Scheme 15, c), and (ii) room-temperature irradiation (396 nm) of ^{Dipp}TerP(PMe$_3$) (**20**) in toluene-d_8 (Scheme 15 a).[82] Recently, we have reported an optimized synthetic route towards phosphafluorene (**22**)

via reduction of $^{Dipp}TerPCl_2$ (**23**) with 2 equivalent of Mg* (Scheme 15, b). This will be further discussed in Chapter 3. Other related terphenyl-based cyclizations in the formation of DBPs were also reported by Ionkin and Marshall in potassium mediated reduction of dichlorophosphanes to give the 5-chlorodibenzophosphole (**26**) (Scheme 15, d),[83] and Wehmschulte's $AlCl_3$-driven Friedel-Crafts reactions of dichlorophosphines (Scheme 15, e).[84] Correspondingly, similar intramolecular cyclizations have also been reported for terphenyl-substituted phosphenium cations, leading to the isolation of 9-phosphafluorenium ions (Scheme 15, f).[85] Thermolysis of aryldichlorophosphine at 200-230 °C with HCl evolution has also been shown to give DBPs derivatives.[84]

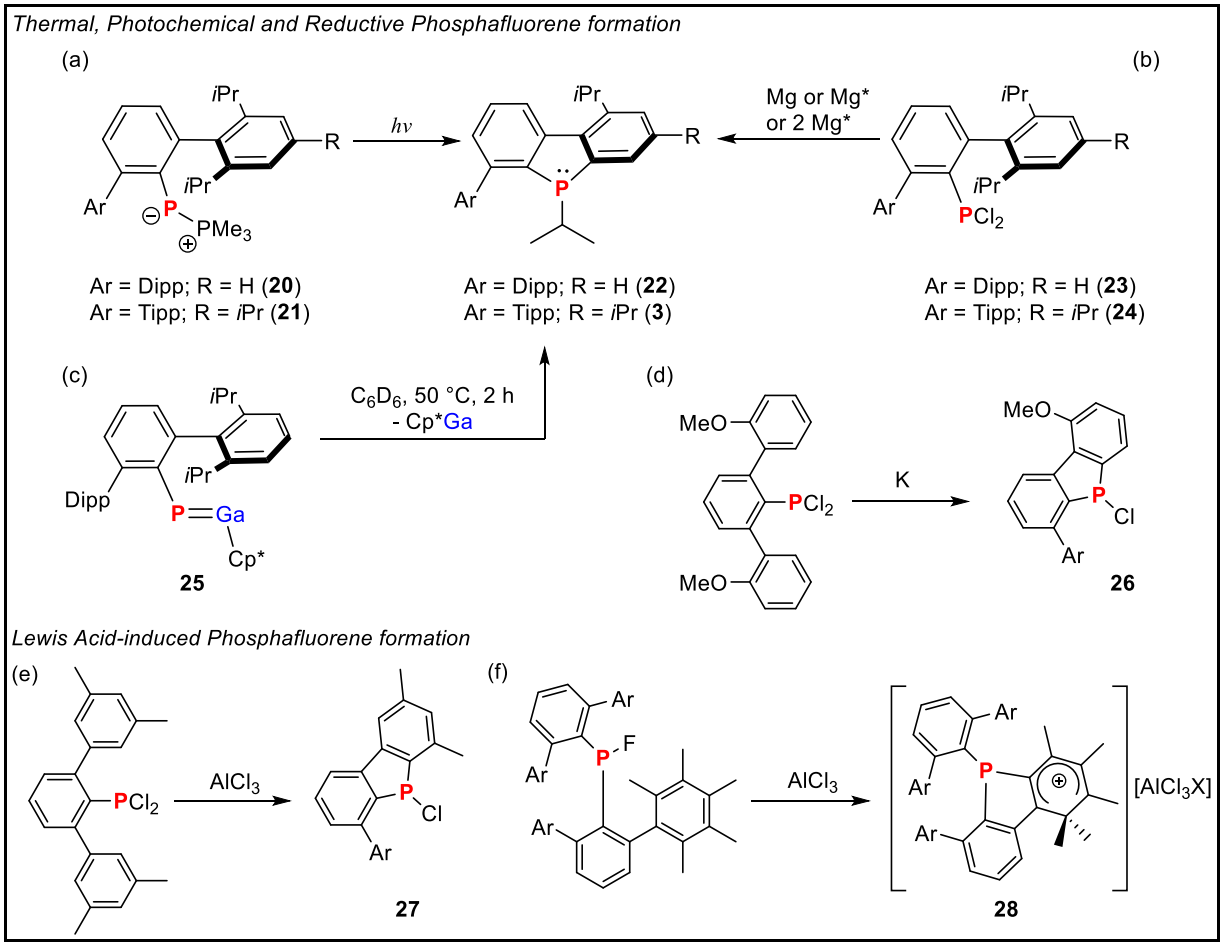

Scheme 15. Diverse strategies towards terphenyl-derived DBPs.

The phosphole ring of the DBPs can be precisely tuned through functionalizations at the phosphorus atom, enabling valency expansion and bond formation to diverse elements (O, S, Se, B, N, P, C) and transition metals. The versatility of P-quarternization strategies for the P atom in dibenzophospholes include oxidation,[86] sulfurization,[87] complexation with metals

(e.g., tungsten, gold,[87] iron or ruthenium,[84]), and related transformations. These structural modifications permit fine-tuning of optoelectronic properties, demonstrating their utility for tailored implementation in photonic and electronic devices. Several promising dibenzophospholes (**29-41**), featuring diverse phosphorus substituents, have been reported for optoelectronic applications. These compounds demonstrate potential utility in devices such as photovoltaics, organic light-emitting diodes (OLEDs), bio-/chemical sensors, and nonlinear optical devices (NLOs) (Scheme 16).[88-89]

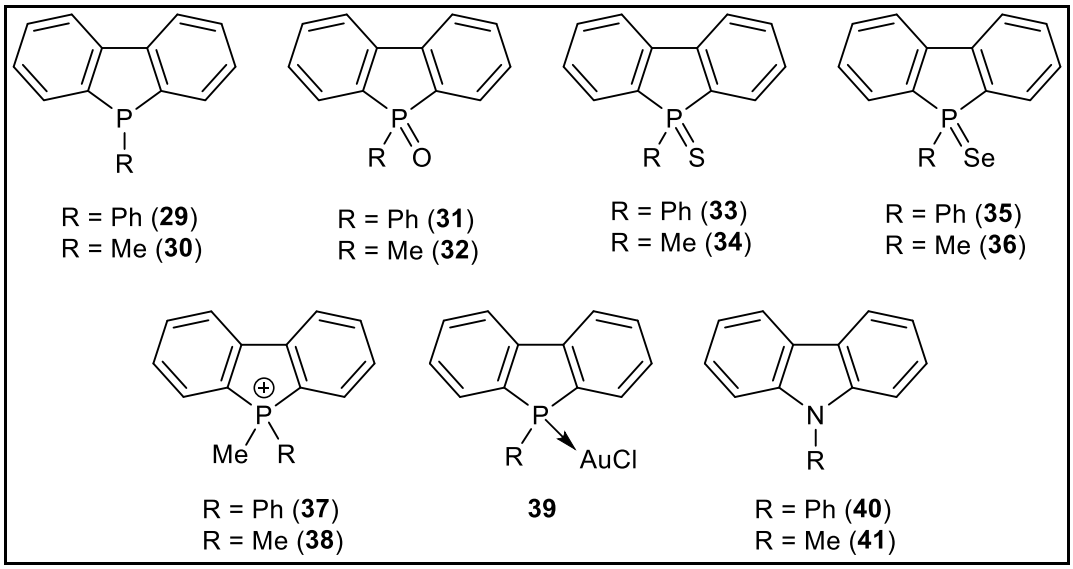

Scheme 16. P-Functionalized dibenzophospholes **29-41** as optoelectronic materials.

1.5 Frustrated Lewis Pairs (FLPs) with DBPs

Frustrated Lewis Pair (FLP) chemistry has undergone significant advancement in recent years, emerging as an essential area in modern chemical research.[90] The foundational concept of FLPs, which involves the synergistic interaction between sterically hindered Lewis acids and bases, has demonstrated remarkable reactivity in the activation of a diverse array of small molecules. FLPs exhibit the unique capability to activate substrates such as H_2, CO_2, SO_2, RNSO, and CO, among others, underscoring their versatility in catalytic and synthetic applications.[90-92] FLPs are typically formed through the combination of sterically encumbered Lewis acids and bases, where the spatial demands of the constituents prevent classical adduct formation, thereby preserving their cooperative reactivity. FLP systems are well-documented in alkyne functionalization. The initial exploration of FLP-mediated alkyne functionalization was first documented in 2009, marking a critical milestone in the field. Early investigations into

the activation of alkynes by frustrated Lewis pairs composed of the strong Lewis acid $B(C_6F_5)_3$ and phosphine donors, showed two distinct pathways dictated critically by the basicity and steric profile of the phosphine.[93-97] Stephan and co-workers demonstrated that by combining the strongly basic, sterically encumbered phosphine (e.g., tBu$_3$P), with strong Lewis acids $B(C_6F_5)_3$ or $Al(C_6F_5)_3$ in phenylacetylene solutions induces alkyne deprotonation. This generates ionic phosphonium alkynylborate salts (**42**, Scheme 17).[93-95] Conversely, less basic or more sterically hindered phosphines (e.g., Ph_3P, Mes_2PH, polyphosphines or chloro/phenoxy-substituted variants) cannot abstract the proton efficiently. Instead, they act as nucleophile in a 1,2-addition across the C≡C bond, to form zwitterionic olefinic adducts (**43**, Scheme 17).[93-95, 97-98]

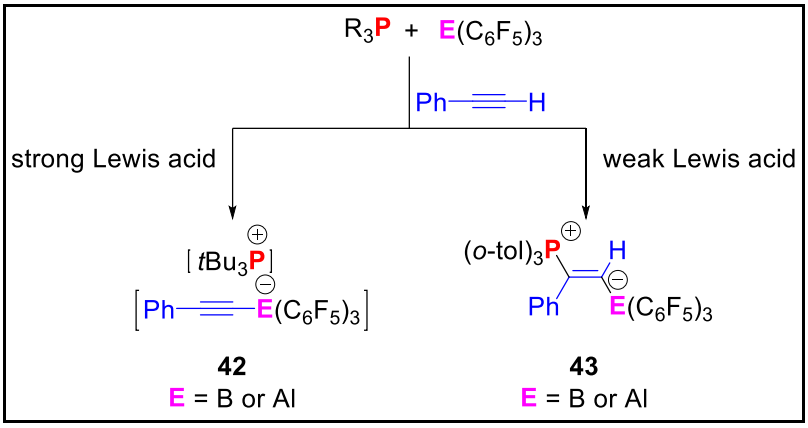

Scheme 17. Two pathways for the activation of alkynes by FLPs. Deprotonation to **42** and 1,2-addition to **43**.

The regio-selectivity of this addition consistently places the phosphonium moiety on the more substituted carbon. This selectivity arises from Lewis acid-induced polarization of the alkyne, which stabilizes a terminal vinyl carbocation intermediate. The observed *trans*-stereochemistry results from nucleophilic approach at the least hindered face of this carbocation.[93] Subsequent studies by the Stephan group confirmed this contradiction based on investigating a diverse array of terminal alkynes, phosphines, and boranes,[96, 99-100] with the unexpected observation that even the classical Lewis adducts like $Ph_3P{\cdot}B(C_6F_5)_3$ which were assumed to be inert due to strong association, yields the 1,2-addition product. However, the isolation of zwitterionic products such as E-$Ph_3P(Ph)C{=}C(H)B(C_6F_5)_3$ confirmed that reversible dissociation of the P−B dative bond enables cooperative activation of alkynes, redefining the scope of FLP chemistry to include 'masked FLPs'.[93-94] Understanding the mechanism of FLP reactions with alkynes is attracting growing research interest. However, the facile and rapid natures of these transformations complicate the kinetic investigation. The most reasonable mechanism involves

initial π-coordination of the Lewis acid center to the alkyne. This proposal aligns with both $Al(C_6F_5)_3$'s established ability to form π-interactions with arene solvents[101] and the observed rapid reaction of terminal alkynes with $E(C_6F_5)_3$ (E = B or Al) Lewis acids (in the absence of bases) to form vinylborane species. Such coordination simultaneously activates the alkyne toward nucleophilic attack and enhances the C–H bond acidity.[94] These studies have not only elucidated the electronic and steric factors governing reactivity but also established FLPs as robust platforms for the selective transformation of unsaturated hydrocarbons.

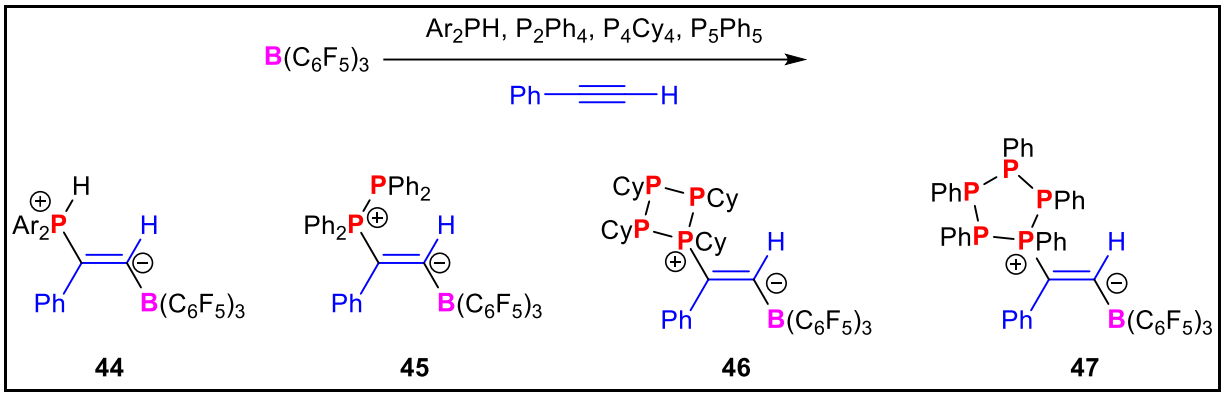

Scheme 18. Products of FLP-alkyne addition reaction.

The scope of phosphorus donors enabling FLP addition reactions has expanded beyond tertiary phosphines to include secondary phosphines (Ar_2PH; Ar = Ph, Mes) and primary phosphines (e.g., $(2,6\text{-}t\text{Bu}_2C_6H_3)PH_2$).[94] Furthermore, polyphosphines (P_2Ph_4, P_4Cy_4, P_5Ph_5) also facilitate these transformations, yielding analogous olefinic zwitterionic phosphonium borate products (Scheme 18). [98] Subsequent work extended this reactivity to chloro- and phenoxy-phosphines, including $t\text{BuPCl}_2$, catecholborane-*t*BuP adducts ($C_6H_4O_2Pt\text{Bu}$), fluorene-derived analogs ($C_{20}H_{12}O_2Pt\text{Bu}$), and tris(aryloxy)phosphines ($(2,6\text{-}t\text{Bu}_2C_6H_3O)_3P$).[99] DBPs exhibit unique electronic properties. Their steric bulk further enables applications as phosphine components in frustrated Lewis pairs (FLPs) with hindered Lewis acids. In chapter 3, we will discuss the reactivity of phosphafluorene**22**) towards terminal alkynes (4-R-C_6H_4-C≡CH) in the presence of $B(C_6F_5)_3$, proving an FLP-type alkenylation strategy for DBPs.

2 Objectives of this work

This doctoral thesis is structured around a central theme: the reactivity and structural diversity of low-valent phosphorus compounds. The objectives of this work are outlined as follows:

1. To synthesize and characterize a series cyanophosphide salts [(^{Dipp}TerPCN)M(crown)] and to explore their oxidation-induced coordination isomerism through various oxidizing reagents (O_2, S_8, N_2O). In addition, to understand the mechanisms, energetics and thermal stabilities associated with CN/NC isomerization using spectroscopic and computational methods.
2. To establish [^{Dipp}TerPCN]$^-$ as a competent cyanophosphide transfer reagent toward main-group electrophiles ($GeCl_2$, PCl_3, $AsCl_3$) and study their structural characteristics via X-ray crystallography and multinuclear NMR spectroscopy.
3. To construct novel ^{Dipp}Ter-substituted phosphafluorene derivatives via P-quaternization and to develop a FLP-mediated alkenylation strategy of this phosphafluorene using $B(C_6F_5)_3$ and terminal arylacetylenes.
4. Elucidating structures, bonding characteristics, and mechanistic insights through a combination of spectroscopy, crystallography, and quantum chemical calculations.

3 Results and Discussion

3.1 Overview

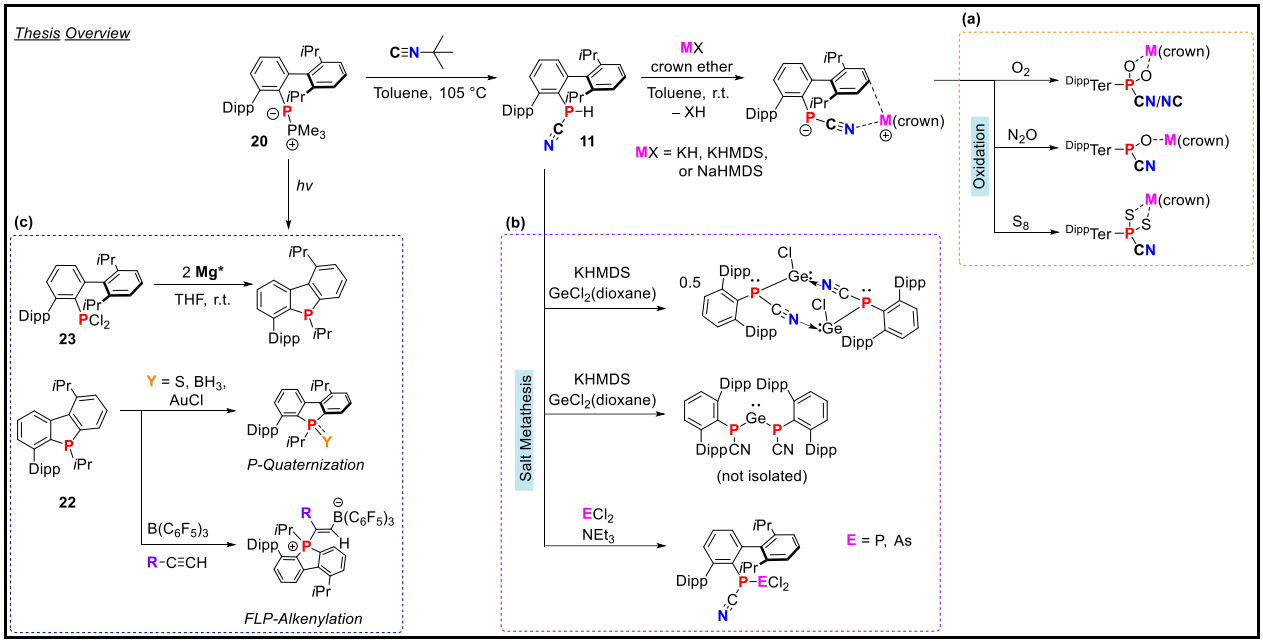

Scheme18. Overview of the thesis; (a) coordination isomerism in dioxophosphorane cyanides, (b) cyanophosphide transfer reactions, and (c) FLP-alkenylation of a phosphafluorene.

In this thesis two principal research domains are discussed: (1) the reactivity of sterically demanding cyanophosphides featuring a ^{Dipp}Ter moiety, and (2) FLP-type alkenylation of a phosphafluorene derivative (Scheme 19, c). The first project is divided into two subprojects: On the one hand the investigation of coordination isomerism in dioxophosphorane cyanides (Scheme 19, a) and on the other hand cyanophosphide transfer reactions (Scheme 19, b). Central to this work is the phospha-Wittig reagent ^{Dipp}Ter–P(PMe$_3$) (**20**), which served as the precursor for synthesizing cyanophosphine (**11**) in Project (1) and previously afforded phosphafluorene (**22**) in Project (2).

In the cyanophosphine subproject, a series of cyanophosphide crown ether salts [(^{Dipp}TerPCN)M(crown)] were isolated and their structural diversity was investigated by single crystal X-ray diffraction experiments (SC-XRD) and multinuclear NMR spectroscopy. Oxidation of these cyanophosphides with oxygen afforded dioxophosphorane cyanides of the general form [^{Dipp}TerPO$_2$(CN)][M(crown)]. In this formal cyanide adducts of ArPO$_2$ we discovered an unprecedented coordination isomerism between the CN and NC forms. The

thermodynamically favored isomer, the P−CN adduct, was determined experimentally and supported by DFT studies. Critically, this isomerism is the first documented at a P(V) center and was absent in sulfur-oxidized $[^{Dipp}TerPS_2(CN)]^-$ and mono-oxidized species, underscoring triplet oxygen's unique role. This phenomenon shows non-transition metal centered coordination versatility with potential applications in catalysis. Building on these findings, subsequent investigation explored cyanophosphide transfer via salt metathesis or base-assisted dehydrohalogenation with ECl_n (E = Ge, n = 2; E = P, As, n = 3).

For project (2), phosphafluorene (**22**) was synthesized via Mg reduction of aryldichlorophosphanes, resulting in a high-yielding route towards **22** and different quaternization strategies have been explored, including coordination to AuCl, BH_3 and sulfurization. The steric bulk of **22** prevented reaction with $B(C_6F_5)_3$, indicating a potential FLP-type system. This was exploited to achieve facile phosphafluorene alkenylation, yielding alkenylphosphonium borate derivatives. To the best our knowledge, this was the first report on FLP-type functionalization of dibenzophospholes, establishing a novel strategy to fine-tune electronics in this important class of compounds.

3.2 Coordination Isomerism in Cyanophosphide Crown Ether Salts

Our group previously reported the deprotonation of cyanophosphines ArP(H)CN (Ar = Mes*, ^{Mes}Ter and ^{Dipp}Ter **11**) with KHMDS to afford the corresponding cyanophopsphides [(ArPCN)K]. However, in contrast to the other variants, only [(^{Dipp}TerPCN)K] and [^{Dipp}TerPCN][K(2.2.2-crypt)] were found to be stable towards KCN elimination.[36] During my doctoral research, I explored the reactivity of cyanophosphines and their cyanophosphide salts, with a focus on ^{Dipp}TerP(H)CN (**11**). The synthesis of **11** was optimized via a scalable one-pot protocol, commencing from 1 g of ^{Dipp}Ter−P(PMe$_3$) (**20**) and employing *t*Bu−NC at 105 °C. At gram scale, an excess of isonitrile and pro-longed heating are required. The synthesis and structural diversity of alkali-metal-crown ether-stabilized cyanophosphide salts of the general formula [(^{Dipp}TerPCN)M(crown)] (M = Na, K; crown = 15-crown-5 or 18-crown-6), particularly in terms of their solid-state arrangements were investigated (Figure 1).

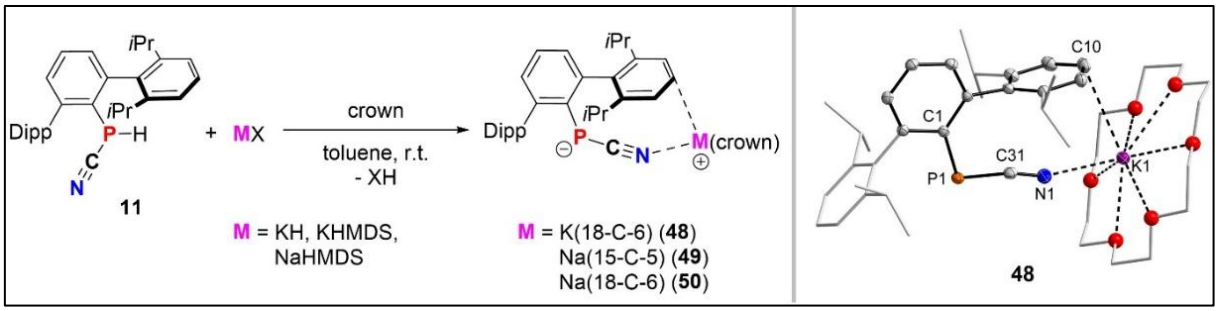

Figure 1. Synthesis of diverse cyanophosphide crown ether salts **48-50** (left) and molecular structure of (^{Dipp}TerPCN)K(18-c-6) **48** (right).

Compounds **48-50** were synthesized via the facile deprotonation of **11** with different alkali metal amides in the presence of crown ethers to afford yellow single crystalline compounds upon crystallization at −30 °C in moderate yields (Figure 1). Gas evolution was observed in the formation of compound **48**, since KH was used in the reaction instead of KHMDS to avoid HN(SiMe$_3$)$_2$ as a byproduct. The quantitative formation of **48-50** is confirmed by ^{1}H NMR spectroscopy in C_6D_6, where the absence of a P−H resonance and the appearance of a deshielded (with respect to **22**) ^{31}P NMR signal at *ca.* −128 ppm after 2 hours indicated the generation of contact ion pairs [(^{Dipp}TerPCN)M(crown)]. **48**, **49** and **50** crystallize in the triclinic space group $P\bar{1}$ (Figure 2). Notably, beside a monomeric ion pair, compound **49** revealed a rare dimeric ion pair structure in the solid state, indicating the significant influence of alkali metal and crown ether selection on supramolecular aggregation (Figure 2, top).

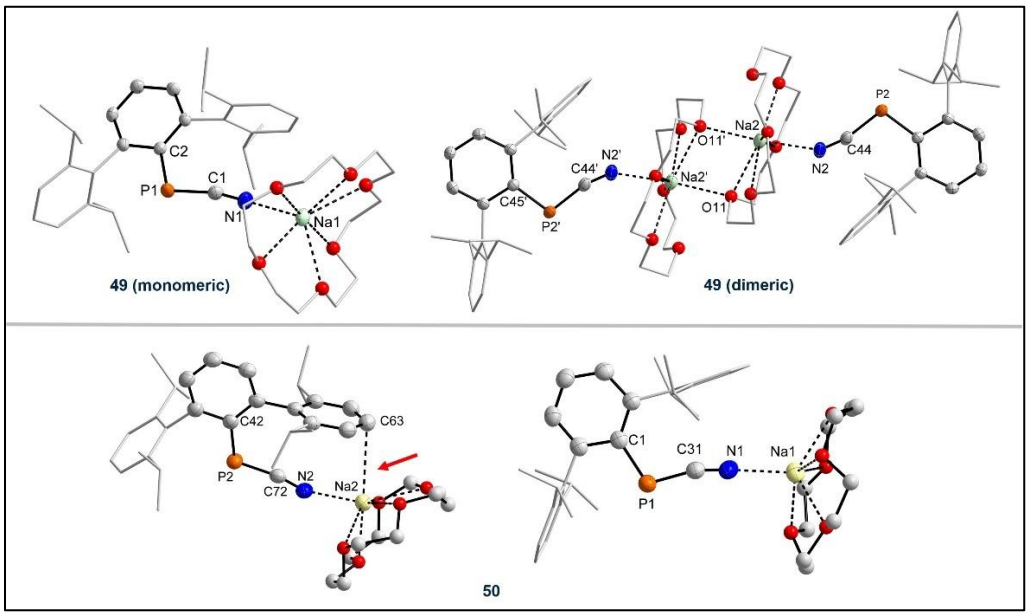

Figure 2. Structural variety in cyanophosphide salts **49** and **50**.

In contrast to [^{Dipp}TerPCN][K(2.2.2-crypt)],[36] all three compounds demonstrated a close interaction between the PCN nitrogen and the metal center (**48**: *d*(N1−K1) = 2.837(1); **49**: *d*(N−Na) = 2.387(2), 2.417(2); **50**: *d*(N−Na) = 2.321(2), 2.334(2) Å; cf. Σr_{vdW}(K−N) = 4.3; (Na−N) = 3.82 Å), along with substantial π-electron delocalization within the cyanophosphide moiety, as evidenced by spectroscopic and crystallographic data. Additionally, there are M−C_{arene} contacts within the sum of the van-der-Waals radii to one of the flanking Dipp-groups in **48** and in one of the independent ion pairs in **50**.[102] Aligned with the thesis objectives, the reactivity of cyanophosphide salts was studied towards oxidants such as O_2, elemental sulfur and N_2O. Facile oxidation with O_2 yields the dioxophosphorane cyanide adducts [^{Dipp}TerPO_2(CN)]$^-$ at moderate yields (Figure 3, top). Surprisingly, these dioxophosphorane species exhibiting an unexpected cyanide/isocyanide isomerism (Figure 3, bottom). In the ^{31}P NMR spectrum of isolated crystals of **48·O₂** and **49·O₂** in C_6D_6 two marginally separated singlets in a ratio of *ca*. 1:1 was detected at −9.0 and −9.3 ppm (**48·O₂**) or −8.5 and −9.3 ppm (**49·O₂**), respectively indicating a mixture of CN/NC isomers. This contrasts **50·O₂**, in which a splitting into two signals at −8.84 and −8.96 ppm was only observed at −30 °C via variable temperature ^{31}P(^{1}H) NMR experiments. Upon heating to 80 °C in toluene-d_8, all compounds clearly show the presence of only one species, which was shown to be the P−CN isomer. Furthermore, IR and Raman spectroscopy showed a low intensity mode at *ca*. 2080 cm^{-1} for the P–NC and a medium intensity mode for the P–CN unit at 2175 cm^{-1} (only in the Raman spectrum), in line with the theoretically predicted spectra. Spectroscopic analyses (particularly variable-temperature ^{31}P NMR and Raman spectroscopy) along with X-ray crystallography

confirmed the simultaneous presence of both isomers, with approximate ratios varying slightly depending on the metal-crown system. The isomerization was found to be reversible and thermally controlled, with the P–CN isomer being thermodynamically favored. DFT and DLPNO-CCSD(T) calculations revealed a significant stabilization energy (~26.5 kJ/mol) for the cyanide isomer, and a calculated isomerization barrier of ~100 kJ/mol, implicating the role of alkali metal ions in facilitating the rearrangement.

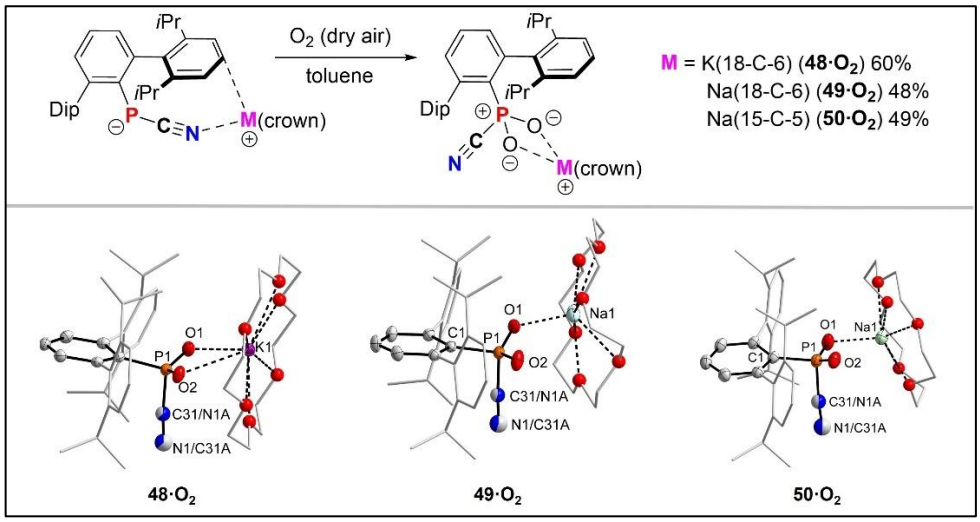

Figure 3. Synthesis of **48·O₂**, **49·O₂**, and **50·O₂** (top) and its molecular structure (bottom), with the disorder represented in the form of cake-diagram-type spheres.

In the solid state structures of $[^{Dipp}TerPO_2(CN)]^-$, the anion exhibits distinct cation interactions: **48·O₂** (K^+) shows two close K···O_P contacts, in, while **49·O₂** and **50·O₂** (Na^+) display only one Na···O_P interaction (Figure 3, bottom). Due to ambiguity in distinguishing the P–CN vs. P–NC bonding modes crystallographically, two structural models were refined for each compound. The P–NC isomer yielded marginally better R-values, but the best fit was achieved with modelling a CN/NC positional disorder, revealing mixed populations: 63:37 (**48·O₂**), 55:45 (**49·O₂**), and 51:49 (**50·O2**) P–NC:P–CN ratios (Figure 3, bottom). Natural Resonance Theory (NRT) and Wiberg Bond Index (WBI) analyses of model systems revealed that the P–CN isomer possesses a higher degree of covalent character and less polarization compared to the P–NC form, rationalizing the greater thermodynamic stability of the former. This formal coordination isomerism is assisted by the metal counterion and to the best of our knowledge the first report on CN isomerization at a P(V) center.

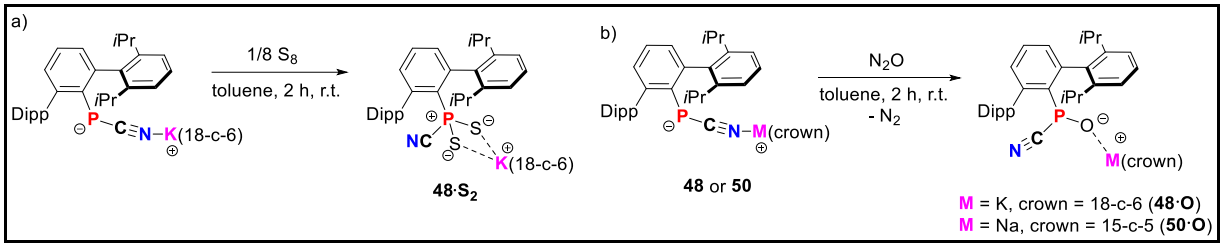

Scheme 20. Reaction of cyanophosphide salts with sulfur (a) and nitrous oxide (b).

Further exploration of the oxidative behavior demonstrated that the use of elemental sulfur (S_8) led exclusively to the dithiophosphorane cyanide adduct $[^{Dipp}TerPS_2(CN)]^-$ (**48 S2**), without any evidence of CN/NC isomerism, implicating a crucial role of triplet oxygen in the CN/NC isomerization process (Scheme 20 a). In contrast, treating the cyanide salts with N_2O (Scheme 20 b) produced anionic phosphinidene monoxide species $[^{Dipp}TerPO(CN)]^-$ (**48 O** and **50 O**), characterized by deshielded ^{31}P NMR resonances at *ca*. 81 ppm and indicative of a P^{III} oxidation state. These were the first examples of anionic phosphinidene monoxide cyanide adducts, representing a novel class of main-group species. The structural features, especially the elongated P–CN bond and pyramidal coordination around phosphorus, supported the assignment. Importantly, we proposed that the CN/NC isomerism occurs via an oxygen-mediated radical intermediate pathway, as supported by cyclic voltammetry (CV) data and the absence of isomerism during oxidation with singlet reagents like S_8 and N_2O.

3.3 Cyanophosphide Transfer Reaction

This paper builds upon previous work to further investigate the potential application of cyanophosphide compounds. Cyanophosphides represent an underexplored class of compounds, and their ambiphilic character has only recently been revealed.[103] This study demonstrates the utility of the stable cyanophosphide salt [^{Dipp}TerPCN]K as a cyanophosphide transfer reagent for synthesizing novel group 14/15 compounds in salt metathesis reactions. Crucially, [^{Dipp}TerPCN]K exhibited superior thermal stability with no significant KCN elimination at 80°C after 24 h, compared to less bulky analogs, enabling its use as a transfer reagent.[12, 82, 104]

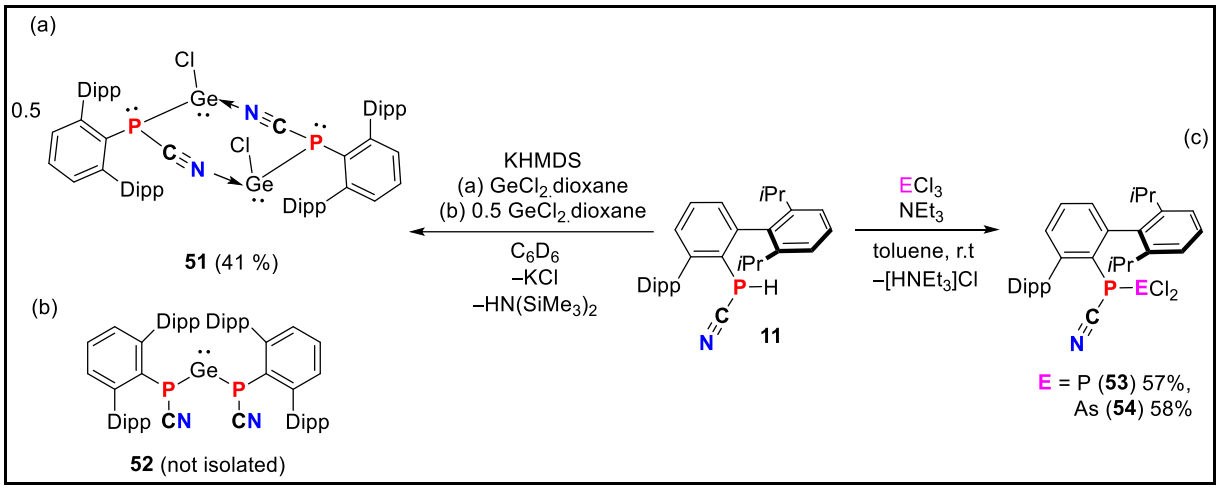

Scheme 21. Salt metathesis of **11** yielded **51** and **52** (a,b) and dehydrohalogenation of **11** with NEt_3 affrorded **53** and **54** (c).

Reaction with $GeCl_2$ (1 equiv.) yielded an unusual dimeric chlorogermylene, [^{Dipp}TerP(CN)GeCl]$_2$ (**51**) (Scheme 21 a), which was characterized by SC-XRD. This revealed an unprecedented 8-membered cyclic structure (Figure 4, left) stabilized by Ge−NCP contacts (Ge−N ~2.05 Å) (cf. Σr_{cov}(Ge−N) = 1.92 A)[15], with elongated, polarized P−Ge (2.54 Å) (cf. Σr_{cov}(Ge−P) = 1.92 A)[15] and Ge−N bonds indicating significant ionic character with minimal back-donation from Ge to the P−CN units, supported by NBO calculations and low Wiberg bond indices. The dimerization is highly exergonic ($\Delta_R G°$ = −136.9 kJ/mol). The ^{31}P NMR spectrum recorded after 1 h at ambient temperature showed a major species at −77.4 ppm with a minor component at −74.3 ppm, while the ^{1}H NMR spectrum showed that starting material **11** was fully consumed. Using 0.5 equivalents $GeCl_2$ generated the sensitive

diphosphanylgermylene [^{Dipp}TerP(CN)]$_2$Ge (**52**) in solution (δ(^{31}P) = −73.9 ppm) (Scheme 21 b), cf. [(*i*Pr$_3$Si)(FTipp$_2$Si)P]$_2$Ge δ(^{31}P) = −62.1 ppm).[105] Attempts to isolate **52** were unsuccessful due to its extreme sensitivity towards moisture. Thus, mainly ^{Dipp}TerP(H)CN was isolated.

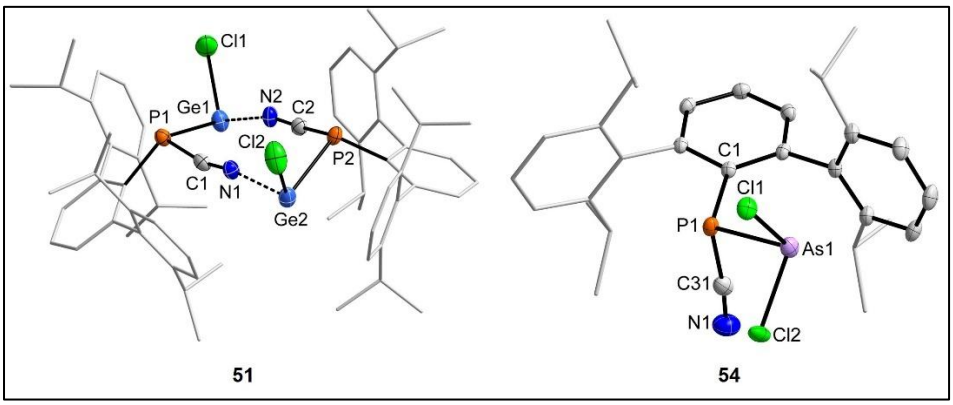

Figure 4. Molecular structure of dimeric chlorogermylene **51** (left) and arsaphosphane **54** (right).

For PCl$_3$ and AsCl$_3$, efficient cyanophosphide transfer via NEt$_3$-assisted dehydrohalogenation produced the diphosphane ^{DippTer}P(CN)PCl$_2$ **53** and arsaphosphane ^{DippTer}P(CN)AsCl$_2$ **54** (Scheme 21 c). Compound **54** was structurally characterized (Figure 4 right), showing a covalent P−As bond (2.3896(6) Å) and trigonal pyramidal geometries at the pnictogen atoms. NMR spectroscopy shows the presence of the second P atom in **53** which appears as a doublet of doublet (showing P-P coupling in ^{13}C NMR, δ (^{13}C) = 116.5 ppm; $^{1}J_{(PP)}$ = 86.6 Hz; $^{2}J_{(PP)}$ = 15.6 Hz), while only a doublet (δ (^{13}C) = 118.2 ppm; $^{1}J_{(PP)}$ = 95.6 Hz) is detected for **54**. This work expands the chemistry cyanophosphide species, accessing rare germylenes and novel pnictogen-phosphorus compounds.

3.4 P-Quaternization and FLP-type Alkenylation of a Phosphafluorene

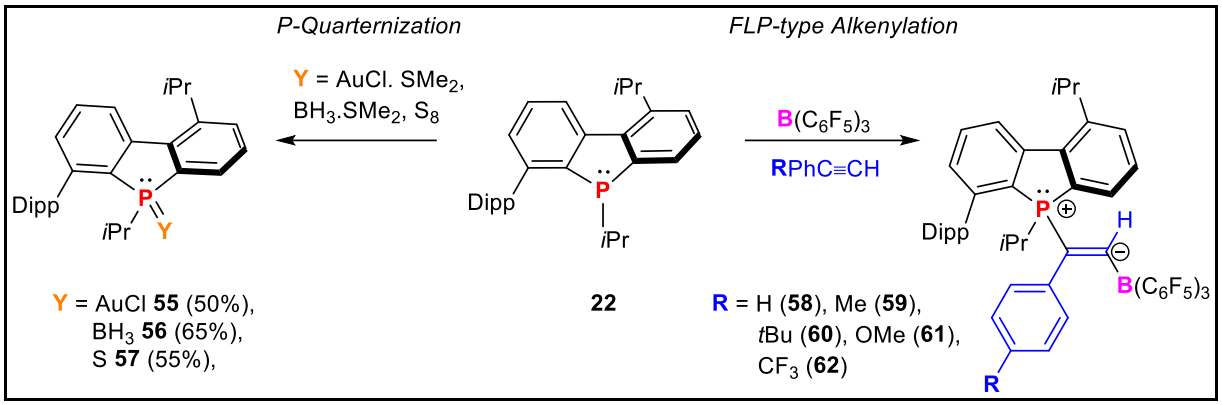

Scheme 22. P-Quaternization (left) and FLP-type alkenylation (right) of a phosphafluorene (**22**).

In this contribution, we have shown the synthesis and functionalization of phosphafluorene (**22**) (a dibenzophosphole, DBP), prepared in 77% yield ($\delta(^{31}P)$= −1.1 ppm) through magnesium-mediated reductive cyclization of readily accessible $^{Dipp}TerPCl_2$ with 2 equiv. of activated magnesium, Mg* (Scheme 15b). Functionalization strategies at the phosphorus center were explored and quarternization of **22** yielded three distinct products. Coordination to AuCl afforded complex **55** ($\delta(^{31}P)$ = 32.4 ppm) featuring a P−Au bond length of 2.2247(6) Å, consistent with known phosphole-Au complexes (Figure 5).[106] The reaction of **22** with $BH_3{\cdot}SMe_2$ gave adduct **56** ($\delta(^{31}P)$= 37.3 ppm, $\delta(^{11}B)$ = −38.4 ppm) which exhibits a P−B bond distance of 1.9269(16) Å, within the range of reported dibenzophosphole-BH_3 adducts.[107] IR spectroscopy confirmed BH_3 coordination with characteristic B−H stretching modes at ~2345 cm-1.[108] Treatment with S_8 produced thiophosphafluorene (**57**) ($\delta(^{31}P)$= 53.4 ppm), showing significant deshielding of the ^{31}P NMR signal consistent with P=S bond formation (Scheme 22, left). X-ray crystallography revealed contracted P−C bonds in **55** and **56** compared to related free phosphafluorenes, consistent with an increased coordination number at phosphorus (Figure 5). Interestingly, combining **22** with $B(C_6F_5)_3$ showed no reaction, indicating frustrated Lewis pair (FLP) formation due to steric hindrance. However, upon addition of terminal phenylacetylenes (R−C_6H_4−C≡CH; R = H, CH_3, *t*Bu, OMe, CF_3), clean and *E*-selective 1,2-addition occurred, generating zwitterionic (*E*)-alkenyl phosphonium borates (**58-62**) in good yields (Scheme 22, right).

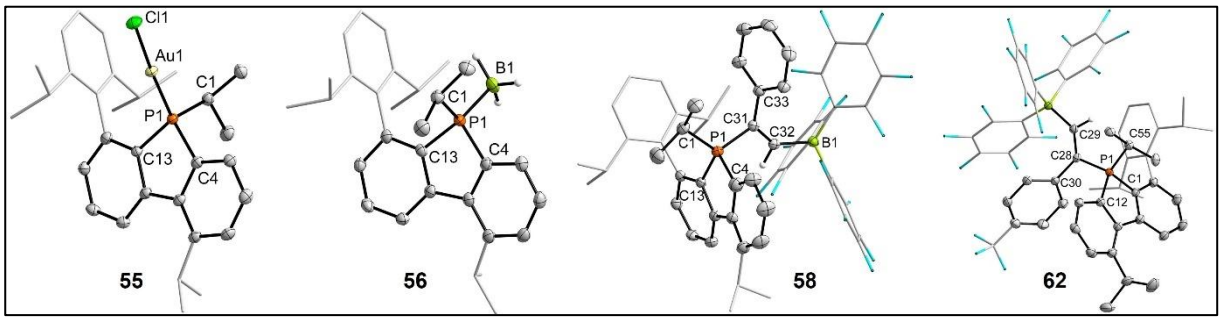

Figure 5. Molecular structures of **55**, **56**, **58** and **62**. Ellipsoids drawn at 50 % with C–H-atoms omitted (except those at C32 (**58**) and C29(**62**)), Dipp-, C_6F_5-, CF_3-, and one of the *i*Pr-groups rendered as wire-frame for clarity.

The process was diastereo-selective, furnishing *E*-configured products with boron adding to the terminal CH group. NMR characterization confirmed the products (**58-62**), showing diagnostic signals for the phosphonium center ($\delta(^{31}P) \approx 36$ ppm), the tetracoordinate boron atoms ($\delta(^{11}B) \approx -15.0$ to -15.4 ppm, d, $J_{P\text{-}B} \approx 18$ Hz), and the alkenyl C=CH proton ($\delta(^{1}H) \approx 7.84\text{-}8.0$ ppm, d, $J_{P\text{-}H} \approx 38$ Hz). SC-XRD experiments of **58** and **62** clearly confirmed the *E*-configuration with boron attached to the alkyne's CH terminus and phosphorus to the CR carbon, alongside activated C=C bonds (~1.34 Å) (Figure 5). The reaction scope demonstrated minimal electronic influence from *para*-substituents in the phenyl acetylenes (EDG/EWG) on the outcome (Scheme 23) or spectroscopic properties, highlighting the robustness of the FLP system.

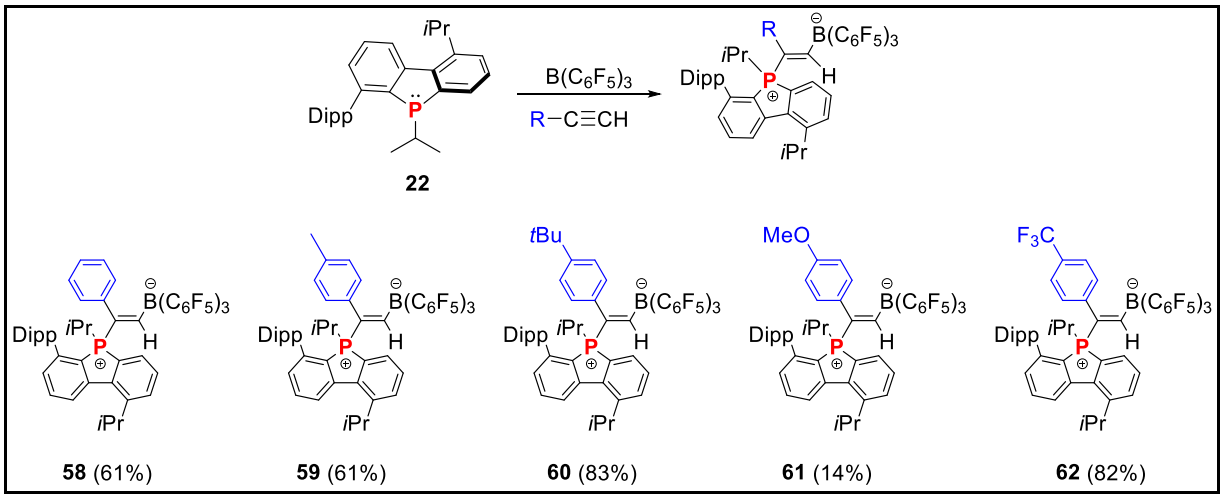

Scheme 23. Reactivity of phosphafluorene (**22**) towards $B(C_6F_5)_3$ in the presence of phenylacetylene derivatives, resulting alkenyl phosphonium borates (**58-62**).

These results present the first example of FLP-type reactivity using a DBP-type phosphorus heterocycle and offer a new avenue for the functionalization of π-conjugated systems. The integration of FLP behaviour with phosphorus heterocycles opens the door for future applications in bond activation, ligand design, and optoelectronic materials.

4 Conclusion

This thesis demonstrates that low-valent phosphorus chemistry provides a rich platform for advancing our understanding of bonding, reactivity, and functional group transfer in main-group systems. Through systematic investigation of the [^{Dipp}TerPCN]$^-$ cyanophosphide anion and ^{Dipp}Ter-derived phosphafluorenes, several key findings emerge that contribute to the growing field of P(I) and P-heterocycle chemistry.

Firstly, the landmark discovery of coordination isomerism in dioxophosphorane cyanides highlights the remarkable structural flexibility of phosphorus compounds. The ability to control and observe reversible isomerization between P−CN and P−NC isomers in phosphorus(V) compounds opens potential avenues in catalysis and the design of functional materials. The findings also contribute to understanding oxidation-state manipulation in phosphorus chemistry, emphasizing the importance of ligand effects and secondary coordination sphere interactions in directing structure and reactivity. This work also emphasizes the importance of radical-mediated processes in achieving such rearrangements and points toward future opportunities in designing isomer-switchable ligands or stimuli-responsive materials.

Secondly, the reactivity of [^{Dipp}TerPCN]$^-$ as a cyanophosphide transfer reagent has been successfully established. Salt metathesis and dehydrohalogenation reactions with $GeCl_2$, PCl_3, and $AsCl_3$ produced a series of structurally diverse P−E bonded species, including chlorogermylene dimers, diphosphanylgermylenes, and group 15 heteroatomic dipnictanes. These results show that cyanophosphide anions are capable of selective and efficient phosphorus transfer, supporting their broader application in constructing complex main-group element architectures.

Thirdly, the FLP-type functionalization of a ^{Dipp}Ter-phosphafluorene reveals a new application of dibenzophosphole scaffolds. The successful activation of terminal arylacetylenes in the presence of $B(C_6F_5)_3$ illustrates the versatility of these heterocycles as Lewis bases in frustrated Lewis pair chemistry. The formation of zwitterionic alkenyl phosphonium borates in an *E*-selective fashion, across a broad range of substituted alkynes, highlights the synthetic potential of phosphafluorene derivatives for targeted functionalization and materials design.

Collectively, these studies not only showcase the multifaceted reactivity of low-valent phosphorus compounds but also provide a foundation for their future applications in

coordination chemistry, ligand development, and small molecule activation. The combination of experimental and theoretical approaches throughout this thesis ensures that the insights gained here can guide future synthetic endeavors and expand the chemical utility of phosphorus-based platforms.

5 Contribution of Work

The following chapter contains the original papers in which the presented results were published. The own contribution of the author of the dissertation to each publication is highlighted separately.

In paper 6.1, the work I undertook is carried out large part of the experiments and analyzed most of the characterization data. In addition, the supporting information corresponding to the paper was written by me. My contribution: 70 %.

In paper 6.2, the work I undertook is carrying out the experiments and analyzing the characterization data. In addition, the supporting information corresponding to the paper was written by me and I was involved in writing co-edited the manuscript. My contribution: 80 %.

In paper 6.3, the work I undertook is carried out all the experimental work, wrote the supporting information and drafted the manuscript. My contribution: 80 %.

6 List of Publications

6.1 Coordination Isomerism in Dioxophosphorane Cyanide

Ayu Afiqah Nasrullah, Edgar Zander, Fabian Dankert, Andrey Petrov, Jonas Surkau, Eszter Baráth and Christian Hering-Junghans

Chem. Sci., **2025**, *16*, 6909−6917

DOI: 10.1039/d4sc07636b

Published: 13th March 2025

Contribution to this paper is 70%.

Chemical Science

ROYAL SOCIETY OF CHEMISTRY

EDGE ARTICLE

View Article Online
View Journal | View Issue

Check for updates

Cite this: *Chem. Sci.*, 2025, **16**, 6909

All publication charges for this article have been paid for by the Royal Society of Chemistry

Received 11th November 2024
Accepted 8th March 2025

DOI: 10.1039/d4sc07636b

rsc.li/chemical-science

Coordination isomerism in dioxophosphorane cyanides†

Ayu Afiqah Nasrullah,[ab] Edgar Zander,[a] Fabian Dankert,[c] Andrey Petrov,[a] Jonas Surkau,[d] Eszter Baráth *[a] and Christian Hering-Junghans *[a]

The 1,3-phosphaazaallene ^{Dipp}TerP = C=N*t*Bu (^{Dipp}Ter = 2,6-(2,6-i$Pr_2C_6H_3$)$_2$–C_6H_3) is thermally labile towards iso-butene elimination and formation of the corresponding cyanophosphine ^{Dipp}TerP(H)CN (**1**). In previous work we have shown facile deprotonation of **1** with K[N(SiMe_3)$_2$] and formation of cyanophosphide [(^{Dipp}TerPCN)K]. We now present the alkali metal tethered cyanophosphides [(^{Dipp}TerPCN)M(crown)] (M = Na, K; crown = 15-c-5, 18-c-6) and their structural diversity in the solid state depending on the metal (M) and the crown ether. Facile oxidation of [^{Dipp}TerPCN][M(crown)] with O_2 yields the formal cyanide adducts of dioxophosphoranes [^{Dipp}TerPO_2(CN)]$^-$. Surprisingly, [^{Dipp}TerPO_2(CN)]$^-$ is obtained as a mixture of the cyanide and isocyanide isomers, indicating a coordination isomerism. This phenomenon is corroborated by experimental and theoretical studies revealing the cyanide isomer to be thermodynamically more stable. The oxidation with elemental sulphur gave the corresponding dithiophosphorane cyanide adduct [^{Dipp}TerPS_2(CN)]$^-$, in which no isomerism was observed. This points to a crucial role of triplet oxygen in the isomerisation process. Monooxidation occurs when [^{Dipp}TerPO_2(CN)]$^-$ salts were treated with N_2O, giving formal anionic phoshinidene monoxide adducts.

Introduction

Aryl-substituted dioxophosphoranes (Ar–PO_2) are the formal heavier analogues of nitroarenes, with a highly electrophilic phosphorus atom. Therefore, R–PO_2 undergoes immediate self-aggregation to give cyclic dimers, trimers or linear oligomers.[1,2] UV-irradiation (λ = 254 nm) of arylphosphiranes Ar–P(C_2H_4) (Ar = Ph,[3] Mes[4]) in a solid argon matrix afforded the phosphinidenes Ar–P in their triplet ground-state (Scheme 1(i)). Subsequent reaction of Ar–P with molecular oxygen ($^3O_2$) at 10 K under irradiation gives phenyldioxophosphorane PhPO_2. The formation of Ph–PO_2 is expected to proceed through a triplet diradical/zwitterionic intermediate with a terminal Ph–P=$O^{(+)}$–$O^{(-)}$ unit, which then rearranges to give cyclic 3-phenyl-1,3,2-dioxophosphorane and eventually Ph–PO_2.[3] In this regard the mechanism may involve triplet–singlet curve crossings, which can only be addressed by sophisticated excited state computations. Considering the extreme electrophilicity of dioxophosphoranes, it is not surprising that mainly Lewis base adducts of R–PO_2 have been reported.

Lewis-base stabilized species include the parent compound HPO_2 which was isolated as its carbodiphosphorane adduct. The phosphinidene H–P is not an intermediate in this case, though.[5] The exposure of NHC phosphinidene Ar–P(NHC) adducts (NHC = N-heterocyclic carbene) to dry air yields the corresponding dioxophosporane NHC adducts of the type R–PO_2(NHC) (Scheme 1(ii)).[6–8] A cyclic phosphine-stabilized amino-dioxophosphorane was synthesized in similar fashion.[9] The OPMe_3 adduct of ^{Dipp}TerPO_2 [^{Dipp}TerPO_2(OPMe_3)] (^{Dipp}Ter = 2,6-(2,6-i$Pr_2C_6H_2$)–C_6H_3) was recently reported, as an unexpected product in the reaction of ^{Dipp}TerP(PMe_3) with SO_2.[10] The dimer of ^{Dipp}TerPO_2, [^{Dipp}TerPO_2]$_2$,[11] was afforded by thermal C_2H_4 liberation from ^{Dipp}TerP(OCH_2)$_2$ or by the addition of catalytic amounts of pyridine or DMAP (DMAP = 4-dimethylaminopyridine) as a Lewis base (Scheme 1(iii)). Cyclic triphosphonates (PO_2)$_3$, the trimers of the corresponding dioxophosphoranes, give an equilibrium mixture with DMAP in $CDCl_3$ containing the trimer and the PO_2(DMAP) adduct, substantiating ligand lability in R–PO_2 base adducts (Scheme 1(iv)).[12]

Our group has recently shown that deprotonation of the cyanophosphines ArP(H)CN (Ar = Mes*, 2,4,6-*t*Bu_3-C_6H_2; ^{Mes}Ter, 2,6-(2,4,6-$Me_3C_6H_2$)–C_6H_3; ^{Dipp}Ter) with K[N(SiMe_3)$_2$]

[a]*Leibniz Institut für Katalyse e.V. (LIKAT), A.-Einstein-Str. 29a, 18059 Rostock, Germany. E-mail: christian.hering-junghans@catalysis.de; eszter.barath@catalysis.de*
[b]*Pusat Persediaan Sains dan Teknologi, Universiti Malaysia Sabah, Jln UMS, 88400 Kota Kinabalu, Sabah, Malaysia*
[c]*Universität Kassel, Institut für Chemie, Heinrich-Plett-Straße 40, 34132 Kassel, Germany*
[d]*Institut für Chemie, Universität Rostock, Albert-Einstein-Straße 3a, 18059 Rostock, Germany*

† Electronic supplementary information (ESI) available: Synthesis and characterization of compounds, NMR spectra, crystallographic, and computational details. CCDC 2401210–2401215, 2427595 and 2427596. For ESI and crystallographic data in CIF or other electronic format see DOI: https://doi.org/10.1039/d4sc07636b

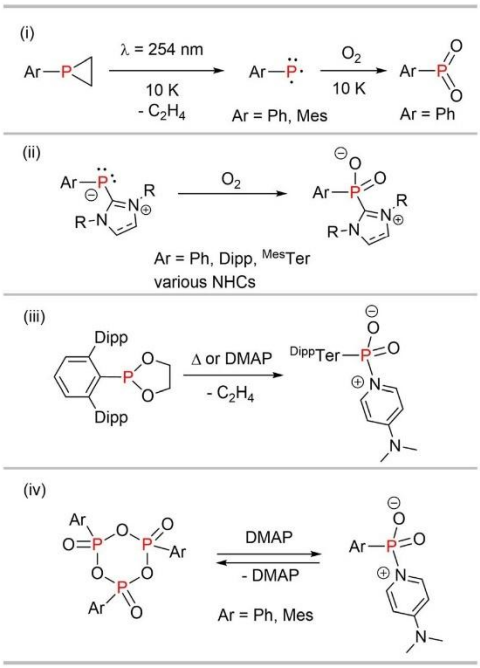

Scheme 1 (i) Generation of phosphinidenes and dioxophosphoranes in Ar matrices. (ii) Synthesis of NHC dioxophosphorane adducts. (iii) DMAP-induced ethylene elimination to access ^{Dipp}TerPO$_2$(DMAP). (iv) Reversible DMAP coordination at dioxophosphoranes.

(KHMDS) afforded the cyanophosphides [(ArPCN)K].[13] Even though [(Mes*PCN)K] ($\delta(^{31}P) = -146.2$ ppm) could be generated in solution, thermal KCN elimination occurred within 16 h at ambient temperature, to give a phosphaindane (**A**, Scheme 2) as the main product, a decomposition product of the free phosphinidene Mes*-P.[14] ^{Mes}TerP(H)CN reacted similarly when treated with 1 eq. of KHMDS, to give after KCN elimination the diphosphene (^{Mes}TerP)$_2$ (**B**, Scheme 2).[15] By contrast [(^{Dipp}TerPCN)K], with a characteristic ^{31}P NMR signal at −142 ppm and [^{Dipp}TerPCN][K(2.2.2-crypt)] were found to be stable towards KCN elimination. It can thus be concluded that [Ar–P(CN)]$^-$ are formal cyanide adducts of phosphinidenes and that air oxidation of the stable [(^{Dipp}TerPCN)K] might result in the formation of the corresponding dioxophosphorane cyanide adducts.

In this contribution we report on a series of alkali metal tethered cyanophosphide [(^{Dipp}TerPCN)M(crown)] (M = Na, K; crown = 18-crown-6, 15-crown-5) salts and outline their structural diversity in the solid state. In addition, the selective double oxidation of the phosphorus atoms in the cyanophosphides with $^3O_2$ is described, giving formal cyanide adducts of dioxophosphoranes. In the case of [^{Dipp}TerP(O$_2$)CN][M(crown)] a nitrile/isonitrile coordination isomerism is observed, a phenomenon that is rare in main group chemistry. By contrast when using S_8 as an oxidant only the dithiophosphorane cyanide adduct is detected, while with N_2O oxygen atom transfer results in the cyanide phosphinidene oxide adducts.

Results & discussion

Structural variety in cyanophosphide salts

First, the synthesis of the cyanophoshine ^{Dipp}TerP(H)CN (**1**) was optimized and was performed on a gram-scale (Scheme 3, top).‡ The combination of ^{Dipp}TerP(PMe$_3$) with three equivalents *t*Bu-NC in toluene and heating to 105 °C for 90 h afforded **1** ($\delta(^{31}P\{^1H\}) = -120.4$ ppm in C_6D_6) as an off-white powder in 84% yield (*cf.* ESI† p. S16 ff.). On a larger scale an excess of the isonitrile and pro-longed heating is required. We first drew our attention towards the stability of [^{Dipp}TerPCN]$^-$ with respect to the alkali metal ion and different crown ethers. Therefore, the

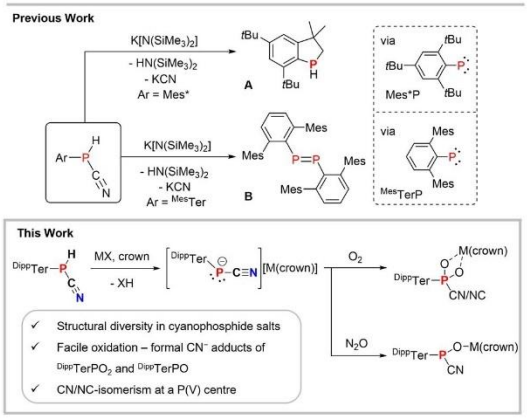

Scheme 2 Cyanophosphines as sources of phosphinidenes and summary of this work.

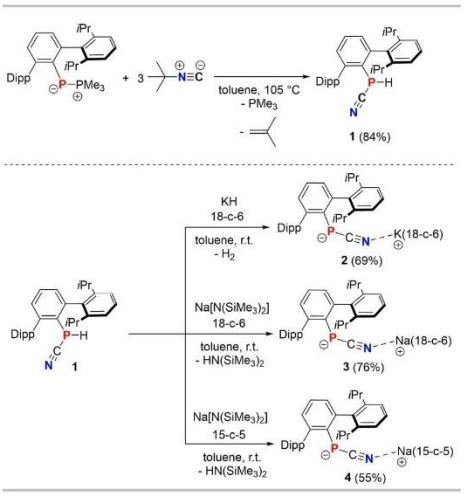

Scheme 3 Optimized synthesis of **1** and syntheses of cyanophosphide salts **2**–**4**.

View Article Online
Edge Article Chemical Science

Table 1 Selected bond lengths [Å], angles [°] of **2**, **3** and **4** and ^{31}P NMR shifts as well as characteristic IR band for the PCN unit. * Shown in Fig. 1

Compound	P–C_{CN}	C_{CN}–N	N–M	P–C_{CN}–N	C_{Ar}–P–C_{CN}	$\delta(^{31}P)$ [ppm]	$\tilde{\nu}$ (PCN) [cm^{-1}]
2 (M = K)	1.770(1)	1.163(2)	2.837(1)	168.6(1)	104.17(5)	−127.2	2045
3[a] (M = Na)	1.767(2)	1.164(3)	2.388(2)	166.4(2)	106.36(8)	−129.3	2049
	1.762(2)*	1.160(3)*	2.417(2)*	165.7(2)*	105.29(8)*		
4[a] (M = Na)	1.752(2)*	1.159(2)*	2.321(2)*	165.5(1)*	106.85(7)*	−129.9	2059
	1.757(2)	1.157(2)	2.334(2)	169.0(2)	104.00(7)		

[a] Two independent molecules in the asymmetric unit.

cyanophosphide species [(^{Dipp}TerPCN)M(L)] (M = K, Na; L = 18-c-6, 15-c-5) were synthesized and comprehensively characterized (Scheme 3, bottom). Deprotonation of **1** with KH, instead of KHMDS, in the presence of 18-c-6 in toluene was accompanied by gas evolution to give a yellow solution. Using KH can be viewed as an alternative base when HN(SiMe$_3$)$_2$ as a byproduct needs to be avoided. A similar color change to yellow is observed when Na[N(SiMe$_3$)$_2$] is used as a base, irrespective of whether 15-c-5 or 18-c-6 is utilized.

The formation of the cyanophosphide salts is indicated in the ^{1}H NMR spectra in C_6D_6 after 2 h by the absence of a PH unit and minimally shielded ^{31}P NMR signals at *ca.* −128 ppm (Table 1). This is indicative of the quantitative formation of the contact ion pairs [(^{Dipp}TerPCN)M(crown)] (**2**, M = K, crown = 18-c-6; **3**, M = Na, crown = 18-c-6; **4**, M = Na, crown = 15-c-5). After recrystallization from toluene at −30 °C, yellow single crystals suitable for SC-XRD experiments of all species were afforded in moderate isolated yields.

2, **3** and **4** crystallize in the triclinic space group $P\bar{1}$ (Fig. 1, *cf.* Fig. S3 and S4†) with varying amounts of toluene in the unit cell. In the solid state there is a structural variety, which will be outlined in the following. In contrast to [^{Dipp}TerPCN][K(2.2.2-crypt)],[13] the N atom of the PCN unit in **2** (Fig. 1, left), **3** (Fig. 1, middle) and **4** (Fig. 1, right) shows a rather close contact to the alkali metal ion in the [M(crown)]$^+$ fragment (**2**: *d*(N1–K1) = 2.837(1); **3**: *d*(N–Na) = 2.387(2), 2.417(2); **4**: *d*(N–Na) = 2.321(2), 2.334(2) Å; *cf.* Σr_{vdW}(K–N) = 4.3; (Na–N) = 3.82 Å). Additionally, there are M–C_{arene} contacts within the sum of the van-der-Waals radii to one of the flanking Dipp groups in **2** (*d*(K1–C10) = 3.464; Σr_{vdW}(K–C) = 4.45 Å) and in one of the independent ion pairs in **4** (*d*(Na2–C63) = 3.106(2) Å; Σr_{vdW}(Na–C) = 3.97 Å).[16] The P–C_{CN} and C_{CN}–N atomic distances (Table 1) correspond to contracted P–C single (*cf.* Σr_{cov}(P–C) = 1.86 Å), and slightly longer C≡N triple bonds (*cf.* Σr_{cov}(C–N) = 1.14 Å), respectively.[17] The P–C_{CN}–N (*ca.* 165°) and C_{Ar}–P–C_{CN} angles (*ca.* 105°) are generally wider when compared to the previously reported [K(2.2.2-crypt)]$^+$ salt.[13] Overall, the [^{Dipp}TerPCN]$^-$ unit closely resembles the isoelectronic ^{Dipp}TerPCO (d(P–C_{CO}) = 1.683(1), *d*(C–O) = 1.156(1) Å),[18] and the CN stretching frequency of *ca.* 2050 cm^{-1} (Table 1) indicates substantial π-electron delocalization in the cyanophosphide unit. Interestingly, in **3** beside a monomeric [(^{Dipp}TerPCN)Na(18-c-6)] ion pair, a dimeric [(^{Dipp}TerPCN)Na(18-c-6)]$_2$ unit was found. The centrosymmetric dimer (Fig. 1, middle), in which the 18-c-6 molecule occupies the equatorial plane of a distorted hexagonal bipyramid around the sodium ions, is formed through coordination of one of the 18-c-6 oxygen atoms to the second sodium, while the second axial position of each sodium in the dimer is occupied by the cyanide N atoms (*d*(N2–Na2 = 2.4172(18) Å; *d*(O11–Na2) = 2.609(3) Å). There are only few examples of dimeric [Na(18-c-6)]$_2^{2+}$ ion pairs,[19,20] and the coordination mode is reminiscent to the one found in [(18-c-6)$_2$Na$_2$(H$_2$O)$_2$]$_{0.5}$[Cd(SCN)$_3$].[21]

It can thus be concluded that the alkali metal ion and the crown ether marginally influence the structure in solution, as indicated by similar NMR data. In the solid state though, significant differences are observed, which can be attributed to packing in the crystal and weak interactions of the alkali metal ion and the flanking ^{Dipp}Ter groups.

Dioxophosphorane cyanide adducts

An initial attempt to crystallize **4** from toluene in the freezer afforded besides yellow microcrystalline material, colorless

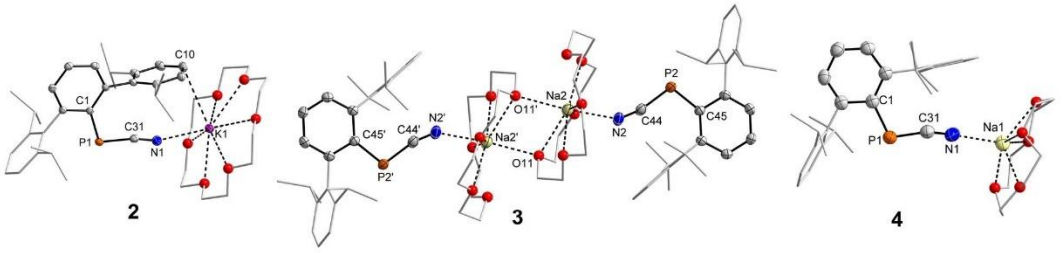

Fig. 1 Molecular structures of **2**, **3** (one of two ion pairs in the asymmetric unit (AsU), ′ symmetry generated: 1 − *x*, 1 − *y*, 1 − *z*) and **4** (one ion pair of two in the AsU). Hydrogen atoms omitted for clarity. Dipp groups shown with mixed wireframe/thermal ellipsoid representations. The iPr-groups and ethylene bridges in the crown ethers are rendered as wireframes. Oxygen atoms rendered as spheres with arbitrary radius. All thermal ellipsoids are drawn at the 50% probability level. Selected bond lengths and angles are shown in Table 1.

View Article Online
Chemical Science Edge Article

blocks suitable for SC-XRD experiments. These were identified as the oxidation product [^{Dipp}TerPO$_2$(CN)][Na(15-c-5)] (**4·O$_2$**).

^{31}P NMR data recorded from the few isolated crystals of **4·O$_2$** showed a signal at −8.3 ppm, in line with those reported for other ArPO$_2$(LB) species (*cf.* PhPO$_2$(dmap) $\delta(^{31}P) = 9.4$ ppm).[12] Concluding that traces of O$_2$ affected the formation of **4·O$_2$**, akin to previous reports on NHC phosphinidene adducts,[6] mixtures of **1**, base and the respective crown ethers were properly degassed and reacted with 1 atm of dry air (Fig. 2, top).

After an initial color change to deep purple in all cases, the solution turned pale-yellow and ^{31}P NMR spectroscopy of the reaction mixtures revealed the quantitative formation of **2·O$_2$**, **3·O$_2$** and **4·O$_2$**. After recrystallization from toluene the compounds were isolated as colorless crystalline solids in moderate yields (Fig. 2, top). In the IR spectrum of isolated **2·O$_2$**, **3·O$_2$** and **4·O$_2$** the CN stretching frequency at *ca.* 2080 cm^{-1} raised the question whether these compounds are the isocyanide adducts with a P–N≡C, rather than with a P–C≡N connectivity. Geometry optimizations and frequency analyses at the PBE0-D3/def2-SVP DFT level of theory, suggested that the mode at *ca.* 2080 cm^{-1} corresponds to the isocyanide-form ($\tilde{\nu}_{PNC,calc.} \approx 2100$ cm^{-1}). Moreover, the calculated IR spectra of the P–C≡N isomers showed that the C–N stretching modes ($\tilde{\nu}_{PCN,calc.} \approx 2210$ cm^{-1}) are of low intensity and should not be detected in the IR spectrum (*cf.* IR spectrum of **4·O$_2$** Fig. 2, bottom), in line with the experimental findings. Consequently, the isolated crystals of **2·O$_2$**, **3·O$_2$** and **4·O$_2$** were also investigated by Raman spectroscopy using a 633 nm red laser. This clearly showed a low intensity mode at *ca.* 2080 cm^{-1} for the P–NC and a medium intensity mode for the P–CN unit at 2175 cm^{-1} (*cf.* **4·O$_2$**, Fig. 2, bottom), in line with the theoretically predicted Raman spectra of [^{Dipp}TerPO$_2$(NC)][M(crown)] and [^{Dipp}TerPO$_2$(CN)][M(crown)], respectively. In the ^{31}P NMR spectrum of isolated crystals of **2·O$_2$** and **3·O$_2$** in C$_6$D$_6$ two marginally separated singlets in a ratio of *ca.* 1 : 1 are detected at −9.0 and −9.3 ppm (**2·O$_2$**) (*cf.* Fig. S24†) or −8.5 and −9.3 ppm (**3·O$_2$**) (*cf.* Fig. S40†), respectively. The presence of both isomers is further indicated by a splitting of the signals for the ^{Dipp}Ter-moiety in the ^{1}H and ^{13}C NMR spectra, which despite only one ^{31}P NMR signal is also observed in **4·O$_2$**. Variable temperature ^{31}P{^{1}H} NMR experiments of **4·O$_2$** in toluene-d$_8$ between −30 and 80 °C clearly show the presence of two species at −30 °C at −8.84 and −8.96 ppm in a nearly 1 : 1 ratio. Coalescence of the two signals is observed at 30 °C accompanied with a gradual downfield-shift of the signal to −8.25 ppm at 80 °C (Fig. S50†). This combined analytical evidence indicates a coordination isomerism at a dioxophosphorane in **2·O$_2$**, **3·O$_2$** and **4·O$_2$**. We thus conclude that upon oxidation of the P atom the CN$^-$ substituent (coordinated to [M(crown)]$^+$) can undergo a CN/NC isomerism giving **2·O$_2$**, **3·O$_2$** and **4·O$_2$** as a mixture of isomers.

2·O$_2$, **3·O$_2$** and **4·O$_2$** all crystallize in the triclinic spacegroup $P\bar{1}$, as their toluene solvates. In all molecular structures the [^{Dipp}TerPO$_2$(CN)]$^-$ anion interacts strongly with the [K(18-c-6)]$^+$ counter-cation through two close K···O$_P$ contacts in **2·O$_2$**, whereas in **3·O$_2$** and **4·O$_2$** only one close Na···O$_P$ contact is detected (Fig. 3). It is difficult to distinguish between the P–CN and P–NC coordination mode in the solid state. Therefore, two structural models were tested in all three cases: (a) with a P–NC unit; (b) with a P–CN unit. The quality of each model was judged by the R_1 and wR_2 values (*cf.* ESI† p. S11), as well as by inspection of the anisotropic displacement parameters (Fig. 3). In both cases the best *R*-values are obtained for the P–NC isomer, however with large displacement parameters for the N atom, which indicates an underlying disorder. This disorder was modelled and revealed approximate 63 : 37 (**2·O$_2$**), 55 : 45 (**3·O$_2$**) and 51 : 49 (**4·O$_2$**) ratios between the P–NC and P–CN form, respectively. This is in line with the observations by ^{31}P NMR and vibrational spectroscopy, *vide supra*.

Next, isolated crystals of **2·O$_2$** and **3·O$_2$**, with an apparent CN/NC isomer mixture, were re-dissolved in C$_6$D$_6$ and heated to 80 °C overnight and the ^{31}P NMR spectra after cooling to room temperature clearly showed only one singlet resonance at −9.3 ppm in both cases, while only one set of signals for the Dipp groups were observed in the ^{1}H and ^{13}C NMR spectra (*cf.* Section 4.4.1 and 4.6.1 of the ESI†). After recrystallization from toluene, Raman spectroscopy only revealed a medium intensity mode at 2175 (**2·O$_2$**, Fig. S28†) or 2176 cm^{-1} (**3·O$_2$**, Fig. S45†), respectively, while no modes were detected in the IR spectra, which is in line with the P–CN isomers.

It can therefore be concluded that the PO$_2$(CN) isomer corresponds to the species with the slightly more shielded ^{31}P NMR signal in the isomer mixture. When a solid sample of **2·O$_2$** is heated to 110 °C for 16 h and is re-dissolved afterwards in C$_6$D$_6$, only the P–CN isomer with an ^{31}P NMR shift of −9.3 ppm is detected (*cf.* Fig. S27†), further corroborated by a ^{13}C NMR signal for the P–CN unit at 124.1 ppm ($^1J_{CP} = 91$ Hz).

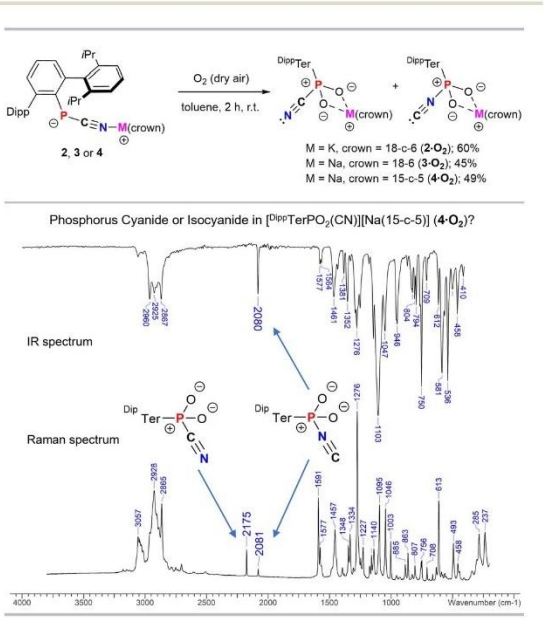

Fig. 2 Synthesis of **2·O$_2$**, **3·O$_2$** and **4·O$_2$** (top) and depiction of the IR- and Raman spectra of **4·O$_2$**.

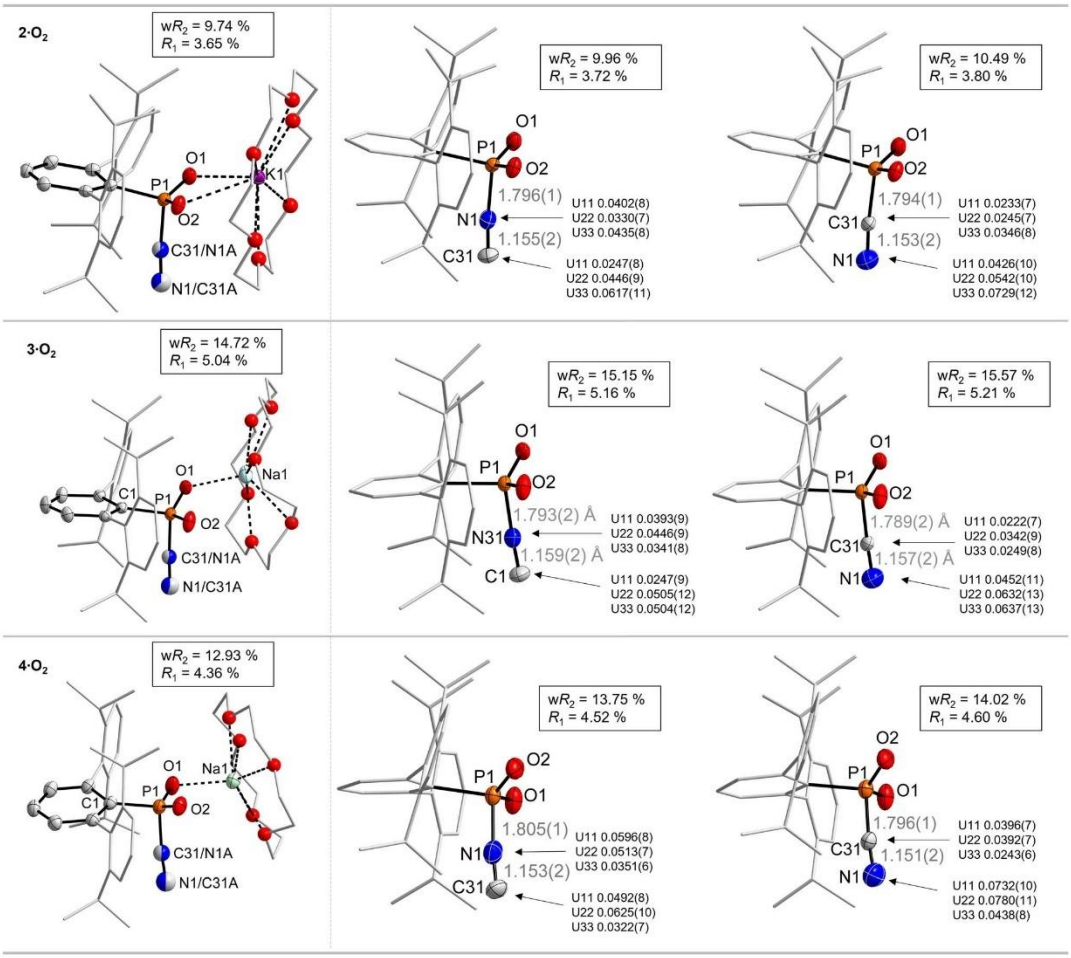

Fig. 3 Molecular structure of $2\cdot O_2$, $3\cdot O_2$ and $4\cdot O_2$ (left), with the disorder represented in the form of cake-diagram-type spheres. ORTEP representations (50% probability) of the respective NC- and CN-isomers of $2\cdot O_2$, $3\cdot O_2$ and $4\cdot O_2$ with refinement and anisotropic displacement parameters for each isomer. For crystallographic details also see the ESI.†

Based on experimental evidence this pointed to the P–CN isomer being thermodynamically favored over the P–NC isomer.

The observed isomerization and crystallization of both isomers in the same crystalline matrix raised the question whether **2** could be oxidized in the solid state when exposed to dry O_2 and if isomerization may occur in the crystalline matrix of **2**. Large accessible voids in the solid-state structure should allow diffusion of O_2 into the crystal lattice. When yellow single crystals of **2** were exposed to O_2 while being agitated with a stir bar, a color change to light purple was observed in the first 10 minutes.

The purple color then quickly faded and the solid turned into an off-white powder, which, when re-dissolved in C_6D_6, clearly showed the presence of an isomer mixture of $\mathbf{2\cdot O_2}$ (*cf.* ESI† Section 4.4.3).

Considering the size of $\mathbf{2\cdot O_2}$, $\mathbf{3\cdot O_2}$ and $\mathbf{4\cdot O_2}$ and overall similar structures, truncated models, namely $[PhPO_2(CN/NC)]M$ (M = Na, K), were chosen for further theoretical studies with the geometry derived from the molecular structures of $\mathbf{2\cdot O_2}$ and $\mathbf{4\cdot O_2}$ in the crystal, respectively. These studies at the DLPNO-CCSD(T)/def2-TZVP level of theory,[22,23] using the PBE0 (ref. 24–26)-D3 (ref. 27 and 28)/def2-TZVP[29] optimized geometries for obtaining the corrections to the free enthalpy (notation: DLPNO-CCSD(T)/def2-TZVP//PBE0-D3/def2-TZVP; *cf.* ESI† p. S76 ff.), revealed that in both cases the $[PhPO_2(CN)]M$ isomer is thermodynamically more stable than the isocyanide form by *ca.* 26.5 kJ mol^{-1}, in line with the experimentally observed presence of only the P–CN isomer after heating $\mathbf{2\ O_2}$ and $\mathbf{3\cdot O_2}$ in C_6D_6 solution, *vide supra*. A transition state that shows N···M interactions was found in both cases, clearly pointing to metal ion involvement in the thermal isomerization process. In both cases

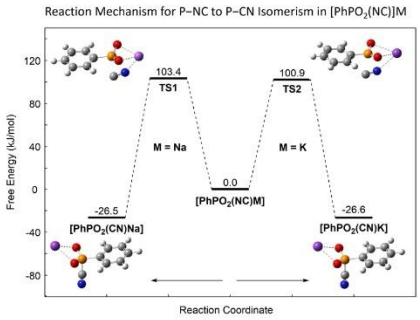

Fig. 4 Computed thermal reaction pathway for the NC/CN isomerism in model compounds $[PhPO_2(NC)]M$ (M = Na, K) (DLPNO-CCSD(T)/def2-TZVP//PBE0-D3/def2TZVP, $c° = 1$ mol L^{-1}).

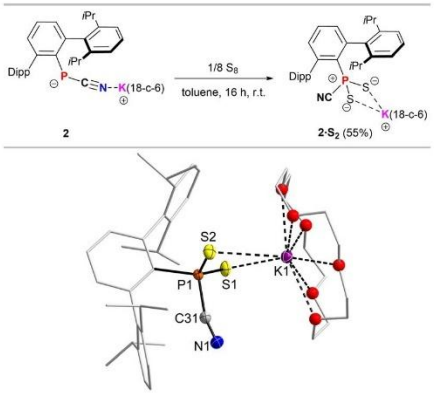

Fig. 5 Synthesis of dithiophosphorane cyanide adduct $2·S_2$ (top). Molecular structure of $2·S_2$ (bottom, one of two molecules in the asymmetric unit). Hydrogen atoms omitted and Dipp groups, ethylene bridges in 18-c-6 rendered as wireframe and O atoms rendered as spheres with arbitrary radius for clarity. Thermal ellipsoids are drawn at the 50% probability level. Selected bond lengths (Å) and angles (°): P1–S1 1.9560(5), P1–S2 1.9663(5), P1–C31 1.822(2), N1–C31 1.149(2), S1–K1 3.3707(5), S2–K1 3.3577(5); S1–P1–S2 120.19(2), C1–P1–S1 114.96(4), C1–P1–S2 107.13(4), N1–C31–P1 164.09(14).

the barrier is *ca.* 100 kJ mol^{-1} (M = Na, 103.4; M = K, 100.9 kJ mol^{-1}) in line with the facile thermal rearrangement at 80 °C in solution and at 110 °C in the solid state (Fig. 4).

As the PO_2–CN isomer was found to be thermodynamically more stable, the isomerization must occur during the initial oxidation step.

Therefore, the electrochemistry of **3** was exemplarily investigated. CV studies in THF showed an irreversible oxidation event with a peak potential of −0.6 V *vs.* Fc/Fc+ (0.1 M $[nBu_4N]PF_6$), accompanied by the aforementioned color change (Fig. S17†). The oxidation at rather negative potential is in line with reports on the related phosphaethynolate salt Na[PCO] (E^{ox} = −0.31 V *vs.* Fc/Fc^+ in THF).[30] We therefore propose initial oxidation of the cyanophosphides by $^3O_2$ to give a neutral P-radical species, which then reacts further with the superoxide anion, to presumably give a linear P–O–O(CN) intermediate. In the final isomerization step the CN-group becomes labile and can bind to the metal-crown cation, and eventually rebound to the P center either as the nitrile or isonitrile.

The involvement of a radical intermediate in the CN/NC isomerism is further supported by the reaction of **2** with elemental sulphur, which after stirring overnight in toluene afforded $[^{Dipp}TerPS_2(CN)][K(18\text{-c-}6)]$ ($\mathbf{2·S_2}$), with no intermediate color change to violet being observed (Fig. 5, top).

$\mathbf{2·S_2}$ shows a ^{31}P NMR signal in C_6D_6 at 32.3 ppm, significantly deshielded when compared to $\mathbf{2·O_2}$. A similar deshielding is observed upon oxygen for sulphur exchange from $PhPO_2(IMe_4)$ ($\delta(^{31}P, CDCl_3) = 0.8$ ppm) to $PhPS_2(IMe_4)$ ($\delta(^{31}P, CDCl_3) = 52.9$ ppm).[6] After recrystallization from toluene $\mathbf{2·S_2}$ was afforded as a toluene solvate, with no indication of an CN/NC isomer mixture in the solid state (*cf.* ESI† p. S13). This is further supported by only one stretching mode in the Raman spectrum at 2154 cm^{-1} (Fig. S37†), while no mode is observed between 2000–2300 cm^{-1} in the IR spectrum. In the solid state (Fig. 5, bottom) the $P–C_{CN}$ distance in $\mathbf{2·S_2}$ (1.822(2) Å) is longer compared to the dioxophosphorane adducts $\mathbf{2·O_2}$, $\mathbf{3·O_2}$ and $\mathbf{4·O_2}$, while the C–N distance is shorter (1.149(2) Å) and in line with a triple bond (*cf.* $\Sigma r_{cov}(C{\equiv}N) = 1.14$ Å),[17] with a P–C–N angle (164.1(1)°) that significantly deviates from linearity, while in $\mathbf{2·O_2}$, $\mathbf{3·O_2}$ and $\mathbf{4·O_2}$ the angles are closer to 180°. Therefore, we assume that the interaction of the cyanophosphides with $^3O_2$ in the first step facilitates the observed isomerisation.

Coordination isomerism in main group species is generally rare. Goicoechea and co-workers have lately described a [B]–OCP to [B]–PCO ([B] = $(HCNDipp)_2B$) isomerism catalysed by *t*Bu–NC (Scheme 4(i)).[31] Inoue and co-workers revealed a thermally induced SiP/PSi-isomerism in the heavier nitrile derivative $\{(SiTol_3)(SiMe_3)_2Si\}SiP(IPr)$ (IPr = $(HCNDipp)_2C$) (Scheme 4(ii)).[32] CN/NC isomerisations in main group species have been observed in magnesium and boron compounds. A MgCN complex with a dipyrromethene ligand (^{Mes}DPM, Scheme 4(iii)) was found to mainly exist as the isocyanide MgNC isomer in the solid state with only minor contribution of the MgCN isomer (95 : 5 ratio).[33] Moreover, it was shown that the borate anion $[(F_3C)_3B–CN]^-$ is thermodynamically more stable than its $[(F_3C)_3B–NC]^-$ isomer by 35.2 kJ mol^{-1} (Scheme 4(iv)), as shown experimentally by DSC measurements.[34]

A potential coordination isomerism in the related species $PO_2(CN)(DABCO)$ (DABCO = 1,4-diazabicyclo(2.2.2)octane) is indicated by ^{31}P NMR spectroscopy, while this phenomenon was not further investigated by the authors.[35] In general, it was shown that the X–CN/X–NC ratio is significantly influenced by the group electronegativity of X, with the X–CN form being favored for more electronegative moieties X.[36–38] These findings are in line with natural resonance theory (NRT) studies carried out on the model complexes $[PhPO_2(CN/NC)]^-$ (*cf.* ESI† p. S78 ff.), which show that there is a higher covalency in the P–CN isomer with the covalent form being predominant (41.8%) and only minor contribution of a non-bonding ionic form (10.4%). For the P–NC isomer the contribution of the ionic form is

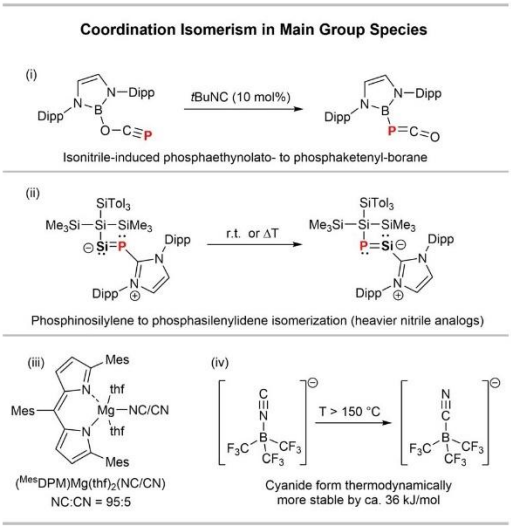

Scheme 4 Examples of (i) [B]-PCO/OCP,[31] (ii) SiP/PSi,[32] (iii) Mg(CN/NC)[33] and (iv) B(CN/NC) isomerisms.[34]

considerably higher (27.8%) (Fig. S61,† middle), which is balanced by a lower covalent character (28.8%). This is also reflected in a larger CN to $PhPO_2$ charge transfer in the $[PhPO_2(CN)]^-$ form of $0.51e^-$ compared to only $0.37e^-$ for the isocyanide isomer, with a higher Wiberg bond index (WBI) for the P–CN isomer (0.72) compared to the P–NC isomer (0.58). The $P–C_{CN}$ bond in the cyanide isomer is also considerably less polarized (P: 31.0%; C: 69.0%) compared to the $P–N_{NC}$ bond (P: 21.6%; N: 78.4%), in line with a smaller ionic character in the PCN isomer. Considering the high group electronegativity of the $^{Dipp}TerPO_2$ the fact that the cyanide form is thermodynamically stable is in line with previous studies.

Phosphinidene monoxide cyanide adducts

Using N_2O as an oxidant with isolated **2** or preparing **2** *in situ* from **1** and KH in toluene solution, a different product with a significantly deshielded ^{31}P NMR signal at 81.1 ppm was obtained (Scheme 5). By comparison with a recent report on the NHC-phosphinidene oxide adduct $^{Mes}TerPO(IMe_4)$ ($\delta(^{31}P)$ = 89.6 ppm),[7] this was assigned to the formal anionic phosphinidene oxide cyanide adduct $[^{Dipp}TerPO(CN)][K(18\text{-c-}6)]$ (**2·O**), which is further corroborated by the ^{31}P NMR shift in the gas phase ($\delta_{calc.}(^{31}P)$ = 72.8 ppm) obtained at the PBE0-D3/def2-TZVP//PBE0-D3-def2-SVP level of theory (Table S6†). Interestingly, the formation of **2·O** is not accompanied by an intermediate color change to purple, further substantiating that the coordination isomerism is related to a radical intermediate.

To the best of our knowledge **2·O** is the only example of an anionic phosphinidene monoxide adduct. Only recently the first free phosphinidene oxide Ar(Bz)N–PO (Ar = 2,6-(3,5-$Tipp_2$-C_6H_3)$_2$–C_6H_3; Bz = benzyl) with a deshielded ^{31}P NMR signal at *ca.* 285 ppm was isolated using an exceedingly bulky aryl-

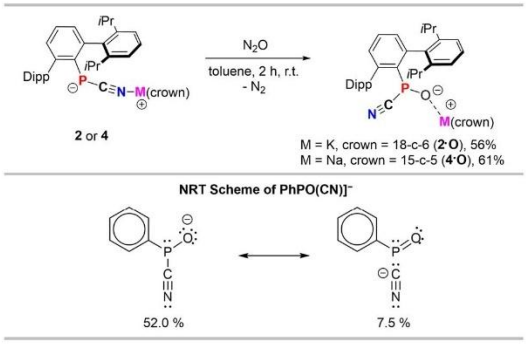

Scheme 5 Synthesis of the phosphinidene monoxide species **2·O** and **4·O** (left) and NRT scheme of the truncated model anion $[PhPO(CN)]^-$.

group.[39] An unstable neutral phosphine-stabilized cyclic aminophosphinidene oxide was recently reported by Nikonov *et al.*, which showed a similar ^{31}P NMR shift (89.6 ppm) compared to **2·O**.[9] SC-XRD quality crystals of **2·O** were obtained from a saturated toluene solution (Fig. 6), which revealed the proposed connectivity with a disordered P(O)CN unit, in a nearly 50 : 50 ratio (*cf.* Fig. S5†), which is in line with a stereochemically active lone pair of electrons on the P atom and both enantiomers of **2·O** being present in the crystal. Despite the disorder, the $P–C_{CN}$ distance (P1A–C31A 1.882(7), P1B–C31B 1.877(9) Å) is clearly elongated compared to **2** (*cf.* 1.770(1) Å), in line with the description of **2·O** as a cyanide adduct of ^{Dipp}TerPO. The P–O distance (P1A–O1A 1.515(2), P1B–O1B 1.528(2) Å) is rather long, when compared to the recently reported free phosphinidene oxide R(Bz)N–PO (*cf.* d(P–O) = 1.447(6) Å), but in line with that in the NHC adduct $^{Mes}TerPO(IMe_4)$ (*cf.* d(P–O) = 1.522(4) Å). The sum of angles at the P atom (Σ<(P) = 302.7(4) °) indicates a trigonal pyramidal coordination environment with

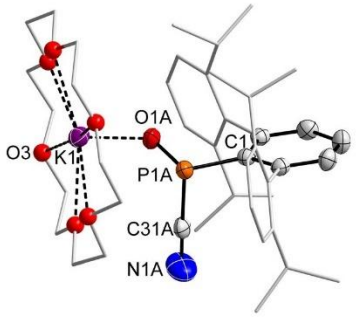

Fig. 6 Molecular structure of **2·O**. Hydrogen atoms omitted and Dipp groups, ethylene bridges in 18-c-6 rendered as wireframe and O atoms rendered as spheres with arbitrary radius for clarity. Thermal ellipsoids are drawn at the 50% probability level. Selected bond lengths (Å) and angles (°) [values of minor part B]: P1A-C1 1.886(2) [1.860(2)], P1A–C31A 1.882(7) [1.877(9)], C31A–N1A 1.151(8) [1.150(9)], O1A-P1A 1.515(2) [1.528(2)], O1A-K1 2.671(2) [2.632(2)]; P1A–C31A–N1A 166(1) [157(1)], O1A–P1A–C31A–104.2(3) [104.6(8)], O1A–P1A–C1 108.04(10) [106.3(1)], C31A–P1A–C1 93.3(5) [89.9(6)].

a short $O_P\cdots K$ contact (2.615(3) Å), rendering this a contact ion pair similar to $\mathbf{2{\cdot}O_2}$ and $\mathbf{4{\cdot}O_2}$. Likewise, $\mathbf{4{\cdot}O}$ was prepared which showed a minimally deshielded ^{31}P NMR signal at 82.9 ppm compared to $\mathbf{2{\cdot}O}$. Noteworthy in this case there is a significant broadening and pseudo-doublet form of the 15-c-5 signal in the ^1H NMR spectrum (*cf.* Fig. S55†). In $\mathbf{2{\cdot}O}$ and $\mathbf{4{\cdot}O}$ two sets of signals for the Dipp-substituents of the ^{Dipp}Ter-group on P are detected in the ^1H and ^{13}C NMR spectra, respectively, which is similar to starting material **1**, and indicates a P center with three different substituents. The ^{13}C NMR signal for the P*C*N unit could not be detected, while there is also no mode in the IR spectrum for the CN-group. This is in line with the theoretically predicted spectrum, with no apparent CN/NC isomerism in this case.

Natural resonance theory (NRT) on the truncated model $[PhPO(CN)]^-$ showed the zwitterionic form with just single bonds on the three-coordinate phosphorus atom to be the major form (Scheme 4). While minor weight is given to a non-bonding form with a Ph–P=O fragment and a cyanide anion, highlighting the polar character of the P–O bond, in line with a Wiberg bond index (WBI) for the P–CN bond of 0.82 and a significant charge transfer from the CN^- fragment to the PhPO-unit of $0.48e^-$.

Conclusions

We have shown that different alkali metal bases (KH, KHMDS, NaHMDS) can be used for the preparation of salts containing the cyanophosphide anion $[^{Dipp}TerPCN]^-$.

Using chelating crown ethers resulted in structural diversity, showing interactions of the encapsulated cations with the flanking Dipp groups of the ^{Dipp}Ter moiety in some cases, while in the case of **3** a rare example of a dimeric $[Na_2(18\text{-c-}6)_2]^{2+}$ cation was found to bridge two cyanophosphides in a centrosymmetric dimer. Independent of whether **2**, **3** or **4** are employed, facile oxidation with dry O_2 afforded the formal cyanide adducts of the dioxophosphorane $^{Dipp}TerPO_2$, as mixtures of cynanide and isocyanide isomers. The coordination isomerism was verified by NMR experiments as well as by vibrational spectroscopy. The cyanide isomer with a PO_2–CN unit was found to be thermodynamically more stable based on experimental data, supplemented by calculations. These calculations also showed involvement of the alkali metal ion in the isomerisation process. With S_8 as an oxidant no indication for a coordination isomerism was found, giving only the cyanide adduct of the dithiophosphorane in $\mathbf{2{\cdot}S_2}$. With N_2O as an oxidant, the anionic phosphinidene oxide adducts $\mathbf{2{\cdot}O}$ and $\mathbf{4{\cdot}O}$ were obtained, which show a ^{31}P NMR shift in the range expected for this rarely documented class of compounds. The trend previously observed for the stepwise oxidation of P^I to P^{III} and eventually P^V is observed in this study as well and shows rather shielded P atoms in the ^{31}P NMR spectra for anionic P^I compound **2** ($\delta(^{31}P) = 128.6$ ppm), a significant deshielding for $\mathbf{2{\cdot}O}$ ($\delta(^{31}P) = 89.6$ ppm), while $\mathbf{2{\cdot}O_2}$ ($\delta(^{31}P) = -9.3$ ppm) is observed in an intermediate range of the ^{31}P NMR chemical shift scale.

Future studies will focus on exploiting the concept of coordination isomerism in P^V compounds for the design of new P^V based catalyst systems.

Data availability

The data supporting this article have been included as part of the ESI.† This includes: synthesis and characterization of compounds, NMR spectra, crystallographic, and computational details. Additionally, a cif-file containing the isomer refinements of $\mathbf{2{\cdot}O_2}$, $\mathbf{3{\cdot}O_2}$ and $\mathbf{4{\cdot}O_2}$ (not uploaded to the CCDC) and a multi-structure *xyz*-file containing all optimized geometries have been uploaded. Crystallographic data for **2** (2401210), **3** (2401211), **4** (2401212), $\mathbf{2{\cdot}O_2}$ (2401213), $\mathbf{3{\cdot}O_2}$ (2427596), $\mathbf{4{\cdot}O_2}$ (2401214), $\mathbf{2{\cdot}S_2}$ (2427595), and $\mathbf{2{\cdot}O}$ (2401215) have been deposited at the CCDC and can be obtained from **https://www.ccdc.cam.ac.uk**.

Author contributions

A. A. N. carried out the experimental work and wrote the ESI.† E. Z. carried out parts of the experimental work. F. D. and C. H.-J. were responsible for solving and refining the SCXRD structures. C. H.-J. carried out the quantum chemical calculations. A. P. carried out CV experiments and analysed the data. J. S. carried out the Raman experiments, analysed and visualized the data. C. H.-J. was responsible for the conceptualization, supervision of the experimental investigations, and wrote the initial draft of the manuscript. C. H.-J., F. D. and E. B. finalized the manuscript. All authors agreed to the submitted content.

Conflicts of interest

There are no conflicts to declare.

Acknowledgements

C. H.-J. acknowledges financial support by an Exploration Grant of the Boehringer Ingelheim Foundation (BIS). A. A. N. thanks the Universiti Malaysia Sabah for funding. F. D. acknowledges the FCI for funding through the Liebig fellowship scheme. We thank our technical and analytical staff for assistance, especially Dr Anke Spannenberg for her support regarding X-ray analysis. We wish to thank the ITMZ at the University of Rostock for access to the cluster computer, and especially Malte Willert for his assistance with the queuing system and software installations. Dr Jonas Bresien (University of Rostock) is acknowledged for providing the SLURM interface for Gaussian and helpful discussions. We want to thank the expert reviewers for valuable input.

Notes and references

‡ Caution! When working with PCN-compounds the release of hydrogen cyanide, especially when cleaning glassware, is possible. Therefore, additional safety precautions and a special waste treatment with hydrogen peroxide are recommended.

1 G. S. Quin, S. Jankowski and L. D. Quin, *Phosphorus, Sulfur Silicon Relat. Elem.*, 1996, **115**, 93–98.
2 L. D. Quin, *Coord. Chem. Rev.*, 1994, **137**, 525–559.
3 A. Mardyukov, D. Niedek and P. R. Schreiner, *J. Am. Chem. Soc.*, 2017, **139**, 5019–5022.
4 X. Li, S. I. Weissman, T.-S. Lin, P. P. Gaspar, A. H. Cowley and A. I. Smirnov, *J. Am. Chem. Soc.*, 1994, **116**, 7899–7900.
5 Z. Liu, A. I. McKay, L. Zhao, C. M. Forsyth, V. Jevtović, M. Petković, G. Frenking and D. Vidović, *J. Am. Chem. Soc.*, 2022, **144**, 7357–7365.
6 D. Bockfeld, T. Bannenberg, P. G. Jones and M. Tamm, *Eur. J. Inorg. Chem.*, 2017, **2017**, 3452–3458.
7 D. Dhara, P. K. Pal, R. Dolai, N. Chrysochos, H. Rawat, B. J. Elvers, I. Krummenacher, H. Braunschweig, C. Schulzke, V. Chandrasekhar, U. D. Priyakumar and A. Jana, *Chem. Commun.*, 2021, **57**, 9546–9549.
8 J.-E. Siewert, B. M. Puerta Lombardi, N. Jannsen, R. Roesler and C. Hering-Junghans, *Inorg. Chem.*, 2023, **62**, 16832–16841.
9 A. G. Baradzenka, S. F. Vyboishchikov, M. Pilkington and G. I. Nikonov, *Chem.–Eur. J.*, 2023, **29**, e202301842.
10 F. Dankert, P. Gupta, T. Wellnitz, W. Baumann and C. Hering-Junghans, *Dalton Trans.*, 2022, **51**, 18642–18651.
11 L. E. English, A. Pajak, C. L. McMullin, J. P. Lowe, M. F. Mahon and D. J. Liptrot, *Chem.–Eur. J.*, 2022, **28**, e202200376.
12 M. I. Arz, V. T. Annibale, N. L. Kelly, J. V. Hanna and I. Manners, *J. Am. Chem. Soc.*, 2019, **141**, 2894–2899.
13 M. Fischer and C. Hering-Junghans, *Chem. Sci.*, 2021, **12**, 10279–10289.
14 A. H. Cowley, F. Gabbai, R. Schluter and D. Atwood, *J. Am. Chem. Soc.*, 1992, **114**, 3142–3144.
15 S. Shah, M. C. Simpson, R. C. Smith and J. D. Protasiewicz, *J. Am. Chem. Soc.*, 2001, **123**, 6925–6926.
16 M. Mantina, A. C. Chamberlin, R. Valero, C. J. Cramer and D. G. Truhlar, *J. Phys. Chem.*, 2009, **113**, 5806–5812.
17 P. Pyykkö and M. Atsumi, *Chem.–Eur. J.*, 2009, **15**, 12770–12779.
18 T. Taeufer, F. Dankert, D. Michalik, J. Pospech, J. Bresien and C. Hering-Junghans, *Chem. Sci.*, 2023, **14**, 3018–3023.
19 K. E. Wentz, A. Molino, S. L. Weisflog, A. Kaur, D. A. Dickie, D. J. D. Wilson and R. J. Gilliard Jr, *Angew. Chem., Int. Ed.*, 2021, **60**, 13065–13072.
20 V. A. Dodonov, O. A. Kushnerova, E. V. Baranov, A. S. Novikov and I. L. Fedushkin, *Dalton Trans.*, 2021, **50**, 8899–8906.
21 H. Zhang, X. Wang and B. K. Teo, *J. Am. Chem. Soc.*, 1996, **118**, 11813–11821.
22 C. Riplinger, B. Sandhoefer, A. Hansen and F. Neese, *J. Chem. Phys.*, 2013, **139**, 134101.
23 C. Riplinger and F. Neese, *J. Chem. Phys.*, 2013, **138**, 034106.
24 C. Adamo and V. Barone, *J. Chem. Phys.*, 1999, **110**, 6158–6170.
25 J. P. Perdew, K. Burke and M. Ernzerhof, *Phys. Rev. Lett.*, 1997, **78**, 1396.
26 J. P. Perdew, K. Burke and M. Ernzerhof, *Phys. Rev. Lett.*, 1996, **77**, 3865–3868.
27 S. Grimme, S. Ehrlich and L. Goerigk, *J. Comput. Chem.*, 2011, **32**, 1456–1465.
28 S. Grimme, J. Antony, S. Ehrlich and H. Krieg, *J. Chem. Phys.*, 2010, **132**, 154104.
29 F. Weigend and R. Ahlrichs, *Phys. Chem. Chem. Phys.*, 2005, **7**, 3297–3305.
30 S. Alidori, D. Heift, G. Santiso-Quinones, Z. Benkő, H. Grützmacher, M. Caporali, L. Gonsalvi, A. Rossin and M. Peruzzini, *Chem.–Eur. J.*, 2012, **18**, 14805–14811.
31 D. W. N. Wilson, M. P. Franco, W. K. Myers, J. E. McGrady and J. M. Goicoechea, *Chem. Sci.*, 2020, **11**, 862–869.
32 M. E. Doleschal, A. Kostenko, J. Y. Liu and S. Inoue, *Nat. Chem.*, 2024, **16**, 2009–2016.
33 G. Ballmann, H. Elsen and S. Harder, *Angew. Chem., Int. Ed.*, 2019, **58**, 15736–15741.
34 M. Finze, E. Bernhardt, H. Willner and C. W. Lehmann, *J. Am. Chem. Soc.*, 2005, **127**, 10712–10722.
35 T. Schneider, K. Schwedtmann, J. Fidelius and J. J. Weigand, *Nat. Syn.*, 2023, **2**, 972–979.
36 S. Petrie, *Phys. Chem. Chem. Phys.*, 1999, **1**, 2897–2905.
37 M. H. Baghal-Vayjooee, J. L. Collister and H. O. Pritchard, *Can. J. Chem.*, 1977, **55**, 2634–2636.
38 M. R. Booth and S. G. Frankiss, *Chem. Commun.*, 1968, 1347–1348.
39 C. Hu, N. H. Rees, M. Pink and J. M. Goicoechea, *Nat. Chem.*, 2024, **16**, 1855–1860.

6.2 Cyanophosphide Transfer Reaction

Ayu Afiqah Nasrullah, Malte Fischer, Fabian Dankert, Eszter Baráth and Christian Hering-Junghans

Organometallics, **2025***, 44,* 788−791

DOI: 10.1021/acs.organomet.5c00012

Published: 17th March 2025

Contribution to this paper is 80%

ORGANOMETALLICS

pubs.acs.org/Organometallics
Communication

Flash Communication: Cyanophosphide Transfer Reactions

Ayu Afiqah Nasrullah, Malte Fischer, Fabian Dankert, Eszter Barath,* and Christian Hering-Junghans*

Cite This: *Organometallics* 2025, 44, 788−791
Read Online

ABSTRACT: Cyanophosphides of the general form $[RPCN]^-$ can be viewed as cyanide adducts of phosphinidenes and are phosphorus species in the (+1)-oxidation state. We have recently reported on the stable cyanophosphide $[^{Dipp}TerPCN]K$ (^{Dipp}Ter = 2,6-$Dipp_2C_6H_3$, Dipp = 2,6-iPrC_6H_3) and now investigate its reactions with ECl_n (E = Ge, n = 2; E = P, As, n = 3) in either salt metathesis or base-assisted dehydrohalogenation reactions. In the case of $GeCl_2$, salt metathesis with $[^{Dipp}TerPCN]K$ afforded the dimer of a chlorogermylene $[^{Dipp}TerP(CN)GeCl]_2$. When only 0.5 equiv of $GeCl_2$ was used, the diphosphanylgermylene $[^{Dipp}TerP(CN)]_2Ge$ was generated in solution. With ECl_3 (E = P, As), facile cyanophosphide transfer was achieved from $^{Dipp}TerP(H)CN$ in NEt_3-assisted dehydrohalogenation, giving diphosphanes or arsaphosphanes of the type $^{Dipp}TerP(CN)ECl_2$ (E = P, As), respectively.

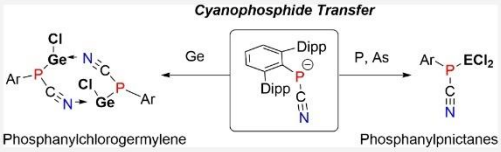

Phosphorus compounds usually occur in the (+3)-oxidation state with two nonbonding electrons, rendering phosphanes of the type PR_3 ubiquitous ligands in coordination chemistry. Phosphanes are also known to coordinate phosphinidenes (R−P),[1] phosphorus species in the (+1)-oxidation state, giving phosphanylidene phosphoranes of the general form R−P(−)−P(+)R_3, which have been known for nearly 60 years.[2] The aryl-substituted variants Mes*P(PMe_3) and ^{Mes}TerP(PMe_3) (**A**, Mes* = 2,4,6-tBu$_3$C$_6$H$_3$; ^{Mes}Ter = 2,6-$Mes_2C_6H_3$, Mes = 2,4,6-$Me_3C_6H_2$; Scheme 1) were popularized by Protasiewicz and co-workers, who reported on the Phospha-Wittig reactivity toward aldehydes, giving phosphaalkenes in facile fashion.[3] Furthermore, the potential of ArP(PMe_3) in formal Ar−P transfer reactions has been explored.[4−6] For example, when ArP(PMe_3) (Ar = Mes*, ^{Mes}Ter, ^{Dipp}Ter) were treated with isonitriles R−NC (R = tBu, Xyl), facile PMe_3 substitution afforded 1,3-phosphaazaallenes of the type ArPCNR (**B**, Scheme 1).[7] ArPCNtBu were shown to undergo thermal *iso*-butene release to give the corresponding cyanophosphines ArP(H)CN (**C**, Scheme 1). Treatment of $^{Dipp}TerP(H)CN$ (**1**) with KHMDS (KHMDS = K[N($SiMe_3$)$_2$]) afforded the stable cyanophosphide $[^{Dipp}TerPCN]K$ (**2**, Scheme 1). Cyanophosphides can be considered as the formal cyanide adducts of phosphinidenes and are thus another class of P-compounds in the (+1)-oxidation state.[8] The notion that $[RPCN]^-$ can be regarded as cyanide adducts of R−P is supported by studies that showed the formation of [PhPCN]M (M^+ = Na, K, $[(Ph_3P)_2N]$) by reacting Ph_5P_5 with MCN.[9] Phosphanyl-substituted cyanophosphides ($[R_2PPCN]^-$; R = Ph, Cy, tBu, N(iPr)$_2$) can also be accessed from cobalt pentaphosphido complexes [(PHDI)Co(η^4-P_5R_2)] (PHDI = bis(2,6-diisopropylphenyl)phenanthrene-9,10-diimine) with the aid of cyanide salts.[10] Moreover, Grützmacher and co-workers recently reported on alkali phosphanyl cyanophosphides {[^{s}P]PCN}M (**D**, Scheme 1; [^{s}P] = $[(H_2CNDipp)_2P]$, M = Na, K).[11] Ambident nucleophilicity has been shown for {[^{s}P]PCN}$^-$, giving either P- (**E**) or N-functionalized species (**F**, Scheme 1, bottom) in salt metatheses reactions. In this contribution, we elucidate the potential of $[^{Dipp}TerPCN]K$ as a cyanophosphide transfer reagent in salt metathesis reactions.

First, we investigated the thermal stability of $[^{Dipp}TerPCN]K$ (**2**) (obtained by combining **1** and KHMDS) with respect to KCN-elimination in a C_6D_6 solution at 80 °C over a period of 24 h. This clearly showed that **2** ($\delta(^{31}P)$ = −141.1 ppm) is the main species in the $^{31}P\{^1H\}$ NMR spectrum after heating, with only minor quantities of a dibenzophosphole derivative as a phosphinidene (^{Dipp}Ter−P) deactivation product being observed (see Figure S5).[4] This contrasts [Mes*PCN]K,[7] which could be generated in solution, but thermal KCN-elimination occurred within 16 h at ambient temperature, to afford phosphaindane **G** (Scheme 1), a known decomposition product of Mes*−P.[12] Likewise, ^{Mes}TerP(H)CN formed the phosphinidene dimer (^{Mes}TerP)$_2$ (**H**, Scheme 1)[6] when treated with KHMDS.

Next, we combined **1** with KHMDS and $GeCl_2$·(dioxane) in a 1:1:1 ratio in a 5:1 mixture of C_6D_6/thf-d_8. The ^{31}P NMR spectrum recorded after 1 h at ambient temperature showed a major species at −77.4 ppm with a minor component at −74.3 ppm, while the ^1H NMR spectrum showed that **1** was fully consumed (Scheme 2(i)). Single crystals were grown from *n*-

Received: January 13, 2025
Revised: March 6, 2025
Accepted: March 12, 2025
Published: March 17, 2025

https://doi.org/10.1021/acs.organomet.5c00012
Organometallics 2025, 44, 788−791

Organometallics pubs.acs.org/Organometallics Communication

Scheme 1. Summary of Our Group's Work on Cyanophosphides (Top) and Examples of Their Ambident Nucleophilicity as Reported by Grützmacher and Co-Workers (Bottom) (NHB = [(H$_2$CNDipp)$_2$B])[11]

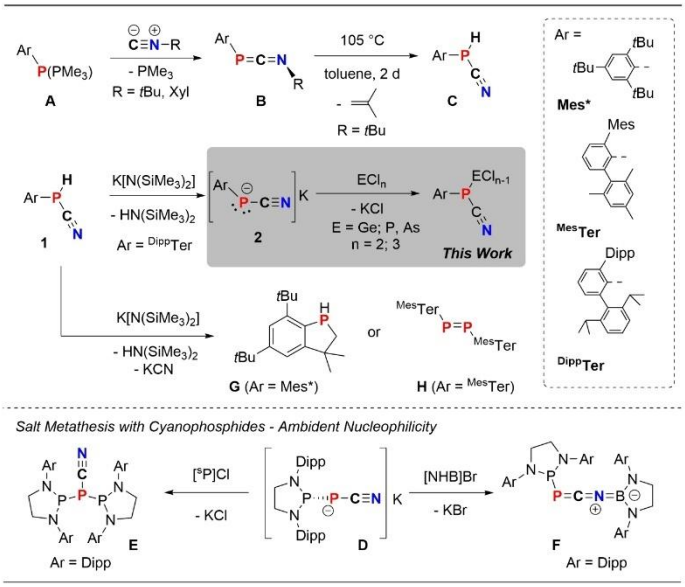

Scheme 2. Reactivity of 1: (i) K[N(SiMe$_3$)$_2$], GeCl$_2$·(dioxane), 5:1 C$_6$D$_6$:thf-d_8, r.t., −KCl, −HN(SiMe$_3$)$_2$; (ii) K[N(SiMe$_3$)$_2$], 0.5 GeCl$_2$·(dioxane), 5:1 C$_6$D$_6$:thf-d_8, r.t., −KCl, −HN(SiMe$_3$)$_2$; (iii) ECl$_3$, NEt$_3$, Toluene, r.t., −[HNEt$_3$]Cl

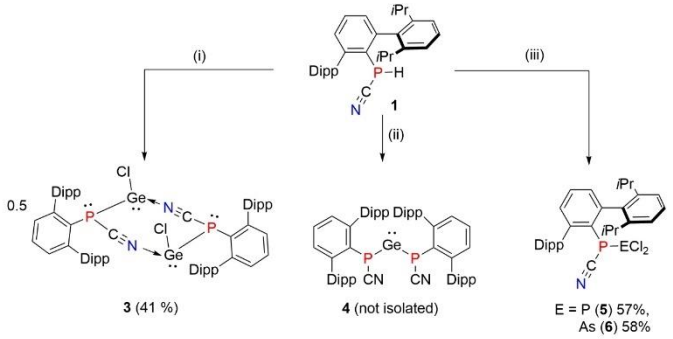

hexane at −30 °C, revealing the formation of the dimeric chlorogermylene [^{Dipp}TerP(CN)GeCl]$_2$ (**3**; δ_{calc}(^{31}P) = −89.4 ppm) (Figure 1). At the DLNPO-CCSD(T)/def2-TZVP//PBE0-D3/def2-SVP(benzene) level of theory, the dimerization was calculated to be strongly exergonic ($\Delta_R G^\circ_{298}$ = −136.9 kJ·mol^{-1}). The dimer is formed through P−CN···Ge contacts (Ge1−N2 2.041(3), Ge2−N1 2.053(3) Å) (cf. Σr_{cov}(Ge−N) = 1.92 Å),[13] with both chlorine atoms on the same side of the eight-membered ring. In the ring, the P−Ge distances are rather long (Ge1−P1 2.5482(9), Ge2−P2 2.5300(9) Å) Σr_{cov}(Ge−P) = 2.32 Å),[13] while the N−C distances indicate only minimal back-donation from Ge to the P−CN units. The long P−Ge and Ge−N distances in **3** point to strongly polarized bonds with high ionic character, which is supported by NBO calculations at the PBE0-D3/def2-TZVP level of theory giving rather low Wiberg bind indexes (WBIs) for the P−Ge (0.62) and Ge−N (0.43) bonds. Moreover, both bonds are significantly polarized toward P (73.6%) or N (88.4%), respectively. The bonding situation is thus best compared with bis-NHC-phosphinidene complexes of [GeCl]$^+$, showing similar P−Ge distances.[14] The angles at Ge are nearly 90 °, while wider angles are detected at P. The P−CN distances (P1−C1 1.763(4), P2−C2 1.761(3) Å) are similar to those in [^{Dipp}TerPCN][K(2.2.2-crypt)] (cf. P1−C31 1.768(1) Å),[7] indicating a sustained [^{Dipp}TerPCN]$^-$ character in **3**, in line with the NBO results. Isolated crystals of **3** show broad signals in the ^{1}H NMR spectrum, and thus, we conclude that both isomers, with Cl on one side of the eight-membered ring or in *trans*-relation, respectively, are present in solution. This is also in line with two signals in the ^{31}P NMR spectrum, *vide supra*. Phosphanylchloro- and diphosphanylgermylenes are rare due to insufficient overlap of the s-type lone pair of electrons (LP) at phosphorus with the lone p-type valence at the Ge atom(s).[15,16]

https://doi.org/10.1021/acs.organomet.5c00012
Organometallics 2025, 44, 788−791

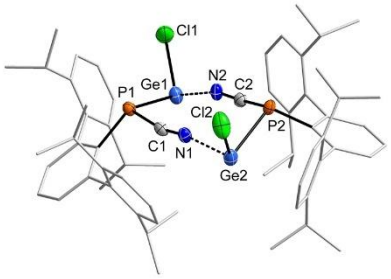

Figure 1. Molecular structure of **3**. H atoms are omitted, and ^{Dipp}Ter groups are rendered as wireframe for clarity. Thermal ellipsoids at 50% probability level. Selected bond lengths (Å) and angles (°): Ge1−N2 2.041(3), Ge1−Cl1 2.2307(11), Ge1−P1 2.5482(9), Ge2−N1 2.053(3), Ge2−Cl2 2.2175(12), Ge2−P2 2.5300(9), P1−C1 1.763(4), P2−C2 1.761(3), P2−C33 1.849(3), N1−C1 1.151(5), N2−C2 1.155(5); Σ(<Ge1) 275.94(9), Σ(<Ge2) 275.17(9), Σ(<P1) 311.9(2), Σ(<P1) 312.2(2), N1−C1−P1 166.6(3), N2−C2−P2 165.9(3).

When the reaction of **1**, $K[N(SiMe_3)_2]$, and $GeCl_2$·(dioxane) was carried out in a 2:2:1 ratio (Scheme 2(ii)), a species with a ^{31}P NMR shift of −73.9 ppm was formed as the main species, indicating the formation of $[^{Dipp}TerP(CN)]_2Ge$ (**4**) (cf. $[(iPr_3Si)(FTipp_2Si)P]_2Ge$ $\delta(^{31}P) = -62.1$ ppm).[16] In the ^{1}H NMR spectrum of the reaction mixture, putative diphosphanylgermylene **4**, dioxane, and $HN(SiMe_3)_2$ are detected in the expected 1:1:2 ratio. Few single crystals (**4cryst**) were grown from a saturated *n*-pentane solution (see SI). A severe disorder of the main structural motif in between the two ^{Dipp}Ter groups precludes a detailed discussion of the structure, yet, the connectivity reveals redistribution of **4**, which is not further discussed due to a certain degree of ambiguity (see the SI for details, Figure S2). Based on ^{1}H and $^{31}P\{^1H\}$ NMR spectroscopy, the formation of **4** in solution is quantitative. Attempts to isolate **4** were unsuccessful, as compound **4** is extremely sensitive to moisture; thus, mainly ^{Dipp}TerP(H)CN was isolated.

After the addition of PCl_3 to a 1:1 mixture of **1** and KHMDS at −78 °C in toluene and warming to ambient temperature, the formation of the desired diphosphane $^{Dipp}TerP(PCl_2)CN$ (**5**) was indicated by two doublets at 182.5 (PCl_2) and −24.8 ppm (PCN) ($^1J_{(PP)}$ = 243.4 Hz). However, there is also a so far unidentified side product at 27.8 ppm in a 2:3 ratio compared to **5**. As an alternative approach, base-assisted dehydrohalogenation was tested next. Therefore, **1** was combined with PCl_3 in a 1:1 ratio in toluene, and a solution of 1 equiv of NEt_3 was added at −78 °C; the mixture was warmed to room temperature overnight (Scheme 2(iii)). After removal of the volatiles and extraction with *n*-hexane, **5** was isolated as an off-white powder in a moderate yield of 57%. X-ray quality crystals of **5** were not obtained; thus, the identity of **5** was confirmed by multinuclear NMR and IR spectroscopy, high-resolution MS, and elemental analysis. In analogous fashion, the arsaphosphane $^{Dipp}TerP(CN)AsCl_2$ (**6**) was prepared in a yield of 58% from a 1:1:1 mixture of **1** with NEt_3 and $AsCl_3$. Both **5** and **6** show similar ^{31}P NMR shifts for the PCN phosphorus atoms at ca. −24.8 (**5**) and −30.8 ppm (**6**), respectively.

The presence of the second phosphorus atom in **5** is also clearly reflected in the ^{13}C NMR signal of the CN group, which appears as a doublet of doublets (**5**: $\delta(^{13}C) = 116.5$ ppm; $^1J_{(PP)} = 86.6$ Hz; $^2J_{(PP)} = 15.6$ Hz), while only a doublet ($\delta(^{13}C) = 118.2$ ppm; $^1J_{PP} = 95.6$ Hz) is detected for **6**. In the ^{1}H and ^{13}C NMR spectra, two sets of signals are detected for the ^{Dipp}Ter-moiety, in line with a trisubstituted pnictogen atom and the formation of **5** and **6** as racemic mixtures. Crystals suitable for SC-XRD of **6** were afforded from a saturated *n*-hexane solution at −30 °C, revealing **6** to crystallize solvent-free in the monoclinic space group $P2_1/n$ with four molecules in the unit cell (Figure 2). The P−As distance (2.3896(6) Å) is

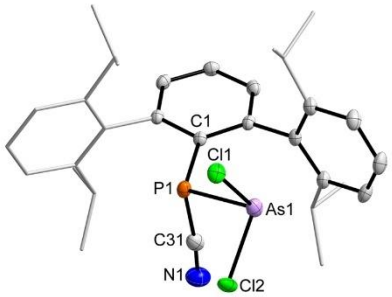

Figure 2. Molecular structure of **6**. H atoms are omitted, and Dipp groups are rendered as wireframe for clarity. Thermal ellipsoids at 50% probability level. Selected bond lengths (Å) and angles (°): P1−C1 1.855(2), P1−As1 2.3896(6), P1−C31 1.799(3), C31−N1 1.142(3), As1−Cl1 2.1877(7), As1−Cl2 2.1965(7); Σ(<P1) 302.5(2), Σ(<As1) 279.48.

in the range expected for a P−As single bond (cf. Σr_{cov}(P−As) = 2.32 Å)[13] (cf. ^{S}IMesP−AstBu$_2$ 2.3133(4) Å, ^{S}IMes = $[(H_2CNMes)_2C]$),[17] indicating a covalent P−As bond, while the P−C_{CN} distance (1.799(3) Å) is longer compared to **3**. Both pnictogen centers are in a trigonal pyramidal coordination environment (Σ>(P) = 302.51°; (As) = 279.48°) with no intermolecular contacts being detected in the solid state.

This work clearly demonstrates the potential of $[^{Dipp}TerPCN]K$ to act as a cyanophosphide transfer reagent, affording the unusual phosphide-substituted chlorogermylene **3**, with an unprecedented eight-membered cyclic dimer formed through Ge···N_{CN} contacts, while with $PnCl_3$ (Pn = P, As), diphosphane **5** and phosphinoarsane **6** were formed. Studies harnessing the dual donor capability of $[^{Dipp}TerPCN]^-$ and attempts to trap diphosphanylgermylene **4** are currently under way.

■ ASSOCIATED CONTENT

Supporting Information

The Supporting Information is available free of charge at https://pubs.acs.org/doi/10.1021/acs.organomet.5c00012.

XYZ coordinates for the optimized structures (XYZ)
Synthesis and characterization of compounds, NMR spectra, and crystallographic and computational details (PDF)

Accession Codes

Deposition Numbers 2416712−2416714 contain the supplementary crystallographic data for this paper. These data can be obtained free of charge via the joint Cambridge Crystallographic Data Centre (CCDC) and Fachinformationszentrum Karlsruhe Access Structures service.

https://doi.org/10.1021/acs.organomet.5c00012
Organometallics 2025, 44, 788−791

AUTHOR INFORMATION

Corresponding Authors

Eszter Barath − *Leibniz Institut für Katalyse e.V. (LIKAT), 18059 Rostock, Germany;* orcid.org/0000-0001-8494-3388; Email: eszter.barath@catalysis.de

Christian Hering-Junghans − *Leibniz Institut für Katalyse e.V. (LIKAT), 18059 Rostock, Germany;* orcid.org/0000-0003-4937-2625; Email: christian.hering-junghans@catalysis.de

Authors

Ayu Afiqah Nasrullah − *Leibniz Institut für Katalyse e.V. (LIKAT), 18059 Rostock, Germany; Pusat Persediaan Sains dan Teknologi, Universiti Malaysia Sabah, 88400 Kota Kinabalu, Sabah, Malaysia*

Malte Fischer − *Leibniz Institut für Katalyse e.V. (LIKAT), 18059 Rostock, Germany;* Present Address: Georg-August-Universität Göttingen, Institut für Anorganische Chemie, Tammannstr. 4, 37077 Göttingen, Germany; orcid.org/0000-0002-2806-1302

Fabian Dankert − *Leibniz Institut für Katalyse e.V. (LIKAT), 18059 Rostock, Germany;* Present Address: Universität Kassel, Institut für Chemie, Heinrich-Plett-Straße 40, 34132 Kassel, Germany; orcid.org/0000-0002-6806-4794

Complete contact information is available at: https://pubs.acs.org/10.1021/acs.organomet.5c00012

Author Contributions

The manuscript was written through contributions of all authors. All authors have given approval to the final version of the manuscript.

Notes

The authors declare no competing financial interest.

ACKNOWLEDGMENTS

C.H.-J. acknowledges the financial support by an Exploration Grant of the Boehringer Ingelheim Foundation (BIS). A.A.N. thanks the Universiti Malaysia Sabah for funding. We thank our technical and analytical staff for assistance, especially Dr. Anke Spannenberg for her support regarding X-ray analysis. We wish to thank the ITMZ at the University of Rostock for access to the cluster computer, and especially Malte Willert for his assistance with the queuing system and software installations. Dr. Jonas Bresien (University of Rostock) is acknowledged for providing the SLURM interface for Gaussian and helpful discussions.

REFERENCES

(1) Protasiewicz, J. D. Coordination-Like Chemistry of Phosphinidenes by Phosphanes. *Eur. J. Inorg. Chem.* **2012**, *2012*, 4539−4549.

(2) Protasiewicz, J. D.; Hering-Junghans, C. Phosphanylidenephosphoranes. In *Encyclopedia of Inorganic and Bioinorganic Chemistry*; Scott, R. A., Ed.; John Wiley & Sons, Ltd., 2022.

(3) Shah, S.; Protasiewicz, D. J. 'Phospha-Wittig' reactions using isolable phosphoranylidenephosphines ArP = PR_3 (Ar = 2,6-$Mes_2C_6H_3$ or 2,4,6-$But_3C_6H_2$). *Chem. Commun.* **1998**, 1585−1586.

(4) Taeufer, T.; Dankert, F.; Michalik, D.; Pospech, J.; Bresien, J.; Hering-Junghans, C. Photochemical formation and reversible base-induced cleavage of a phosphagallene. *Chem. Sci.* **2023**, *14*, 3018−3023.

(5) (a) Gupta, P.; Siewert, J.-E.; Wellnitz, T.; Fischer, M.; Baumann, W.; Beweries, T.; Hering-Junghans, C. Reactivity of phospha−Wittig reagents towards NHCs and NHOs. *Dalton Transactions* **2021**, *50*, 1838−1844. (b) Fischer, M.; Nees, S.; Kupfer, T.; Goettel, J. T.; Braunschweig, H.; Hering-Junghans, C. Isolable Phospha- and Arsaalumenes. *J. Am. Chem. Soc.* **2021**, *143*, 4106−4111. (c) García-Romero, Á.; Hu, C.; Pink, M.; Goicoechea, J. M. A. Crystalline Unsupported Phosphagallene and Phosphaindene. *J. Am. Chem. Soc.* **2025**, *147*, 1231−1239.

(6) Shah, S.; Simpson, M. C.; Smith, R. C.; Protasiewicz, J. D. Three Different Fates for Phosphinidenes Generated by Photocleavage of Phospha-Wittig Reagents $ArPPMe_3$. *J. Am. Chem. Soc.* **2001**, *123*, 6925−6926.

(7) Fischer, M.; Hering-Junghans, C. On 1,3-phosphaazaallenes and their diverse reactivity. *Chem. Sci.* **2021**, *12*, 10279−10289.

(8) Ellis, B. D.; Macdonald, C. L. B. Stable compounds containing heavier group 15 elements in the + 1 oxidation state. *Coord. Chem. Rev.* **2007**, *251*, 936−973.

(9) Schmidpeter, A.; Zirzow, K.-H.; Burget, G.; Huttner, G.; Jibril, I. Cyanidabbau von $(PhP)_5$: Bildung, Struktur und Reaktionen des Phenyl-cyanphosphid-Ions. *Chem. Ber.* **1984**, *117*, 1695−1706.

(10) Hoidn, C. M.; Maier, T. M.; Trabitsch, K.; Weigand, J. J.; Wolf, R. [3 + 2] Fragmentation of a Pentaphosphido Ligand by Cyanide. *Angew. Chem., Int. Ed.* **2019**, *58*, 18931−18936.

(11) Li, Z.; Borger, J. E.; Müller, F.; Harmer, J. R.; Su, C.-Y.; Grützmacher, H. Phosphanyl Cyanophosphide Salts: Versatile PCN Building Blocks. *Angew. Chem., Int. Ed.* **2019**, *58*, 11429−11433.

(12) Cowley, A. H.; Gabbai, F.; Schluter, R.; Atwood, D. New approaches to the generation of phosphinidenes. *J. Am. Chem. Soc.* **1992**, *114*, 3142−3144.

(13) Pyykkö, P.; Atsumi, M. Molecular Double-Bond Covalent Radii for Elements Li−E112. *Chem. A Eur. J.* **2009**, *15*, 12770−12779.

(14) Siewert, J.-E.; Schumann, A.; Wellnitz, T.; Dankert, F.; Hering-Junghans, C. Triphosphiranes as phosphinidene-transfer agents − synthesis of regular and chelating NHC phosphinidene adducts. *Dalton Trans.* **2023**, *52*, 15747−15756. (b) Hadlington, T. J.; Kostenko, A.; Driess, M. Synthesis and Coordination Ability of a Donor-Stabilised Bis-Phosphinidene. *Chem. A Eur. J.* **2021**, *27*, 2476−2482.

(15) (a) Izod, K.; Rayner, D. G.; El-Hamruni, S. M.; Harrington, R. W.; Baisch, U. Stabilization of a Diphosphagermylene through pπ−pπ Interactions with a Trigonal-Planar Phosphorus Center. *Angew. Chem., Int. Ed.* **2014**, *53*, 3636−3640. (b) du Mont, W.-W.; Schumann, H. Chloro (di-tert-butylphosphino)germanediyl and -stannanediyl: Stable Germanium(II) and Tin(II) Organophosphorus Compounds. *Angew. Chem., Int. Ed. Engl.* **1975**, *14*, 368−368.

(16) Driess, M.; Janoschek, R.; Pritzkow, H.; Rell, S.; Winkler, U. Diphosphanyl- and Diarsanyl-Substituted Carbene Homologues: Germanediyls, Stannanediyls, and Plumbanediyls with Remarkable Electronic Structures. *Angew. Chem., Int. Ed. Engl.* **1995**, *34* (15), 1614−1616.

(17) Balmer, M.; Gottschling, H.; von Hänisch, C. Phosphaalkene-substituted organo-group 15 compounds: synthesis and characterisation of (NHC)P−EtBu_2 (E = P, As, Sb and Bi). *Chem. Commun.* **2018**, *54*, 2659−2661.

https://doi.org/10.1021/acs.organomet.5c00012
Organometallics 2025, 44, 788−791

6.3 FLP-type Alkenylation of a Phosphafluorene

Ayu Afiqah Nasrullah, Eszter Baráth and Christian Hering-Junghans

Dalton Trans., **2025** submitted (Status: xx.06.2025)

Contribution to this paper is 80%

ARTICLE

FLP-type Alkenylation of a Phosphafluorene

Ayu Afiqah Nasrullah,[a,b] Eszter Baráth*,[a] and Christian Hering-Junghans*,[a]

Received 00th January 20xx,
Accepted 00th January 20xx

DOI: 10.1039/x0xx00000x

Phosphafluorenes, in which the chemically vulnerable C-9 position of the fluorene core has been replaced with phosphorus, demonstrate enhanced stability compared to conventional fluorene-based materials and belong to the general class of dibenzophospholes (DBPs). Phosphafluorene formation is commonly observed in the reductive functionalization of terphenyl-based dihalophosphanes. In here, we outline a high-yielding route towards phosphafluorene **1**, starting from readily available ^{Dipp}TerPCl$_2$ (^{Dipp}Ter = 2,6-Dipp-C$_6$H$_3$; Dipp = 2,6-*i*Pr$_2$-C$_6$H$_3$). Different quarternization strategies of **1** are outlined, including a complex with AuCl, its BH$_3$ adduct, and its corresponding sulphide. Interestingly, facile alkenylation of **1** was achieved in the presence of B(C$_6$F$_5$)$_3$ and various phenylacetylene derivatives. This FLP-type alkenylation is *E*-selective giving zwitterionic phosphonium borates.

Introduction

Phosphanylidenephosphoranes of the general form RP(PR'$_3$) are also referred to as Phospha-Wittig reagents.[1] Specifically, aryl-substituted variants are commonly used in phosphaalkene synthesis in the so-called phospha-Wittig reaction. The first aryl-substituted phosphanylidenephosphoranes, ArP(PMe$_3$), were synthesized by Protasiewicz and co-workers in 1998 through the combination of Ar–PCl$_2$ with an excess of PMe$_3$ and zinc powder.[2] To date a limited number of ArP(PMe$_3$) (Ar = 2,4,6-*t*Bu$_3$-C$_6$H$_2$, Mes*;[2] 2,6-(2,6-Cl$_2$C$_6$H$_2$)$_2$-C$_6$H$_3$, ^{Cl}Ter;[3] 2,6-(2,4,6-Me$_3$-C$_6$H$_2$)$_2$-C$_6$H$_3$, ^{Mes}Ter;[2, 4] 2,6-(2,4,6-*i*Pr$_3$-C$_6$H$_2$)$_2$-C$_6$H$_3$, ^{Tipp}Ter;[5] 2,6-(2,6-*i*Pr$_2$-C$_6$H$_2$)$_2$-C$_6$H$_3$, ^{Dipp}Ter;[6] 1,1,3,3,5,5,7,7-octaethyl-1,2,3,5,6,7-hexahydro-s-indacen-4-yl, EIND[7]) have been reported and their utility in Wittig-type reactions has been explored. Moreover, it was shown that Phospha-Wittig reagents offer a pathway for the generation of arylphosphinidenes, Ar–P, under photochemical conditions. For example, when ^{Tipp}TerP(PMe$_3$) was irradiated at 365 nm the formation of a phosphafluorene was described, through insertion of the phosphinidene into one of the C$_{Ar}$-C$_{iPr}$ bonds of the Tipp groups.[5] Our group observed ^{Dipp}Ter–P generation and deactivation to give phosphafluorene **1** via the thermal decomposition of the isolated phosphagallene, ^{Dipp}TerPGaCp* at 50 °C for 2 h (Scheme 1, a), or through the irradiation (396 nm) of ^{Dipp}TerP(PMe$_3$) in toluene-d_8 at room temperature (Scheme 1, b).[8] These findings complement earlier work on phosphafluorene formation via the reduction of ^{Tipp}TerPCl$_2$ with magnesium (Scheme 1, f).[9]

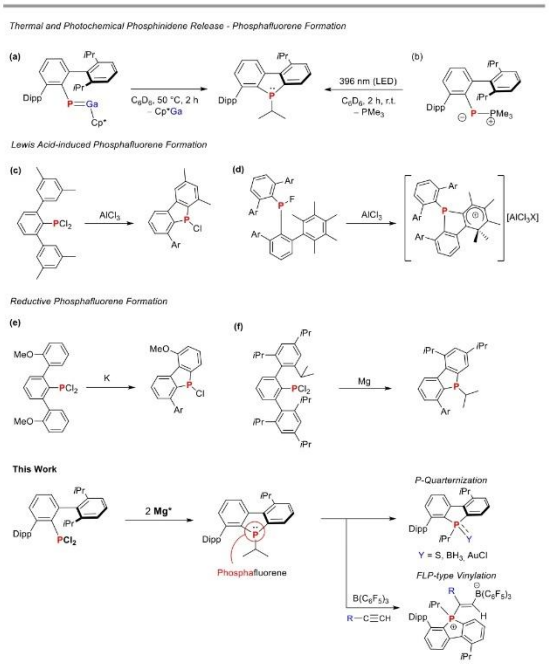

Scheme 1. (a) Thermal phosphinidene release from a phosphagallene, (b) Photochemical PMe$_3$ release from ^{Dipp}TerP(PMe$_3$); (c,d) Lewis acid induced phosphafluorene formation in terphenyl-substituted halophosphanes; (e,f) Reductive approaches towards phosphafluorenes from dichlorophosphanes (e, f); and summary of this work.

[a] *Leibniz Institut für Katalyse e.V. (LIKAT), A.-Einstein-Str. 29a, 18059 Rostock (Germany). Email: eszter.barath@catalysis.de, Christian.hering-junghans@catalysis.de*

[b] *Pusat Persediaan Sains dan Teknologi, Universiti Malaysia Sabah, Jln UMS, 88400, Kota Kinabalu, Sabah (Malaysia).*

Supplementary Information available: Synthesis of compounds, NMR spectra and crystallographic details. CCDC 2466772-2466775. See DOI: 10.1039/x0xx00000x

It was later shown that the reducing agent plays an important role in the outcome of the reaction.[10] Related cyclizations of terphenyl-based dichlorophosphanes were also described by Marshall[11] in the reduction with potassium (Scheme 1, e), and by Wehmschulte and co-workers in AlCl$_3$-mediated Friedel-

Crafts type reactions (Scheme 1, c).[12] Similar intramolecular cyclizations have also been described for terphenyl-substituted phosphenium cations, allowing the isolation of the 9-phospha fluorenium ions (Scheme 1, d).[13]

Phosphafluorenes belong to the broader class of dibenzophospholes (DBPs),[14] which are a family of compounds that have garnered significant interest due to their unique electronic properties and potential applications in materials science and catalysis. DBPs are important building blocks for organic π-conjugated compounds, which have enormous potential as optoelectronic materials for example in light-emitting diodes (OLED), organic field-effect transistors, nonlinear optical devices, and organic solar cells.[15-18] In recent years, monodentate non–symmetrical dibenzophospholes have emerged as ligands in rhodium-catalyzed hydroformylations.[19] Phosphafluorenes, in which the chemically vulnerable C-9 position of the fluorene is replaced with phosphorus, demonstrate enhanced stability compared to conventional fluorene-based materials. They usually show fluorescence in the UV region, while the photophysical properties can be precisely tuned through functionalization, especially quarternization at the phosphorus atom. Examples of quarternization strategies on the P center of phosphafluorenes (DBPs) include oxidation,[20] sulfurization,[21] complexation with tungsten, gold,[21] iron or ruthenium,[12] and related transformation. These structural modifications enable precise tuning of optoelectronic properties, highlighting their potential for tailored application in photonic and electronic devices.[14]

DBPs can also be viewed as sterically encumbered phosphines, rendering them suitable candidates for frustrated Lewis pair (FLP) applications when paired with sterically hindered Lewis acids. The functionalization of alkynes using FLPs has been intensively studied.[22] The outcome of the reactions greatly depends on the basicity of the phosphine used. In the case of P/B-FLPs two outcomes are possible: (a) phosphonium alkynyl-borates, through deprotonation of the alkyne, or (b) addition to the alkynes resulting in zwitterionic alkenyl phosphonium borates, when less basic phosphines were employed.[23 24 25]

In this contribution, we report on different quarternization products of phosphafluorene **1** using BH_3, S_8 or AuCl. Moreover, the reactivity of **1** towards terminal alkynes (4-R-C_6H_4-C≡C–H) in the presence of $B(C_6F_5)_3$ was investigated, proving an FLP-type alkenylation strategy for DBPs (Scheme 1, bottom).

Results and Discussion

At first, the synthesis of phosphafluorene **1** was optimized, adopting the route Power and co-workers used to make a ^{Tipp}TerPCl$_2$-derived phosphafluorene (Scheme 1, f).[9] The reaction of ^{Dipp}TerPCl$_2$ with two equivalents of activated magnesium (Mg*) in THF at room temperature overnight produced a light orange, fluffy solid of **1** in 77 % yield after work-up (Scheme 2, top). The best results were obtained when using two equivalents of activated magnesium, while stoichiometric amounts gave **1** in lower yield.

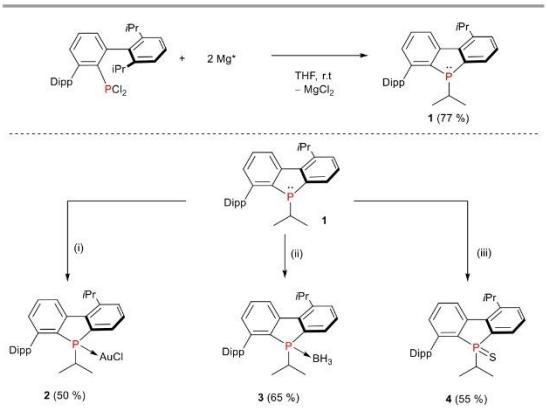

Scheme 2. Synthesis of phosphafluorene **1** (top). Quarternization of the phosphorus center in **1**: (i) AuCl·SMe_2, toluene, 16 h, r.t.; (ii) H_3B·SMe_2, *n*-hexane, 16 h, r.t.; (iii) 1/8 S_8, CH_2Cl_2, 16 h, r.t.

Phosphafluorene **1**, formed as the sole product through the insertion of the P atom into one of the *o*-C(Ar)–C(*i*Pr) bonds. Its structure was confirmed by ^{31}P NMR spectroscopy in C_6D_6 ($\delta(^{31}P\{^1H\})$ = −1.1 ppm), consistent with our previous observations in the decomposition of a phosphagallene (Scheme 1, a).[8] Despite their intriguing electronic properties, phosphafluorenes remain understudied in terms of their reactivity. The flexible coordination behavior of the endocyclic phosphorus atom, along with the accessibility of its lone pair offers significant potential for structural diversification. Thus, chemical modifications at the P-center of **1**, particularly through coordination to transition metals, sulfurization, and reactions with Lewis acids were studied (Scheme 2, bottom). The combination of **1** with (Me_2S)AuCl in toluene and stirring overnight at ambient temperature in the absence of light resulted in the formation of complex **2** (Scheme 2, i). Recrystallization of the crude product from a 1:5 CH_2Cl_2:*n*-hexane solution at −30 °C afforded colourless single crystals suitable for single crystal X-ray diffraction (SCXRD) analysis and **2** was isolated in 50 % yield. The $^{31}P\{^1H\}$ NMR shift in C_6D_6 at 32.4 ppm indicated the formation of complex **2** and quarternization of the P atom. Characteristic of **1** is that one of the Me-groups of the *i*Pr-groups on the P atom is rather shielded, while appearing as a pseudo triplet. Upon coordination of AuCl, the $^3J_{P-H}$ coupling constant increases and results in a clear doublet of doublet splitting of the signal. Generally, all compounds derived from **1** show a rather complex ^{1}H NMR spectrum with all methyl groups being magnetically inequivalent, due to C_1 symmetry in solution.

Next, **1** was treated with borane dimethylsulfide (Me_2S·BH_3), which afforded phosphafluorene BH_3 adduct **3** in 65 % yield after crystallization from *n*-heptane at −30 °C as colourless single crystalline material. The $^{31}P\{^1H\}$ and $^{11}B\{^1H\}$ NMR spectra of **3** in C_6D_6 displayed characteristic shifts at 37.3 ppm and −38.4 ppm, respectively, indicating tetracoordinate P and B atoms. Additionally, the BH_3 moiety was detected by IR spectroscopy, with weak B–H stretching modes centred at ca. 2345 cm^{-1}.[26]

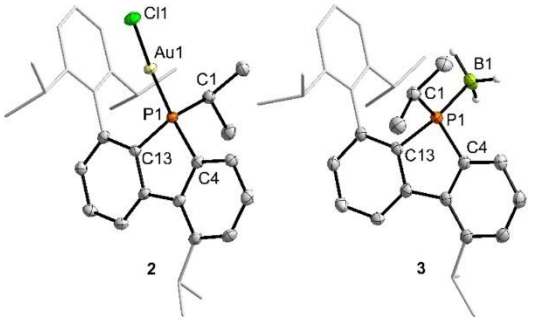

Figure 1. Molecular structures of **2** and **3**. Ellipsoids drawn at 50 % with C-H-atoms omitted, Dipp- and one of the *i*Pr-groups rendered as wire-frame for clarity. Selected bond lengths [Å] and angles [°] of **2**: C1–P1 1.845(2), C4–P1 1.798(2), C13–P1 1.805(2), P1–Au1 2.2247(6), Cl1–Au1 2.2885(6); C4–P1–C13 91.83(10), C4–P1–C1 106.46(10), C13–P1–C1 105.84(10), C4–P1–Au1 114.61(7), C13–P1–Au1 121.62(7), C1–P1–Au1 113.71(8); C5–C4–P1–C13 179.9(2). **3**: P1–C4 1.7991(13), P1–C13 1.8102(13), P1–C1 1.8435(14), P1–B1 1.9269(16); C4–P1–C13 91.52(6), C4–P1–C1 108.29(6), C13–P1–C1 107.20(6), C4–P1–B1 111.38(7), C13–P1–B1 121.08(6), C1–P1–B1 114.62(7); C13–P1–C4–C9 -178.84(12).

In the ^{1}H NMR spectrum, the expected quartet resonance for BH_3 is significantly broadened and overlaps with the signals of the *i*Pr-Me groups and could therefore not be unambiguously assigned. Similarly to **2**, the shielded Me-groups of the iPr-groups on the P atom changes into a doublet of doublets.

As a last quarternization strategy the reaction of **1** with elemental sulfur was conducted, cleanly furnishing thiophosphafluorene **4** as a pale-yellow solid in 55 % isolated yield. The ^{31}P NMR signal of **4** ($\delta(^{31}P\{^{1}H\})$ = 53.4 ppm; $\Delta_{1\text{-}4}(\delta(^{31}P))$ = +54.5 ppm)) is notably deshielded compared to **2** and **3**, consistent with P=S bond formation. A similar deshielding is observed in related dibenzophosphapentaphenes upon sulfurization (cf. $\Delta(\delta(^{31}P))$ = +48.9 ppm).[21] Single-crystal X-ray diffraction experiments (SC-XRD) revealed that **2** and **3** crystallize in the monoclinic space groups $P2_1/c$ and $P2_1/n$, respectively. Both **2** and **3** show a four-coordinate P atom (Σ(<P) = 304.1(1) (**2**), 307.01(6) ° (**3**)). The P–C_{Ar} distances (**2**: 1.798(2), 1.805(2); **3**: 1.799(1), 1.810(1) Å) are shorter compared to the related free phosphafluorene derived from ^{Tipp}TerPCl$_2$ (cf. 1.805(11), 1.817(4) Å).[9] Similarly, the P–C_{iPr} (**2**: 1.845(2); **3**: 1.844(1) Å) bonds are contracted as compared to the related phosphafluorene. The P1–Au1 bond distance (2.2247(6) Å) in **2** aligns with reported gold(I)-phosphole complexes,[27] while the P–B distance in BH_3-adduct **3** (1.9269(16) Å) is in the range of reported dibenzophosphole BH_3 adducts.[28]

In an effort to identify alternative Lewis acid to $H_3B{\cdot}SMe_3$, we explored bulkier derivatives such as $B(C_6F_5)_3$. When **1** and $B(C_6F_5)_3$ were combined in a 1:1 ratio in C_6D_6, no discernible reaction was observed according to ^{31}P NMR spectroscopy. This lack of reactivity suggests frustrated Lewis pair (FLP) behaviour arising from steric congestion between the Lewis acid and base. Upon addition of one equivalent phenylacetylene to the reaction mixture in C_6D_6, the color of the solution changes from light orange to dark red. NMR data of the reaction mixture showed complete conversion to a new species. Layering of the reaction mixture in C_6D_6 with *n*-hexane at ambient temperature and standing overnight afforded a white powder of ArPC(Ph)=C(H)B$(C_6F_5)_3$ (**5**; Ar= 1-(2,6-diisopropylphenyl)-5,9-diisopropyl-9-phosphafluorene) and was isolated in 61 % yield. Compound **5** features a ^{1}H NMR resonance at 7.84 ppm (d, $^{3}J_{P-H}$ = 38.0 Hz) assigned to the alkenyl C=CH moiety (cf. Ph_3P(PhC=CH)B$(C_6F_5)_3$: $\delta(^{1}H)$ = 8.32 ppm, $^{3}J_{P-H}$ = 36.0 Hz).[23] The ^{31}P NMR signal at 36.1 ppm is in line with a phosphonium center, whereas the ^{19}F NMR spectrum showed three sets of signals for the *o*-, *p*-, and *m*-fluorine atoms of the C_6F_5 groups located at $\delta(^{19}F)$ −130.5, −161.7, and −166 ppm, respectively, in line with reported FLP-type activations of phenylacetylene and free rotation about the B–C axis.[23] In the ^{11}B NMR spectrum, a signal at −15.4 ppm (d, $^{3}J_{P-H}$ = 18.0 Hz) is in line with a four-coordinate boron center and a phosphonium borate zwitterionic species. Collectively these data, suggested that **5** is exclusively the 1,2-addition product (Scheme 3, bottom). This assumption was confirmed by X-ray crystallography showing that the phosphine and borane added to the alkyne in (*E*)-fashion with the B adding to the CH terminus of the alkyne (Figure 2, left).[24] The solid-state structure reveals P–C_{Ar} (1.792(2), 1.801(2) Å) and P–C_{iPr} (1.828(2) Å) distances similar to those found in **2** and **3** (*vide supra*). The P–$C_{C=C}$ distance (1.828(2) Å) is in the range of a contracted P–C single bond (Σr_{cov}(P–C) = 1.86 Å)[29] and minimally longer than in Ph_3P(PhC=CH)B$(C_6F_5)_3$ (cf. 1.806(1) Å).[23] The C31–C32 distance (1.344(2), cf. Σr_{cov}(C=C) = 1.34 Å)[29] clearly indicates activation of the alkyne unit, with the P and B atoms being in *trans*-orientation with respect to the C=C bond. Notably, the C=C*H* proton is oriented towards the phosphafluorene moiety.

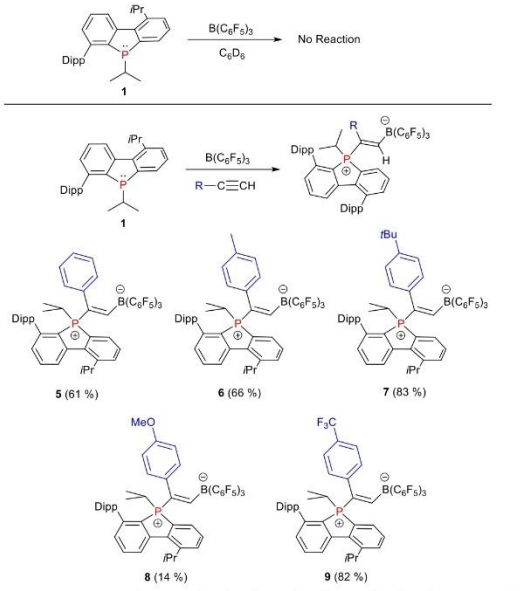

Scheme 3. Reactivity of **1** towards $B(C_6F_5)_3$ in the absence (top) and presence of phenylacetylene derivatives, giving alkenyl phosphonium borates **5**-**9**.

Motivated by these findings, we next tested a series of *para*-substituted phenylacetylene (RPhC≡CH where R = CH_3 (**6**), *t*Bu (**7**), OMe (**8**), CF_3 (**9**)) to investigate possible substituent effects on this FLP reactivity. Reaction of these alkynes with the **1**/$B(C_6F_5)_3$ FLP system proceeded analogously to **5**, yielding diverse zwitterionic alkenyl phosphonium borate products (Scheme 3), which underlines the generality of this functionalization strategy.[24] This FLP-type alkenylation of a P-heterocycle is also related to the chemistry of phosphinine-borane adducts towards phenylacetylene.[30] The ^{31}P NMR shifts for **6**-**9** are clustered near 36.0 ppm, clearly showing minimal influence of the *para*-substituent. All compounds (**6**-**9**) displayed ^{19}F NMR signals for the $B(C_6F_5)_3$ moiety in the range of −130.5 (*ortho*-F), −161.7 (*para*-F), and −166.0 (*meta*-F), mirroring **5**, and thereby indicating a similar $B(C_6F_5)_3$ moiety in all alkenylation products **5**-**9**. Notably, **9** showed an additional singlet at −63.3 ppm in the ^{19}F NMR spectrum assignable to the CF_3 group. The ^{11}B NMR spectra of **6**-**9** uniformly exhibited resonances near −15.0 ppm (d, $^3J_{P-B}$ = 18 Hz) as expected for borate-type activation products. These observations suggest minimal electronic influence from the *para*-substituents of phenylacetylenes (EDG/EWG) on the regio- and chemoselectively of the alkenylation. In all derivatives the C=CH resonance is deshielded at ca. 8 ppm and a $^3J_{P-H}$ coupling constant of ca. 38 Hz.

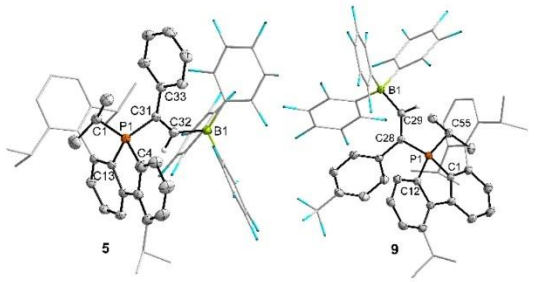

Figure 2. Molecular structures of **5** and **9**. Ellipsoids drawn at 50 % with C-H-atoms omitted (except those at C32 (**5**) and C29(**9**)), Dipp-, C_6F_5-, CF_3- and one of the *i*Pr-groups rendered as wire-frame for clarity. Selected bond lengths [Å] and angles [°] of **5**: P1–C4 1.7915(18), P1–C13 1.8014(16), P1–C1 1.8282(18), P1–C31 1.8282(17), B1–C32 1.648(2), C31–C32 1.344(2); C4 P1 C13 93.34(8), C4–P1–C1 110.49(8), C13–P1–C1 113.17(8), C4–P1–C31 107.19(8), C13–P1–C31 112.12(7), C1–P1–C31 117.64(8), C32–C31–P1 112.79(12), C31–C32–B1 138.96(15); C4–P1–C31–C32 65.08(14). **9**: C1–P1 1.8007(14), C12–P1 1.7807(14), C28–P1 1.7969(13), C55–P1 1.8326(14), C28–C29 1.3433(19), C29–B1 1.642(2); C12–P1–C28 108.96(6), C12–P1–C1 93.52(6), C28–P1–C1 122.55(6), C12–P1–C55 108.64(7), C28–P1–C55 113.19(6), C1–P1–C55 107.71(6), C29–C28–P1 116.86(10), C28–C29–B1 136.79(13); C29–C28–P1–C12 137.25(11).

These results underscore the robustness of FLP-mediated alkyne activation, where steric and electronic perturbations at the *para*-position are effectively reduced by the conjugated aromatic system, preserving the core electronic structure of the adduct.

Single crystals of **9** suitable for SC-XRD were obtained from layering the C_6D_6 reaction mixture with *n*-heptane at room temperature. As previously observed in **5**, the alkyne activation is (*E*)-selective, with boron attached to the CH terminus (Figure 2, right). All key structural parameters are similar to those found in **5**. However, the orientation of the C=C*H* proton is different, which is not oriented towards the P-*i*Pr group.

Conclusions

We outline a facile synthetic route towards phosphafluorene **1** starting from readily accessible $^{Dipp}TerPCl_2$ in a reductive approach. Quarternization of **1** with AuCl, BH_3, and sulphur afforded P-functionalized species **2**-**4**, respectively. When **1** was combined with $B(C_6F_5)_3$ no reaction was observed. When adding phenylacetylene to the mixture, clean FLP-type alkenylation of the P in **1** was noted giving (*E*)-configured alkenyl phosphonium borate **5**. This novel alkenylation strategy for DBPs was extended and facile conversion with *para*-substituted phenylacetylenes was achieved giving species **6**-**9**. To the best of our knowledge this is the first report on FLP-type functionalization of DBPs and the generality of the concept with respect to the DBP-precursors is currently investigated.

Author contributions

A.A.N. carried out the experimental work, wrote the supporting information and drafted the manuscript. C.H.-J. was responsible for the conceptualization, supervision of the experimental investigations, solved and refined the SCXRD structures. C.H.-J. and E.B. finalized the manuscript. All authors agreed to the submitted content.

Conflicts of interest

There are no conflicts to declare.

Data availability

The data supporting this article have been included as part of the Supplementary Information. This includes: Synthesis and characterization of compounds, NMR spectra and crystallographic details.

Crystallographic data **2** (2466772), **3** (2466773), **5** (2466774) and **9** (2466775) have been deposited at the CCDC and can be obtained from https://www.ccdc.cam.ac.uk.

Acknowledgements

A.A.N. thanks the Universiti Malaysia Sabah for funding. We thank our technical and analytical staff for assistance, especially Dr. Anke Spannenberg for her support regarding X-ray analysis.

Notes and references

1 J. D. Protasiewicz, *Eur. J. Inorg. Chem.*, 2012, **2012**, 4539-4549.
2 S. Shah and J. D. Protasiewicz, *Chem. Commun.*, 1998, 1585-1586.

3 Rhett C. Smith, T. Ren and John D. Protasiewicz, *Eur. J. Inorg. Chem.*, 2002, **2002**, 2779-2783.
4 S. Shah, G. P. A. Yap and J. D. Protasiewicz, *J. Organomet. Chem.*, 2000, **608**, 12-20.
5 S. Shah, M. C. Simpson, R. C. Smith and J. D. Protasiewicz, *J. Am. Chem. Soc.*, 2001, **123**, 6925-6926.
6 P. Gupta, J.-E. Siewert, T. Wellnitz, M. Fischer, W. Baumann, T. Beweries and C. Hering-Junghans, *Dalton Trans.*, 2021, **50**, 1838-1844.
7 K. Takeuchi, H.-o. Taguchi, I. Tanigawa, S. Tsujimoto, T. Matsuo, H. Tanaka, K. Yoshizawa and F. Ozawa, *Angew. Chem. Int. Ed.*, 2016, **55**, 15347-15350.
8 T. Taeufer, F. Dankert, D. Michalik, J. Pospech, J. Bresien and C. Hering-Junghans, *Chem. Sci.*, 2023, **14**, 3018-3023.
9 B. Twamley, C. D. Sofield, M. M. Olmstead and P. P. Power, *J. Am. Chem. Soc.*, 1999, **121**, 3357-3367.
10 R. C. Smith, S. Shah and J. D. Protasiewicz, *J. Organomet. Chem.*, 2002, **646**, 255-261.
11 A. S. Ionkin and W. J. Marshall, *Heteroatom Chem.*, 2003, **14**, 360-364.
12 A. A. Diaz, J. D. Young, M. A. Khan and R. J. Wehmschulte, *Inorg. Chem.*, 2006, **45**, 5568-5575.
13 M. Olaru, D. Duvinage, Y. Naß, L. A. Malaspina, S. Mebs and J. Beckmann, *Angew. Chem. Int. Ed.*, 2020, **59**, 14414-14417.
14 P. Hibner-Kulicka, J. A. Joule, J. Skalik and P. Bałczewski, *RSC Advances*, 2017, **7**, 9194-9236.
15 J. Yin, R.-F. Chen, S.-L. Zhang, Q.-D. Ling and W. Huang, *J. Phys. Chem. A*, 2010, **114**, 3655-3667.
16 H.-C. Su, O. Fadhel, C.-J. Yang, T.-Y. Cho, C. Fave, M. Hissler, C.-C. Wu and R. Réau, *J. Am. Chem. Soc.*, 2006, **128**, 983-995.
17 C.-H. Lin, C.-W. Hsu, J.-L. Liao, Y.-M. Cheng, Y. Chi, T.-Y. Lin, M.-W. Chung, P.-T. Chou, G.-H. Lee, C.-H. Chang, C.-Y. Shih and C.-L. Ho, *J. Mat. Chem.*, 2012, **22**, 10684-10694.
18 X. Deng, S. Liu, Y. Sun, D. Zhong, D. Jia, X. Yang, B. Su, Y. Sun, G. Zhou, B. Jiao and Z. Wu, *Dyes and Pigments*, 2023, **209**, 110885.
19 A. Oukhrib, L. Bonnafoux, A. Panossian, S. Waifang, D. H. Nguyen, M. Urrutigoity, F. Colobert, M. Gouygou and F. R. Leroux, *Tetrahedron*, 2014, **70**, 1431-1436.
20 H. A. van Kalkeren, S. H. A. M. Leenders, C. R. A. Hommersom, F. P. J. T. Rutjes and F. L. van Delft, *Chem. Eur. J.*, 2011, **17**, 11290-11295.
21 P.-A. Bouit, A. Escande, R. Szűcs, D. Szieberth, C. Lescop, L. Nyulászi, M. Hissler and R. Réau, *J. Am. Chem. Soc.*, 2012, **134**, 6524-6527.
22 J. Guo, M. Yan and D. W. Stephan, *Org. Chem. Front.*, 2024, **11**, 2375-2396.
23 M. A. Dureen and D. W. Stephan, *J. Am. Chem. Soc.*, 2009, **131**, 8396-8397.
24 M. A. Dureen, C. C. Brown and D. W. Stephan, *Organometallics*, 2010, **29**, 6594-6607.
25 C. Jiang, O. Blacque and H. Berke, *Organometallics*, 2010, **29**, 125-133.
26 26. C. A. Jaska, H. Dorn, A. J. Lough and I. Manners, *Chem. Eur. J.*, 2003, **9**, 271-281.
27 S. Attar, W. H. Bearden, N. W. Alcock, E. C. Alyea and J. H. Nelson, *Inorg. Chem.*, 1990, **29**, 425-433.
28 V. Diemer, A. Berthelot, J. Bayardon, S. Jugé, F. R. Leroux and F. Colobert, *J. Org. Chem.*, 2012, **77**, 6117-6127.
29 P. Pyykkö and M. Atsumi, *Chem. Eur. J.*, 2009, **15**, 12770-12779.
30 J. Lin, F. Wossidlo., N. T. Coles, M. Weber, S. Steinhauer, T. Böttcher and C. Müller, *Chem. Eur. J.*, 2022, **28**, e202104135.

Please do not adjust margins

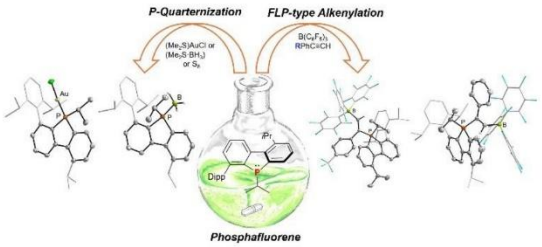

TOC Entry. Quarternization strategies of a phosphafluorene, including coordination to AuCl and adduct formation with BH_3 are discussed. In the presence of $B(C_6F_5)_3$ and alkynes the facile alkenylation of the P atom is achieved.

7 References

[1] J. D. Protasiewicz, C. Hering-Junghans, in *Encycl. Inorg. BioInorg. Chem.*, pp. 1-27.
[2] J. D. Protasiewicz, *Eur. J. Inorg. Chem.* **2012**, *2012*, 4539-4549.
[3] W. Mahler, A. B. Burg, *J. Am. Chem. Soc.* **1958**, *80*, 6161-6167.
[4] A. B. Burg, W. Mahler, *J. Am. Chem. Soc.* **1961**, *83*, 2388-2389.
[5] E. Urnėžius, S. Shah, J. D. Protasiewicz, *Phosphorus, Sulfur, Silicon Relat. Elem.* **1999**, *144*, 137-139.
[6] T. L. Breen, D. W. Stephan, *J. Am. Chem. Soc.* **1995**, *117*, 11914-11921.
[7] S. Shah, J. D. Protasiewicz, *Chem. Commun.* **1998**, 1585-1586.
[8] K. Takeuchi, H.-o. Taguchi, I. Tanigawa, S. Tsujimoto, T. Matsuo, H. Tanaka, K. Yoshizawa, F. Ozawa, *Angew. Chem. Int. Ed.* **2016**, *55*, 15347-15350.
[9] Rhett C. Smith, T. Ren, John D. Protasiewicz, *Eur. J. Inorg. Chem.* **2002**, *2002*, 2779-2783.
[10] S. Shah, G. P. A. Yap, J. D. Protasiewicz, *J. Organomet. Chem* **2000**, *608*, 12-20.
[11] P. Gupta, J.-E. Siewert, T. Wellnitz, M. Fischer, W. Baumann, T. Beweries, C. Hering-Junghans, *Dalton Trans.* **2021**, *50*, 1838-1844.
[12] S. Shah, M. C. Simpson, R. C. Smith, J. D. Protasiewicz, *J. Am. Chem. Soc.* **2001**, *123*, 6925-6926.
[13] C. Smit, T. A. Van der Knaap, F. Bickelhaupt, *Tetrahedron Lett.* **1983**, *24*, 2031-2034.
[14] L. Weber, *Chem. Rev.* **1992**, *92*, 1839-1906.
[15] P. Pyykkö, M. Atsumi, *Chem. Eur. J.* **2009**, *15*, 12770-12779.
[16] A. B. Burg, *J. Inorg. Nucl. Chem* **1971**, *33*, 1575-1581.
[17] D. Weber, E. Fluck, *Z. fur Anorg. Allg. Chem.* **1976**, *424*, 103-107.
[18] G. Fritz, T. Vaahs, H. Fleischer, E. Matern, *Z. fur Anorg. Allg. Chem.* **1989**, *570*, 54-66.
[19] G. Fritz, T. Vaahs, H. Fleischer, E. Matern, *Angew. Chem.* **1989**, *101*, 324-325.
[20] F. Zurmühlen, M. Regitz, *Angew. Chem.* **1987**, *99*, 65-67.
[21] M. Sanchez, R. Réau, C. J. Marsden, M. Regitz, G. Bertrand, *Chem. Eur. J.* **1999**, *5*, 274-279.
[22] R. Armbrust, M. Sanchez, R. Reau, U. Bergstraesser, M. Regitz, G. Bertrand, *J. Am. Chem. Soc.* **1995**, *117*, 10785-10786.
[23] P. Le Floch, A. Marinetti, L. Ricard, F. Mathey, *J. Am. Chem. Soc.* **1990**, *112*, 2407-2410.
[24] M. Stubenhofer, C. Kuntz, M. Bodensteiner, A. Y. Timoshkin, M. Scheer, *Organometallics* **2013**, *32*, 3521-3528.
[25] D. V. Partyka, M. P. Washington, J. B. Updegraff III, R. A. Woloszynek, J. D. Protasiewicz, *Angew. Chem.* **2008**, *120*, 7599-7602.
[26] B. A. Surgenor, M. Bühl, A. M. Z. Slawin, J. D. Woollins, P. Kilian, *Angew. Chem.* **2012**, *124*, 10297-10300.
[27] B. A. Surgenor, B. A. Chalmers, K. S. Athukorala Arachchige, A. M. Z. Slawin, J. D. Woollins, M. Bühl, P. Kilian, *Inorg. Chem.* **2014**, *53*, 6856-6866.
[28] A. Marinetti, S. Bauer, L. Ricard, F. Mathey, *Organometallics* **1990**, *9*, 793-798.
[29] X. Chen, R. C. Smith, J. D. Protasiewicz, *Chem. Commun.* **2004**, 146-147.
[30] U. J. Kilgore, H. Fan, M. Pink, E. Urnezius, J. D. Protasiewicz, D. J. Mindiola, *Chem. Commun.* **2009**, 4521-4523.
[31] T. Krachko, J. C. Slootweg, *Eur. J. Inorg. Chem.* **2018**, *2018*, 2734-2754.
[32] A. Doddi, M. Peters, M. Tamm, *Chem. Rev.* **2019**, *119*, 6994-7112.
[33] K. Powers, C. Hering-Junghans, R. McDonald, M. J. Ferguson, E. Rivard, *Polyhedron* **2016**, *108*, 8-14.
[34] M. M. Roy, E. Rivard, *Acc. Chem. Res.* **2017**, *50*, 2017-2025.
[35] C. E. Knappke, J. M. Neudörfl, A. J. von Wangelin, *Org. Biomol. Chem.* **2010**, *8*, 1695-1705.
[36] M. Fischer, C. Hering-Junghans, *Chem. Sci.* **2021**, *12*, 10279-10289.
[37] H. Sitzmann, M. F. Lappert, C. Dohmeier, C. Üffing, H. Schnöckel, *J. Organomet. Chem* **1998**, *561*, 203-208.
[38] M. Fischer, S. Nees, T. Kupfer, J. T. Goettel, H. Braunschweig, C. Hering-Junghans, *J. Am. Chem. Soc.* **2021**, *143*, 4106-4111.
[39] A. Hofmann, T. Tröster, T. Kupfer, H. Braunschweig, *Chem. Sci.* **2019**, *10*, 3421-3428.
[40] F. Dankert, C. Hering-Junghans, *Chem. Commun.* **2022**, *58*, 1242-1262.

[41] F. Dankert, J. E. Siewert, P. Gupta, F. Weigend, C. Hering-Junghans, *Angew. Chem. Int. Ed.* **2022**, *61*, e202207064.
[42] H. P. DeGroot, T. P. Hanusa, in *Encycl. Inorg. BioInorg. Chem.*, pp. 1-13.
[43] R. C. Dobbie, P. D. Gosling, B. P. Straughan, *J. Chem. Soc., Dalton Trans.* **1975**, 2368-2373.
[44] C. Schulten, G. von Frantzius, G. Schnakenburg, R. Streubel, *Heteroat. Chem.* **2011**, *22*, 275-286.
[45] E. Ionescu, G. von Frantzius, P. G. Jones, R. Streubel, *Organometallics* **2005**, *24*, 2237-2240.
[46] A. Maraval, A. Igau, C. Lepetit, A. Chrostowska, J.-M. Sotiropoulos, G. Pfister-Guillouzo, B. Donnadieu, J. P. Majoral, *Organometallics* **2001**, *20*, 25-34.
[47] A. Schmidpeter, F. Zwaschka, *Angew. Chem. Int. Ed. in English* **1977**, *16*, 704-705.
[48] A. Schmidpeter, G. Burget, F. Zwaschka, W. Sheldrick, *Z. fur Anorg. Allg. Chem.* **1985**, *527*, 17-32.
[49] J. F. Binder, S. C. Kosnik, P. B. J. St Onge, C. L. Macdonald, *Chem. Eur. J.* **2018**, *24*, 14644-14648.
[50] B. D. Ellis, C. L. B. Macdonald, *Coord. Chem. Rev.* **2007**, *251*, 936-973.
[51] R. M. Deng, K. B. Dillon, *J. Chem. Soc., Chem. Commun.* **1981**, 1170-1171.
[52] A. Schmidpeter, K. H. Zirzow, G. Burget, G. Huttner, I. Jibril, *Chem. Ber.* **1984**, *117*, 1695-1706.
[53] Z. Li, J. E. Borger, F. Müller, J. R. Harmer, C. Y. Su, H. Grützmacher, *Angew. Chem. Int. Ed.* **2019**, *58*, 11429-11433.
[54] C. M. Hoidn, T. M. Maier, K. Trabitsch, J. J. Weigand, R. Wolf, *Angew. Chem. Int. Ed.* **2019**, *58*, 18931-18936.
[55] L. E. English, A. Pajak, C. L. McMullin, J. P. Lowe, M. F. Mahon, D. J. Liptrot, *Chem. Eur. J.* **2022**, *28*, e202200376.
[56] F. Dankert, P. Gupta, T. Wellnitz, W. Baumann, C. Hering-Junghans, *Dalton Trans.* **2022**, *51*, 18642-18651.
[57] D. Bockfeld, T. Bannenberg, P. G. Jones, M. Tamm, *Eur. J. Inorg. Chem.* **2017**, *2017*, 3452-3458.
[58] D. Dhara, P. K. Pal, R. Dolai, N. Chrysochos, H. Rawat, B. J. Elvers, I. Krummenacher, H. Braunschweig, C. Schulzke, V. Chandrasekhar, U. D. Priyakumar, A. Jana, *Chem. Commun.* **2021**, *57*, 9546-9549.
[59] M. I. Arz, V. T. Annibale, N. L. Kelly, J. V. Hanna, I. Manners, *J. Am. Chem. Soc.* **2019**, *141*, 2894-2899.
[60] A. G. Baradzenka, S. F. Vyboishchikov, M. Pilkington, G. I. Nikonov, *Chem. Eur. J.* **2023**, *29*, e202301842.
[61] X. Zhao, X. Chu, G. Rauhut, C. Chen, C. Song, B. Lu, X. Zeng, *Angew. Chem. Int. Ed.* **2019**, *58*, 12164-12169.
[62] A. Mardyukov, D. Niedek, P. R. Schreiner, *J. Am. Chem. Soc.* **2017**, *139*, 5019-5022.
[63] L. D. Quin, *Coord. Chem. Rev.* **1994**, *137*, 525-559.
[64] A. A. Nasrullah, E. Zander, F. Dankert, A. Petrov, J. Surkau, E. Baráth, C. Hering-Junghans, *Chem. Sci.* **2025**, *16*, 6909-6917.
[65] G. Ballmann, H. Elsen, S. Harder, *Angew. Chem. Int. Ed.* **2019**, *58*, 15736-15741.
[66] M. Finze, E. Bernhardt, H. Willner, C. W. Lehmann, *J. Am. Chem. Soc.* **2005**, *127*, 10712-10722.
[67] D. W. Wilson, M. P. Franco, W. K. Myers, J. E. McGrady, J. M. Goicoechea, *Chem. Sci.* **2020**, *11*, 862-869.
[68] M. E. Doleschal, A. Kostenko, J. Y. Liu, S. Inoue, *Nat. Chem.* **2024**, 1-8.
[69] A. A. Nasrullah, M. Fischer, F. Dankert, E. Barath, C. Hering-Junghans, *Organometallics* **2025**, *44*, 788-791.
[70] P. Hibner-Kulicka, J. A. Joule, J. Skalik, P. Bałczewski, *RSC Adv.* **2017**, *7*, 9194-9236.
[71] T. Baumgartner, R. Réau, *Chem. Rev.* **2006**, *106*, 4681-4727.
[72] T. Baumgartner, *Acc. Chem. Res.* **2014**, *47*, 1613-1622.
[73] M. G. Hobbs, T. Baumgartner, *Eur. J. Inorg. Chem.* **2007**, *2007*, 3611-3628.
[74] D. Joly, P. A. Bouit, M. Hissler, *J. Mater. Chem. C* **2016**, *4*, 3686-3698.

[75] M. Gouygou, O. Dechy-Cabaret, K. Fourmy, D. U. C. Nguyen, *Catal. Sci. Technol.* **2015**, *5*.
[76] G. Wittig, G. Geissler, *Justus Liebigs Ann. Chem.* **1953**, *580*, 44-57.
[77] S. Ogawa, Y. Tajiri, N. Furukawa, *Bull. Chem. Soc. Jpn.* **2006**, *64*, 3182-3184.
[78] G. Wittig, E. Kochendoerfer, *Chem. Ber.* **1964**, *97*, 741-746.
[79] H. Hattori, K. Ishida, N. Sakai, *Synthesis* **2024**, *56*, 193-219.
[80] B. Twamley, C. D. Sofield, M. M. Olmstead, P. P. Power, *J. Am. Chem. Soc.* **1999**, *121*, 3357-3367.
[81] R. C. Smith, S. Shah, J. D. Protasiewicz, *J. Organomet. Chem* **2002**, *646*, 255-261.
[82] T. Taeufer, F. Dankert, D. Michalik, J. Pospech, J. Bresien, C. Hering-Junghans, *Chem. Sci.* **2023**, *14*, 3018-3023.
[83] A. S. Ionkin, W. J. Marshall, *Heteroat. Chem.* **2003**, *14*, 360-364.
[84] A. A. Diaz, J. D. Young, M. A. Khan, R. J. Wehmschulte, *Inorg. Chem.* **2006**, *45*, 5568-5575.
[85] M. Olaru, D. Duvinage, Y. Naß, L. A. Malaspina, S. Mebs, J. Beckmann, *Angew. Chem. Int. Ed.* **2020**, *59*, 14414-14417.
[86] H. A. van Kalkeren, S. H. A. M. Leenders, C. R. A. Hommersom, F. P. J. T. Rutjes, F. L. van Delft, *Chem. Eur. J.* **2011**, *17*, 11290-11295.
[87] P.-A. Bouit, A. Escande, R. Szűcs, D. Szieberth, C. Lescop, L. Nyulászi, M. Hissler, R. Réau, *J. Am. Chem. Soc.* **2012**, *134*, 6524-6527.
[88] H.-C. Su, O. Fadhel, C.-J. Yang, T.-Y. Cho, C. Fave, M. Hissler, C.-C. Wu, R. Réau, *J. Am. Chem. Soc.* **2006**, *128*, 983-995.
[89] J. Yin, R.-F. Chen, S.-L. Zhang, Q.-D. Ling, W. Huang, *J. Phys. Chem. A.* **2010**, *114*, 3655-3667.
[90] D. W. Stephan, G. Erker, *Angew. Chem. Int. Ed.* **2010**, *49*, 46-76.
[91] D. W. Stephan, *Science* **2016**, *354*.
[92] A. L. Travis, S. C. Binding, H. Zaher, T. A. Q. Arnold, J.-C. Buffet, D. O'Hare, *Dalton Trans.* **2013**, *42*, 2431-2437.
[93] M. A. Dureen, D. W. Stephan, *J. Am. Chem. Soc.* **2009**, *131*, 8396-8397.
[94] M. A. Dureen, C. C. Brown, D. W. Stephan, *Organometallics* **2010**, *29*, 6594-6607.
[95] C. Jiang, O. Blacque, H. Berke, *Organometallics* **2010**, *29*, 125-133.
[96] M. A. Dureen, C. C. Brown, D. W. Stephan, *Organometallics* **2010**, *29*, 6422-6432.
[97] H. Kim, D. W. Stephan, *Dalton Trans.* **2023**, *52*, 5023-5027.
[98] S. J. Geier, M. A. Dureen, E. Y. Ouyang, D. W. Stephan, *Chem. Eur. J.* **2010**, *16*, 988-993.
[99] C. B. Caputo, S. J. Geier, E. Y. Ouyang, C. Kreitner, D. W. Stephan, *Dalton Trans.* **2012**, *41*, 237-242.
[100] J. Guo, M. Yan, D. W. Stephan, *Org. Chem. Front.* **2024**, *11*, 2375-2396.
[101] G. S. Hair, A. H. Cowley, R. A. Jones, B. G. McBurnett, A. Voigt, *J. Am. Chem. Soc.* **1999**, *121*, 4922-4923.
[102] M. Mantina, A. C. Chamberlin, R. Valero, C. J. Cramer, D. G. Truhlar, *J. Phys. Chem. A.* **2009**, *113*, 5806-5812.
[103] Z. Li, J. E. Borger, F. Müller, J. R. Harmer, C.-Y. Su, H. Grützmacher, *Angew. Chem. Int. Ed.* **2019**, *58*, 11429-11433.
[104] A. H. Cowley, F. Gabbai, R. Schluter, D. Atwood, *J. Am. Chem. Soc.* **1992**, *114*, 3142-3144.
[105] M. Driess, R. Janoschek, H. Pritzkow, S. Rell, U. Winkler, *Angew. Chem. Int. Ed. in English* **1995**, *34*, 1614-1616.
[106] S. Attar, W. H. Bearden, N. W. Alcock, E. C. Alyea, J. H. Nelson, *Inorg. Chem.* **1990**, *29*, 425-433.
[107] V. Diemer, A. Berthelot, J. Bayardon, S. Jugé, F. d. r. R. Leroux, F. Colobert, *J. Org. Chem.* **2012**, *77*, 6117-6127.
[108] C. A. Jaska, H. Dorn, A. J. Lough, I. Manners, *Chem. Eur. J.* **2003**, *9*, 271-281.

8 Curriculum Vitae

AYU AFIQAH NASRULLAH
Ziolkowskistr.8B,18059 Rostock,
Germany.
Phone: +49 176 32204965
Email: ayu.nasrullah@catalysis.de
Born: 13 Feb 1987
Status: Married.
Nationality: Malaysian

ACADEMIC QUALIFICATION

2022 – 2025 **PhD in Inorganic Chemistry** at Leibniz Institute for Catalysis (LIKAT), Rostock Germany.
Supervisors: Dr. Christian Hering-Junghans, Prof. Dr. Eszter Baráth.
PhD Thesis: "The Chemistry of Cyanophosphide and Phosphafluorene: Insight of Structure and Reactivity"
PhD defense on 28th Oct 2025

2011 – 2014 **Master of Science (Natural Products Chemistry)** at University of Malaya, Kuala Lumpur, Malaysia.
Supervisor: Prof. Dr. Khalijah Awang and late Dr. Mat Ropi Mukhtar.
Master Thesis: "Phytochemicals and Bioactivities of *Cryptocarya Nigra* (Lauraceae)"

2006 – 2010 **Bachelor of Science (Applied Chemistry)** at University of Malaya, Kuala Lumpur, Malaysia.
Honours – CGPA: 2.97/4.00
Bachelor Thesis: Chemical constituent of *Neonauclea sp.1* (Rubiaceae).

2005 – 2006 **Pre-University (Foundation of Science)** at Centre for Foundation Studies in Science (PASUM), University of Malaya, Kuala Lumpur, Malaysia.
Honours – CGPA: 3.33/4.00

2004 **Malaysian Education Certification – SPM** (Pure Science) at Convent Girls High School, Ipoh, Perak, Malaysia.
Results: 7 A's 3 B's

PROFESIONAL EXPERIENCES

2019 – Feb 2022 **Chemistry Coordinator** at Preparatory Centre for Science and Technology, University Malaysia Sabah (UMS), Kota Kinabalu, Sabah, Malaysia.
Subjects: General Chemistry (Pre-University Level)

2015 – Feb 2022 **Lecturer** at Preparatory Centre for Science and Technology, University Malaysia Sabah (UMS), Kota Kinabalu, Sabah, Malaysia.
Subjects: General Chemistry (Pre-University Level)

2013 – 2015 **Tutor and Lab Demonstrator** at Preparatory Centre for Science and Technology, University Malaysia Sabah (UMS), Kota Kinabalu, Sabah, Malaysia.
Subjects: Pre-University chemistry

2010-2013 **Research Assistant** during master's degree at Chemistry Department, Faculty of Science, University of Malaya (UM), Kuala Lumpur, Malaysia.

PUBLICATIONS

11 Nasrullah, A. A., Baráth, E., & Hering-Junghans, C. FLP-type Alkenylation of a Phosphafluorene. *Dalton Trans.* **2025**, *54*, 15795-15800.

10 Nasrullah, A. A., Fischer, M., Dankert, F., Barath, E., & Hering-Junghans, C. Flash Communication: Cyanophosphide Transfer Reactions. *Organomet.* **2025**, *44*(7), 788-791.

9 Nasrullah, A. A., Zander, E., Dankert, F., Petrov, A., Surkau, J., Baráth, E., & Hering-Junghans, C. Coordination isomerism in dioxophosphorane cyanides. *Chem. Sci.* **2025**, *16*(16), 6909-6917.

8 Hematpoor, A., Liew, S.Y., Omar, H., Shilpi, J.A., Zahari, A., Syamsir, D.R., Salleh, H.M., Tohar, N., Theng Kim, R.P., Qureshi, A.K. and Nasrullah, A.A. Toxicity of Malaysian Medicinal Plant Extracts Against Sitophilus oryzae and Rhyzopertha dominica. *Pertanika Journal of Tropical Agricultural Science* **2022**, *45*(4).

7. S. N. S. Bakri, N. Juhan, C. H. Che Hussin, A.A. Nasrullah, *International Journal of Education, Psychology and Counseling* **2022**, *7*, 469-478.

6. Rajak, M. A. A., Nasrullah, A. A., Bakri, S. N. S., & Lasaraiya, S. Impak Modul Pembelajaran Berasaskan Masalah-Sains, Teknologi, Kejuruteraan dan Matematik kepada Pelajar Sekolah Menengah di Luar Bandar: Kajian Perbandingan. *International Journal of Education, Psychology and Counseling* **2022**, *7*(48), 458-468.

5. Yunus, M. M., Nasrullah, A. A., Dahon, N. H., & Pelah, N. A. A Preliminary Study on the Graphic Development for Lab Instrumentation Model. *Transactions on Science and Technology* **2021**, *8*(3-3), 599-603.

4. Nasrullah, A. A., Dahon, N. H., Rajak, M. A. A., Yunus, M. M., Abd Latip, N. A., Arshad, S. E., & Yusslee, E. M. F. M. A Preliminary Study on STEM Encouragement in Chemistry Subject: The Learning Experience of SMK Usukan Students in STEM AUMS Warrior Program. *Transactions on Science and Technology* **2021**, *8*(3-2), 388-393.

3 Nasrullah, A. A., Rajak, M. A. A., Dahon, N. H., Yunus, M. M., Latip, N. A. A., Arshad, S. E., & Din, W. A. The effectiveness of the inverted classroom learning model for pre-university chemistry students: The preliminary study. *International Journal of Advanced Research in Education and Society* **2019**, *1*(2), 49-56.

2. Dahon, N.H., Kassim, M.J., Razali, N.N., Yusslee, M.F.M., Nasrullah, A.A., Basri, N.F. FTIR

Analysis on Phase Transformation of Rust In The Presence of Gambir. *Journal of Global Science Research* **2018**, *1*, 54-62.

1. Ayu Afiqah Nasrullah, Azeana Zahari, Jamaludin Mohamad, Khalijah Awang. Antiplasmodial Alkaloids from the bark of *Crytocarya nigra* (Lauraceae). *Molecules* **2013**, *18* (7), 8009-8017.

CONFERENCES

8 **Oral** A. A. Nasrullah; F. Dankert, E. Zander, J. Surkau, E. Barath, C.Hering-Junghans. "Coordination Isomerism in Dioxophosphorane Cyanides"; February **2025**, 21st European Workshop on Pnictogen Chemistry, EWPC in Innsbruck, Austria.

7 **Poster** A. A. Nasrullah; F. Dankert, E. Zander, J. Surkau, E. Barath, C.Hering-Junghans. "Diverse Reactivity of Cyanophosphide," September **2024**, 24th Norddeutches Doktorandenkolloquium, NDDK in Rostock, Germany.

6 **Poster** A. A. Nasrullah; S. Chakrabortty; P. Kamer; S. Tin; E. Baráth; J. de Vries. "Chemo selective synthesis of cyclohexane derivatives via the hydrogenation of aromatic ketones using unligated RhCl3 precursor," March **2023**, 56th Jahrestreffen Deutscher Katalytiker in Weimar, Germany.

5 **Oral** Ayu Afiqah Nasrullah, Nur Hazwani Dahon, Mohd Azrul Abdul Rajak, Megawati Mohd Yunus, Nur Anneliza Abd. Latip, Sazmal Effendi Arshad, and Eddy Mohd Farid Mohd Yusslee. "A Preliminary Study on STEM Encouragement in Chemistry Subject: The Learning Experience of SMK Usukan Students in STEM AUMS Warrior Program", August **2021**, The First UMS Colloquium on Fundamental Research and Application (UMS-CoFA2020), University Malaysia Sabah, Sabah, Malaysia. (Online)

4 **Invited Speaker** Ayu Afiqah Nasrullah. "Experience with Online Final Examination during Pandemic Covid-19", July **2020**, Webinar Tel@Ums "Soaring Above Challenges Together", University Malaysia Sabah, Sabah, Malaysia. (Online)

3 **Oral** Ayu Afiqah Nasrullah, Mohd Azrul Abdul Rajak, Nur Hazwani Dahon, Megawati Mohd Yunus, Nur Anneliza Abd. Latip, Sazmal Effendi Arshad, Wardatul Akmam Din. "The Effectiveness of The Inverted Classroom Learning Model for Pre-University Chemistry Students: The Preliminary Study", June **2019**, International Conference on Business, Education, Innovation and Social Sciences (ICBEISS 2019), Asian Scholar Network at Seri Pacific Hotel, Kuala Lumpur, Malaysia.

2 **Oral** Ayu Afiqah Nasrullah. "Phytochemical Analysis of Atherosperminine Isolated from *Cryptocarya nigra* (Lauraceae)", December **2016**, International Conference on Education, Mathematics and Science 2016 (ICEMS 2016) in conjunction with 4th International Postgraduate Conference on Science and Mathematics 2016 (IPCMS 2016) at Faculty of Science and Mathematics, Sultan Idris Education University, Tanjung Malim, Perak, Malaysia.

1 **Oral** Ayu Afiqah Nasrullah, Mat Ropi Mukhtar, Khalijah Awang, and A. Hamid A. Hadi. "Alkaloids Isolated from *Cryptocarya nigra* (Lauraceae)", December **2011**, 7th Mathematics and Physical Science Graduate Congress (7th MPSGC) at Faculty of Science, National University Singapore (NUS), Singapore.

FURTHER SKILL

Languages Malay (native), English (fluent), German (beginner)

IT skill MS Office (Word, Excel, PowerPoint), Endnote, ChemDraw, Mestre Nova, Scifinder, Reaxys

REFEREES

Dr. habil Christian Hering-Junghans
Leibniz-Institut für Katalyse e. V.
Albert-Einstein-Straße 29A
18059 Rostock
christian.hering-junghans@catalysis.de

Prof. Dr. habil Eszter Baráth
Leibniz-Institut für Katalyse e. V.
Albert-Einstein-Straße 29A
18059 Rostock
eszter.barath@catalysis.de

ChM. Dr. Newati Wid
Preparatory Centre for Science and Technology, University Malaysia Sabah,
Kota Kinabalu, Sabah, Malaysia.
newati@ums.edu.my

Assoc. Prof Ts. Dr. Sazmal Effendi Arshad
Faculty of Science and Natural Resource, University Malaysia Sabah,
Kota Kinabalu, Sabah, Malaysia.
sazmal@ums.edu.my

Prof Dr. Khalijah Awang
Dept of Chemistry, Faculty of Science,
University Malaya, 50603 Lembah Pantai,
Kuala Lumpur, Malaysia
khalijah@um.edu.my